WORK OF THE STAFF AND COMMITTEES

In any professional institution such as our own, a considerable amount of work is carried on behind the scenes, of which only a small part ever comes to the notice of the general membership. The vast bulk of the administrative work is naturally performed by the secretariat, under the direction of the General Secretary, who can call upon the knowledge and experience of the several specialized officers on his staff.

The Institution is fortunate in its permanent staff, and at this time, just at the close of our General Secretary's tour of India on behalf of the Institution, and on the eve of his return to normal duties, it is fitting to express on behalf of the Council and members a tribute to him, to the Assistant Secretary who has deputized so successfully for him during his absence, and to the permanent officers and other members of the staff who perform the many duties without which the Institution could not exist.

Next to the secretariat and staff, the bulk of the Institution's work is carried out by the Standing Committees appointed by the General Council. On these, and in particular on the Professional Purposes, the Membership, the Programme and Papers, and the Education and Examinations Committees, fall the major tasks. Their meetings are frequent and lengthy, and in many cases involve extra work in the preparation of reports and in obtaining information outside the actual meetings.

The Institution's task would be more difficult if it were not for the Local Section Committees who, on a small scale, reproduce the pattern of the Standing Committees. The increase in the number and strength of the Local Sections as the Institution grows is greatly to the benefit of the membership in general.

The membership of the Institution has reason for being particularly grateful to the relatively small number of people who devote much spare time to work on these and the other Committees. Although they are appointed annually by the General Council, in many cases the personnel of Committees changes much less frequently, so that some members serve for quite a number of years. In this, as in other spheres, experience is valuable and the General Council therefore feels most reluctant to lose the services of those who have shown themselves willing and capable in Committee work.

Nevertheless, it is the wish of the Council to encourage new talent from the membership of the Institution, and to make new appointments to Committees from time to time. Many members must have the knowledge and ability to participate in Committee work, thereby relieving some of the senior members who have served for a long time on one or more of the various Standing Committees.

Ours is a young Institution, but one with a future which is assured. It is most desirable in such an Institution that qualified members, even though young in years, should have every opportunity, if they so desire, of contributing their quota to the work of the Institution.

With this object in view, the Council, through the General Secretary, will always be pleased to hear from any member who considers that he has the qualifications and, most important, the enthusiasm to take part in Committee work. Even though no vacancies may exist immediately, it will be very valuable for the Council to have a list of names from which Committee members could be selected in the future.

W. E. M.

137

NOTICES

His late Majesty King George VI

As stated in the last issue of the *Journal* the President, on behalf of the Council and members, sent a message to Her Majesty The Queen conveying deep sympathy in the loss of His late Majesty and expressing the Institution's constant loyalty to Her Majesty.

The following reply has been received from the Queen's Secretary:—

"I am commanded by The Queen to express to you and to all those on whose behalf you wrote her sincere thanks for your kind message of sympathy in her great loss.

"Her Majesty greatly appreciates their thought of her and her family at this time."

Obituaries

Council has learned with regret of the death of Frank Wilmout Wicks who was elected an Associate Member in 1927. Mr. Wicks was chief instructor at a commercial radio school before his retirement in 1947. Up to the time of his death at the age of 70 years, he continued to take a keen interest in the Institution.

* * *

Council also records with regret the death of Frederick George Boyd (Associate) at the age of 44 years. Mr. Boyd, who was a senior engineer in E.M.I. Factories, Ltd., was elected in 1947. During the war he served in the R.A.F., reaching the rank of Flight Lieutenant.

Radio Components Show

The Ninth Private Exhibition of the Radio and Electronic Component Manufacturers' Federation will be held at Grosvenor House, Park Lane, London, from Monday, April 7th, to Wednesday, April 9th. Admission is by invitation only and members wishing to attend the exhibition should get in touch with the Institution Librarian.

Radio Industry Appointments

Mr. G. Darnley Smith has been elected chairman of the Radio Industry Council in succession to Mr. J. W. Ridgeway, O.B.E. (Member), who has been chairman since 1948. Mr. Darnley Smith was chairman in 1947 and has been chairman of the Industry Television Policy Committee since its formation in 1948. Mr. G. A. Marriott, B.A. (Member), was elected vice-chairman.

Mr. P. H. Spagnoletti, B.A., and Mr. E. K. Balcombe were re-elected chairman and vice-chairman respectively of the British Radio Equipment Manufacturers Association, a constituent association of the Radio Industry Council. At the annual general meeting of the Association Mr. Spagnoletti said that 590,000 British radio receivers and chassis were exported last year, an all-time record.

Radio Show Dates

The Radio Industry Council announces that the 19th National Radio Show will be held at Earls Court, London, from Tuesday, August 26th, to Saturday, September 6th. There will be restricted admission on August 26th.

The Northern Radio Show, City Hall, Manchester, is to be opened at 12 noon on Wednesday, April 23rd, and the opening speeches will be broadcast. It has not yet been announced who will open the Show.

The Physical Society's 36th Exhibition

The 36th Exhibition of the Physical Society will be held at Imperial College, South Kensington, London, S.W.7, from Thursday, April 3rd, to Tuesday, April 8th (excluding Sunday). Only Fellows of the Society and the Press will be admitted from 10 a.m. to 6 p.m. on the first day.

There will be two sessions each day: from 10 a.m. to 1 p.m. and from 2 p.m. to 9 p.m. Members may obtain tickets from the Institution's Librarian for admission, (*a*) to both sessions on a particular day, or (*b*) to any morning session, or (*c*) to any evening session.

The Exhibition will take place in the Main Building of the Royal College of Science, Imperial Institute Road, and in the Huxley Building, opposite the Science Museum in Exhibition Road. Tickets will admit their holders to both buildings.

Transfer of Examination Entries

In the past the Education and Examinations Committee has allowed the transfer of examination entries to the next examination in the case of illness or other unavoidable circumstances. Many candidates have taken undue advantage of this concession at considerable cost and inconvenience to the Institution.

It has therefore been decided that with effect from the November 1952 examination, no entry will be transferable once it has been accepted and examination fees will not be returned nor transferred for other purposes.

IMPROVEMENTS IN DESIGN AND OPERATION OF IMAGE ICONOSCOPE TYPE CAMERA TUBES *

by

J. E. Cope,† L. W. Germany† and R. Theile, Dr. Phil.†

A Paper presented at the Fifth Session of the 1951 Radio Convention on August 23rd in the Cavendish Laboratory, Cambridge

SUMMARY

Television camera tubes using high-velocity electrons for scanning show a number of undesirable characteristics. These include spurious signals and edge flare, which are due to non-uniform secondary electron redistribution effects and, in addition, there is no true "black level" information in the picture signal.

Effects due to uneven redistribution can be considerably reduced if the average storage surface potential is shifted negatively from that reached under normal operating conditions. In an improved design of the "Photicon" image iconoscope, this potential change is achieved by flooding the storage surface with low-velocity electrons, which are emitted from a large annular photo-emissive surface surrounding the storage plate. Suitably biased electrodes direct the low-velocity electron rain in such a manner as to compensate for the non-uniformity of the residual redistribution.

The use of the new tube also allows simplification of the camera control unit. As the "black" picture signal is constant in relation to the interline pulses produced by beam suppression, it is no longer necessary to evaluate the blackest part of the picture signal in order to set the "black level." A simple "clamp circuit" is sufficient and results in a very satisfactory transmission of the average brightness component of the picture.

1. Introduction

Amongst the various types of television camera tubes at present in use, the image iconoscope has retained a place as a useful and practical device, producing pictures with excellent definition and tonal gradation. The sensitivity is sufficient for studio use and for field television under reasonable light conditions. The tube is relatively robust in construction and not sensitive to light overloading.

The output current does not, however, contain a black reference level and may under low light conditions contain objectionable shading signals. This latter fault is due to the non-uniform secondary electron redistribution on the storage surface peculiar to high-velocity electron scanned pick-up tubes. This imposes some limitations; for instance, readjustment of shading and black level controls is likely to be needed when the light distribution in the scene is changed and, furthermore, the tonal gradation of dark objects

near the bottom of the picture is not faithfully reproduced. It has long been thought that this non-uniform redistribution of secondaries could be equalized by a flood of low-velocity electrons directed on to the storage surface, but until recently no really satisfactory scheme for applying this idea to improve the image iconoscope has been evolved.

Recent work on these lines has been more successful and has resulted in the development of the "photo-electron-stabilized" (P.E.S.) Photicon.[1]

2. Analysis of the Operation of the Image Iconoscope

In order to appreciate the factors influencing the design of the new tube, it is necessary to understand the operation of picture generation in the normal image iconoscope. Fig. 1 shows the tube[2, 3] diagrammatically. The scene to be televised is focused on to the homogeneous semi-transparent photo-cathode, and the electrons released are imaged on to the storage plate. This plate is scanned obliquely by a beam of high-velocity electrons, thereby evaluating the charge pattern produced by the photo-electron

bombardment. The velocity of both beam and photo-electrons is of the order of 1,000 V. The storage plate usually consists of a thin mica sheet, one side of which is activated for a high secondary emission ratio, the other being backed with a conducting layer forming the signal plate. The storage surface can be represented as a large number of discrete capacitances to this common electrode. The inside wall of the glass bulb is coated with a metallic film, which serves as an anode for the image converter section and as a collector for the secondary electrons released from the storage surface.
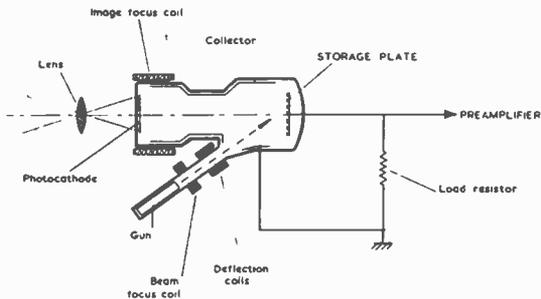

Fig. 1.—*Diagram of an image iconoscope type pick-up tube.*

Under the high-velocity bombardment by either scanning beam or photo-electrons, the storage surface, which has a secondary emission ratio greater than unity, emits secondaries and, therefore, due to the loss of these electrons, assumes a positive potential. Thus a bias voltage is developed which makes the flow of the secondaries to the collector progressively more difficult until the so-called equilibrium potential is reached, when only the faster electrons, equal in number to the number of primaries, escape to the collector.

The equilibrium potential is of the order of three volts but the exact value is determined by the actual material used for the storage surface, since the secondary emission ratio and the distribution of the initial velocity of the secondaries vary with different materials.

In the scanning process, the balance between the total number of electrons arriving at, and leaving, the storage surface is maintained over a complete picture cycle. (To be strictly accurate this is only true for a still picture, but the consideration of this steady state is sufficient for analysis.) All secondaries in excess of the number of primaries must fall back on to the

storage surface. This "redistribution" of low-velocity electrons forms a negative charge layer on the storage surface. Thus, after scanning, the potential of the surface drifts negatively from the equilibrium potential. Those areas corresponding to bright parts of the picture tend to return to the equilibrium potential due to photo-electron bombardment, and in this way the picture charge pattern is formed. The existence of redistribution is therefore quite essential to form a picture, and a storage surface with a high secondary emission ratio ensures that sufficient electrons are available.

The first limitation in the picture generation is now apparent. It has been shown that the picture charge pattern development is restricted to the limits set by the positive equilibrium potential and the maximum negative drift therefrom due to redistribution. This means that the signal, which is proportional to the elementary charge, cannot exceed a certain level irrespective of the scene brightness. The storage efficiency therefore decreases as the light level is increased. On the other hand, this results in a very satisfactory transfer characteristic, enabling a wide range of light to be handled and providing a reasonably good match to the average receiving cathode ray tube, the final picture having a very good tonal gradation.

The rain of redistributed secondary electrons, however, is not uniform over the storage area, as it is modulated by the surface potential which changes with the motion of the scanning beam. As the spot under beam electron bombardment assumes the positive equilibrium potential, the area just scanned becomes the most positive part of the surface and attracts the low-velocity secondary electrons released by the beam while scanning the following lines. There is a tendency, therefore, for the redistributed electrons to migrate in the opposite direction to the motion of the scanning beam across the storage surface. The electrons are accumulated in those areas scanned first, with a deficiency along the edges where scanning ends. This non-uniformity of redistribution is the cause of shading signals and edge flare. As a negative value of the storage surface potential generates a signal corresponding to "dark" or "black," the background of the picture is shaded from left to right and top to bottom, the top left-hand corner appearing dark, the bottom and right-hand edges appearing white, as illustrated in Fig. 2a.
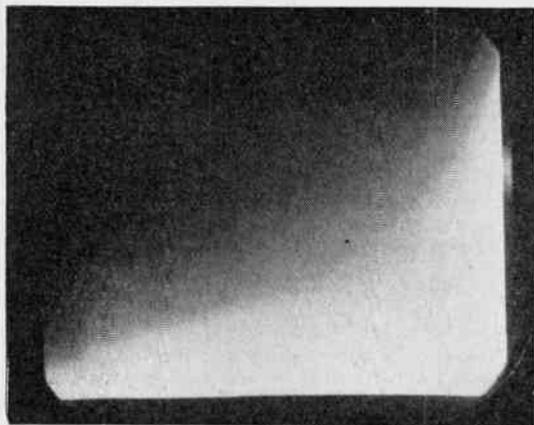
(a) *Typical nature of background shading due to spurious signals without light on the photo-cathode.*

Fig. 2.—Television pictures showing typical properties of image iconoscope type tubes.

The absence of redistribution along the edges where scanning ends causes considerable trouble. Edge flare is especially marked in the frame direction as the deficiency at the ends of most of the line scan is partially made good by re-distribution of secondaries from the following lines, but those lines at the bottom of the picture are less fortunate as the beam returns abruptly to the top of the raster. The bottom edge of the storage area therefore remains at or near the equilibrium potential and thus very little charge can be developed. Therefore the modulation fades out towards the lower edge of the picture, leaving a white spurious signal.

So far redistribution from the scanning beam only has been considered. The photo-electrons produce secondary electrons which are also re-distributed because the current balance applies equally to both beam and photo-electrons. The redistribution due to the photo-electron bombardment is dependent on the picture content and adds to the beam redistribution. If the scene is composed of relatively small areas of light and shade scattered over the picture area, the charge condition over the storage surface is equalized and, as is well known, if sufficient light is present on the scene, shading is much reduced (Figs. 2b and 2c). It is quite possible to equalize the residual spurious signal by the addition of suitable compensating waveforms of line and frame frequency, provided that the picture content is fairly constant. In order to suppress edge flare completely, however, the
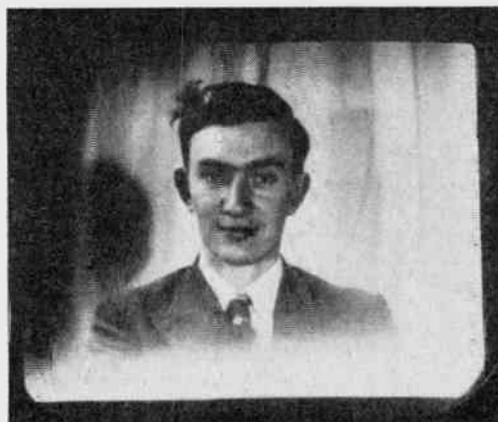
(b) *Edge flare in pictures taken with insufficient scene light.*

(c) *Picture taken with high scene light still showing slight edge flare in dark areas at the bottom.*

required light level must be fairly high in the lower parts of the scene. Unfortunately, typical scenes to be televised contain extended dark areas along the bottom edge, for example, persons wearing dark clothes, as shown in Fig. 2. Bottom flare is, therefore, a serious limitation in the use of the image iconoscope type of tube.

The remaining fault to be considered is the absence of black reference level in the signal output waveform. This is due to the fact that the signal output cannot maintain a direct current and that there are no pulses having a constant relationship to the "black" signal, which might be used as a reference level. This can clearly be seen by analysing the signal waveform as

141

it appears after being clamped at the end of each line (see Fig. 3).[4] If no light is present on the photo-cathode, only the shading signals are generated, and the general character of the waveform is indicated in the diagram. A raster of 10 lines is shown in order that signals in the line periods can be clearly seen. The signal level present during the beam suppression periods corresponds to zero signal plate current and is clamped to a constant value, signals above this level corresponding to "white" (less electrons escaping from the storage surface than arriving) whilst signals below this level correspond to "black."

Fig. 3.—*Diagram of an image iconoscope signal after "clamping" over one frame period without light on the photo-cathode.*

The shading signals shown in Fig. 2a appear as deviations from the signal plate current in both directions and the time integrals of all positive and negative components are equal over the frame period. It will be seen that the shading signal waveform tends to rise as scanning proceeds in both line and frame directions. Fig. 4 shows the actual oscillograms taken on a 405-line Photicon camera chain. As the individual line waveforms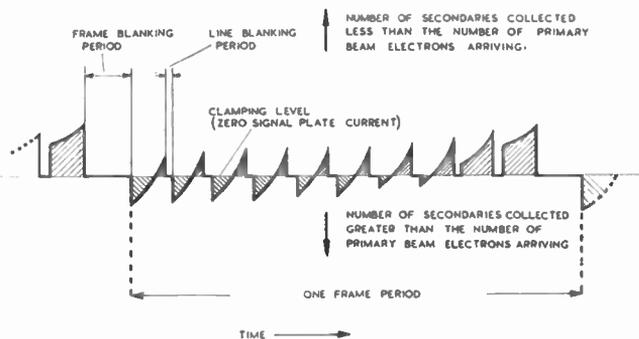 are not resolved, the oscillogram appears as a band (whose width is given by the line components) with the zero line of the clamped interline pulses passing through the electrical mean of the signal.

If light from a picture is now admitted to the photo-cathode, the corresponding signal is superimposed. This is shown in Fig. 4b for a pattern of horizontal black-and-white bars with a low degree of illumination. Here the picture appears as a modulation of the shading waveform, as the redistribution of secondaries released by the beam is predominant. When the light is increased the signal is developed in both positive and negative directions from a base line formed by the shading signal which, if the light level is high enough, becomes reduced, giving a signal nearly symmetrical about the zero line (Fig. 4c). It is obvious that the relationship between the black level and the interline pulses is not constant with changing scene illumination due to the current balance having to be maintained. As this current balance applies to the total signal plate current caused by both beam and photo-electron bombardment, the interline level will not necessarily represent the electrical mean of the signal in the presence of a
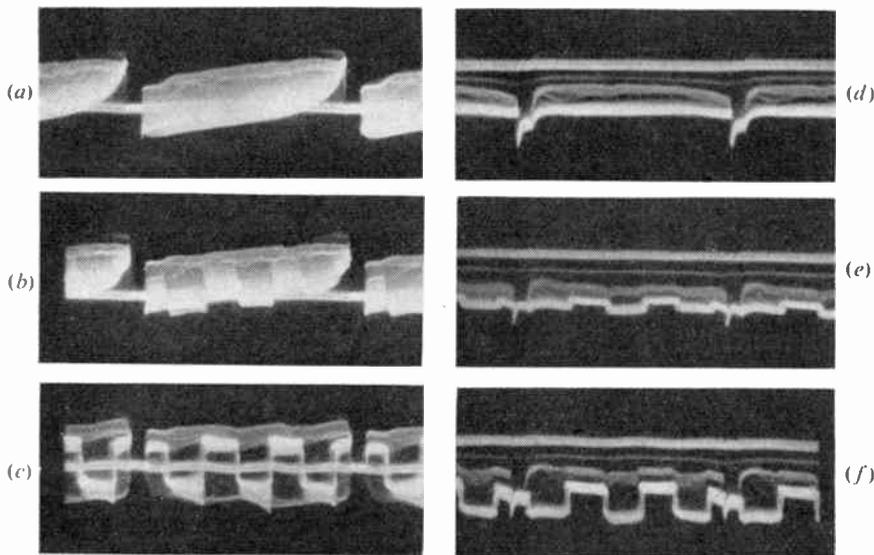

Fig. 4.—*Oscillograms of an image iconoscope signal after "clamping" over one frame period, televising a pattern of black-and-white horizontal bars:*
(a), (b), (c) without shading correction, light level increasing
(d), (e), (f) with shading correction, light level increasing.

142

picture. This level is obtained by beam suppression and thus may not correspond to zero signal plate current since the photo current is not periodically interrupted. This again shows how indefinite the relationship between the beam suppression level and picture "black" can be. A clamp circuit operating during the interline periods cannot therefore evaluate the black level. If the scene light level is gradually reduced, the black and white peaks of the picture waveform tend to an average grey level, as illustrated in the right-hand group of Fig. 4 where shading correction waveforms have been added to the signal before clamping. The top line in the oscillogram represents the clamping level, the shift having been introduced by the method of shading correction used. It is clearly demonstrated that the relationship between the clamping level and picture "black" varies with the scene brightness and the lack of suitable reference pulses makes necessary an additional d.c. restoration circuit in the camera control unit.
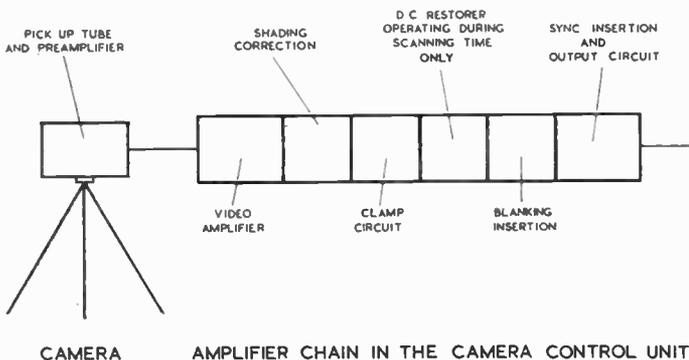

Fig. 5.—*Block diagram of the amplifier chain in a "Photicon" camera control unit.*

Referring to Fig. 5, which shows a block diagram of the amplifier chain used with the normal Photicon camera, this d.c. restorer is connected between the clamp circuit and the blanking insertion, and evaluates the darkest part of the picture signal, establishing this value as the black level. Although this scheme helps, it fails if there are no real black parts in the scene. If, for example, a uniform white field is televised and a small black area inserted, the level of the picture changes enormously, resulting in the so-called "Wimbledon effect."

3. Improved Operation of Image Iconoscope Tubes

The analysis given in the preceding section has shown that modifications in the operation and design of image iconoscope tubes are necessary in order to overcome edge flare, shading signals and the absence of true black level information.

Edge flare can be reduced by the "rim and back lighting technique" which is used on iconoscopes in telecine equipment in the U.S.A.[5,6] The improvement in this case is mainly due to electrons, released by the illumination of the mosaic rim, replacing the deficiency of redistribution in the region where scanning ends. In the case of the image iconoscope, this principle could be made to work if the storage plate was photo-sensitized. However, the desired electron source close to the edges could be more practically provided by the scanning beam itself if operated in a suitable manner,[7] the beam being made to continue scanning beyond the edge corresponding to the actual end of the picture as determined by amplifier blanking. This can be done by delaying the camera frame synchronizing pulse and reducing the camera blanking time. During this overscan period the beam current can be increased by a suitable pulse generating appreciable redistribution of secondaries which fall into the bottom area of the picture. To avoid the limitation imposed by the current balance of an insulator, the area scanned in this interval should be made conductive and connected to a suitable bias voltage. Obviously this scheme is more efficient if the fly-back time of the raster is kept as short as possible. Such a system, although somewhat complicated, does reduce edge flare.

The discovery of "back lighting" in iconoscopes,[8,9] which increases the useful signal with a reduction in shading signals, was more or less accidental and explanations of the reason for the improvement have been vague. According to our investigations, the following explanation seems to be satisfactory: that electrons are released from the always slightly photo-sensitive wall coating and are attracted by the more positive areas of the mosaic, thereby reducing the shading signals.

143

The principle of the rim and back lighting technique, now that it is more clearly understood, shows the manner in which the major faults of high-velocity electron-scanned tubes can be eliminated. It follows directly from the analysis given in the preceding section that the addition of an electron charge to those areas of the storage surface with electron deficiency, must result in an improved charge condition over the entire surface. Moreover, an addition of further electrons on all parts of the surface will result in greater efficiency of both picture charge pattern formation and signal generation. The mean surface potential is shifted negatively with respect to the collector, and therefore, more secondary electrons per primary electron can leave from all parts of the surface and the redistribution with all its disadvantages is correspondingly reduced. The current balance is maintained by the external supply of electrons which also form the necessary charge layer into which the picture pattern is impressed. To maintain the improved operating condition, additional charge must be supplied to every frame period, either in the form of a burst of electrons during the blanking time—which is a suitable method for film transmission with "memory scanning"[10]—or continuously for normal storage operation.

A continuous replacement can be achieved by flooding the storage surface with a diffuse rain of low-velocity electrons which do not produce any appreciable secondary emission. There have been many proposals in the past to incorporate such an irradiation in an iconoscope, one of the earliest[11] being shown in Fig. 6a. Here an additional neck, containing a thermionic cathode and an accelerating grid electrode, is sealed in the glass envelope, the neck being inclined obliquely towards the mosaic surface. There was no practical success with such an arrangement, many worse spurious signals being introduced. Proposals to replace the thermionic cathode by a photo-cathode which is illuminated through a suitably shaded transparency, and the emission from which is imaged on to the storage surface,[12] could not eliminate the fundamental limitations due to the use of an electron source of small dimensions relative to, and offset from, the storage plate. Neither is there anything better known of the more elegant proposal[13] to employ a symmetrical electron source consisting of a rectangular frame of four filaments with slot electrodes.
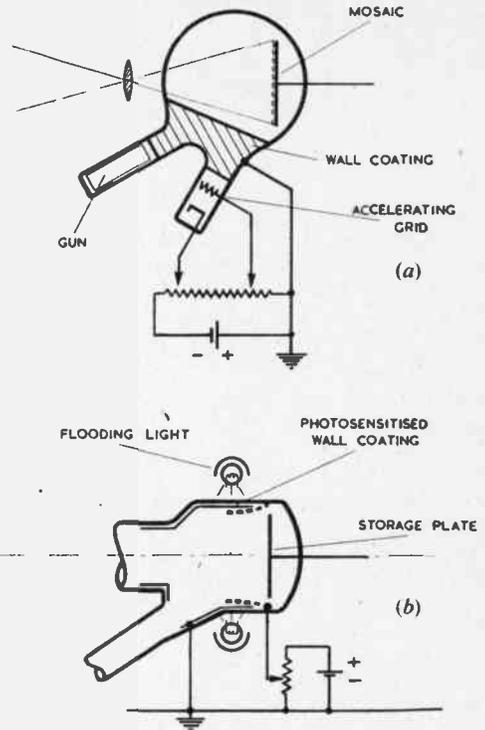

Fig. 6.—*Arrangements to irradiate the storage surface with low-velocity electrons.*

Investigations were carried out in our own laboratories to obtain improved results with Photicon tubes by introducing a potential shift of the storage surface using a flood of low velocity electrons, and it was soon realized that one of the reasons why many previous attempts, described for iconoscopes, had achieved little success was the fact that the irradiation was too local in origin and direction. It was found that a more diffuse irradiation could be obtained by using a large-area semi-transparent photocathode, suitably illuminated, surrounding the storage plate, with a suitable accelerator in the form of a mesh electrode as shown in Fig. 6b.[14] The electrons released are accelerated into the space in front of the storage surface by a potential applied between the grid and the emitting surface. The electrons land on the storage surface causing the required negative drift of the surface potential to a limiting value decided by the accelerating potential, initial electron velocity, and the angle of incidence to the

144

storage plate. Using an extended photo-surface as an electron source, a fairly uniform surface potential shift could be obtained.

The control of illumination governs the quantity of electrons available for the surface irradiation. If the irradiating current density is too high, no appreciable picture charge pattern can develop, since the photo-current will be comparatively small and the surface potential will be determined mainly by the irradiation. The density of the irradiation should rather be so adjusted as to enable the areas corresponding to the brightest parts of the picture to approach the equilibrium potential. The arrangement in Fig. 6b, when adjusted to this optimum compromise, gave promising results in reduction of shading and provides the signal with a constant black level reference, but edge flare was still evident. It was then realized that a satisfactory solution in all respects could be achieved only if the irradiation was made non-uniform: in fact a reciprocal of the non-uniform surface potential produced by the beam redistribution. Such an arrangement[14] is incorporated in the P.E.S. Photicon now to be described.

4. Construction and Operation of the P.E.S. Photicon

The main feature of this new tube is the provision of two strip electrodes mounted parallel and close to those edges of the storage surface where the scanning motion ends. To avoid an increase in the tube output capacity, these electrodes do not overlap the signal plate and are spaced a few millimetres from the storage surface, as shown in Figs. 7 and 8. These electrodes replace the accelerating grid used in the previous construction (Fig. 6b). The tube has a large-area semi-transparent photo-cathode surrounding the storage plate and extending to the shoulder of the glass envelope. The strip electrodes are connected to leads brought out through the glass wall of the bulb and are connected to adjustable positive potentials in the order of a few volts, whereby an asymmetric electrostatic field is established relative to the photo-sensitive wall coating. Electrons, released by suitably illuminating this photo-surface, are attracted towards the strip electrodes, filling the areas of the storage surface adjacent to them. As the strips are mounted close to those areas deficient in beam redistribution, the equalization of the storage surface charge can now be achieved. In addition, the asymmetrical field
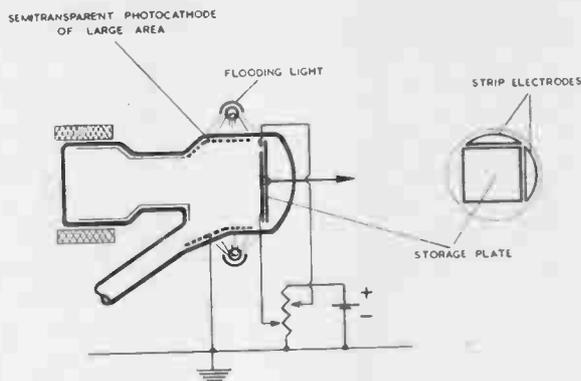

Fig. 7.— Diagram of the P.E.S. Photicon.

Fig. 8.— Photographs showing the P.E.S. Photicon and the storage plate assembly.

produces some second-order effects supporting the equalization, since the tendency of the secondaries to migrate against the beam motion is to some extent lessened, and the positive strip, acting as a part of the collector, improves collection efficiency along the bottom of the picture.

The surface potential is now stabilized by the combined action of the secondary electron redistribution and the low-velocity electron flood. Considering the case of scanning a black field with no picture photo-electron bombardment, it will be seen that the entire storage surface stabilizes to a slightly negative value relative to
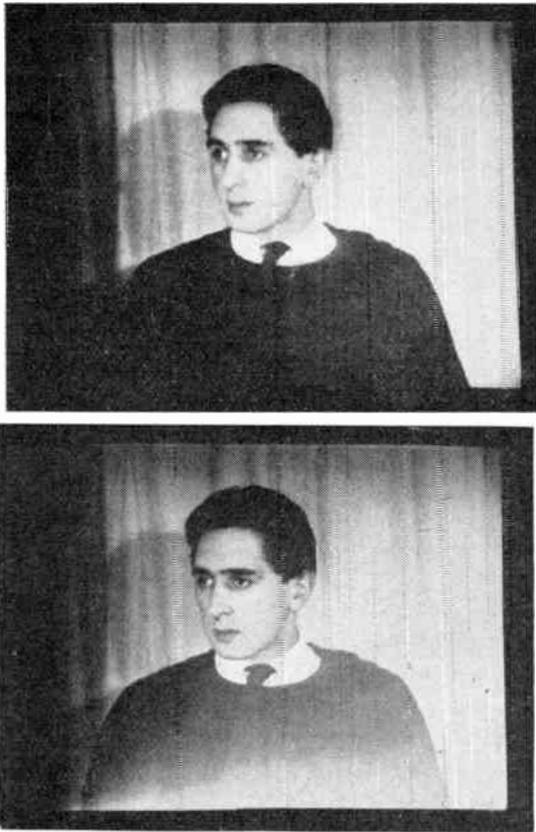
145

Fig. 9.—Pictures taken with a Photicon with and without the application of the described bias technique.

the collector. The analysis has shown that the beam redistribution provides a copious electron charge over the top part of the frame. This area, being already stabilized negatively, requires no electrons from the auxiliary photo-cathode if the beam current and the associated secondary electron redistribution is strong enough. If this is not the case, then additional electrons from the flood land until the surface is charged to a slightly negative potential.

The bottom area of the storage surface is mainly stabilized by the low-velocity electron rain which fills those parts normally lacking electrons. It is quite possible, by a suitable adjustment of the strip potentials, to obtain enough, or even a surplus, of charge in the area scanned by the last lines of the frame. The edge flare is thus eliminated and pictures with dark

146

areas at the bottom are faithfully reproduced, as illustrated in Fig. 9, where television pictures are shown photographed with and without the application of the new storage surface biasing technique under operating conditions identical in all other respects.

It is now clear that, in the absence of light on the picture photo-cathode, the surface potential will eventually stabilize to a uniform negative level because of the electrons released by the continuously emitting auxiliary photo-surface. The storage surface can therefore be said to be "photo-electron stabilized" (abbreviated P.E.S.).

Analysing the output waveforms of the new tube we see that in Fig. 10a, unlike Fig. 3, a black field now has a uniform level. The scanning beam tends to establish the positive equilibrium potential whilst discharging the surface, and on the average more secondaries leave the storage surface than arrive at any point in the path of the scanning beam. The signal plate current component resulting from the beam electron bombardment is now constant, not fluctuating or changing in polarity as in Fig. 3, but unidirectional to the level which is present during the blanking periods. As the flooding current is a counterbalance, the overall equilibrium for one complete scanning cycle has no longer to be maintained by the beam current alone. Since all parts of the storage surface are stabilized approximately to the same potential, the signal output is substantially free from spurious signals.

When a scene is televised, those areas of the storage surface corresponding to the bright parts of the picture are prevented from assuming the full negative charge level, since they lose charge by secondary emission. There are two competing forces which influence the surface potential of an illuminated picture point; on the one hand the stabilization towards the negative limit determined by the redistribution and flooding, and on the other hand stabilization towards the positive equilibrium potential of secondary emission if picture photo-electrons are present. As the flooding source and beam redistribution are fixed, the resulting potential of each picture element is dependent on the local brightness in the scene.

The beam, while exploring the storage surface, is presented with a charge layer modulated with the picture content. By the scanning action each element is returned to the positive equilibrium
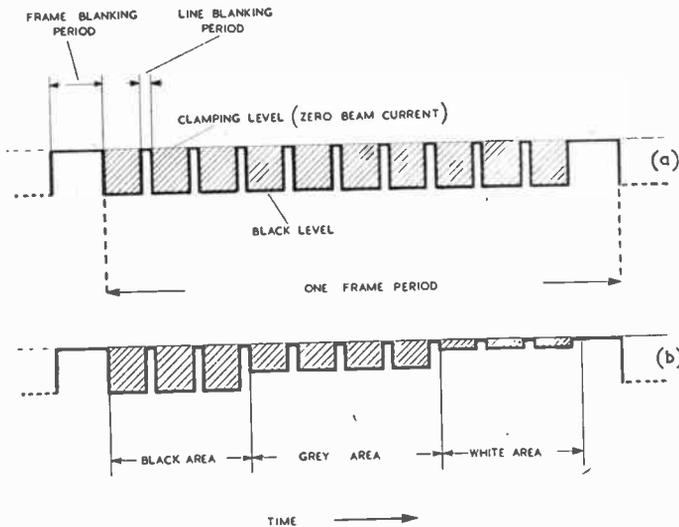
Fig. 10.—*Diagram of the P.E.S. Photicon output signal waveform after clamping on the same time base as Fig. 3, televising a black frame (a) and a frame of three tones (b).*

potential. The greater the predischarge by the picture photo-electrons, the smaller is the residual level to be discharged to equilibrium under scanning and, therefore, the signal output current, related to the zero beam current level (the clamping level), is inversely dependent on the scene brightness, as illustrated in Fig. 10*b* for the three examples of black, grey and white areas. If sufficient electrons are supplied from the auxiliary source, such that even for a peak white area, the storage surface is not completely discharged, then the signal after clamping is unidirectional to the interline pulse and the peak values of the signal current, which correspond to "black," have a constant relationship to this level and are independent of the picture content. Clamping to the interline level, therefore, faithfully reproduces the average brightness of the scene in a camera chain using the P.E.S. Photicon, and the d.c. restorer shown in Fig. 5 is no longer necessary.

The constancy of the black level can be seen in the oscillograms (Fig. 11), which show the line waveforms at the output of the camera preamplifier, generated by scanning a white vertical bar on a black field, with and without the application of the bias technique, for different degrees of scene illumination. The output waveform for no illumination (Fig. 11*a*) is quite in accordance with the sketch Fig. 10*a*. As the

light is increased (*b-d*), the picture is developed from this uniform black level in the direction of the interline pulse, but the amplitude of "black" to interline pulse remains constant. The oscillograms illustrate also the reduction in spurious signals, as all the scanned lines have substantially the same wave shape, and the resulting television picture (*e*) is free from the usual shading in the dark background. The same series of pictures taken with the bias lights and strip potentials switched off is shown in Fig. 11 (*f-k*). Comparison of the two groups shows the improvement obtained in practice with the new tube.

The fact that the interline level corresponds to white (or whiter than peak white of the picture) and not to black is inconvenient, and necessitates constancy of beam current and electron flood. Experience has shown that this constancy can be reasonably well maintained and it is not considered to be a serious disadvantage. A possible alternative to this arrangement has been adopted on a Tele-Cine equipment. A strip of black material has been placed down the side of the photo-cathode to ensure a definite "black" signal at the start of each line. The clamp circuit then operates on this signal. Reference to Fig. 11 shows that clamping to a "black" signal is perfectly satisfactory in the P.E.S. tube.

There are two difficulties here: the black signal must occur during the blanking time prescribed by the system standards and when a long camera cable is used very little time is available for scanning this inserted black; also there is a slight relative movement of the photo-electron image and the scanning beam on the storage surface, due to the changing influence of the earth's field when panning or tilting the camera.

In the course of the development of the P.E.S. Photicon an arrangement was tried combining the asymmetrical electrode configuration (Fig. 7) with a common symmetrical accelerator close to the photo-surface (as indicated in Fig. 6*b*), in order to obtain greater potential shift over the entire storage surface. Although it is possible to achieve higher efficiency of signal generation, the picture quality is then deteriorated by second-order effects. Among these are chromatic
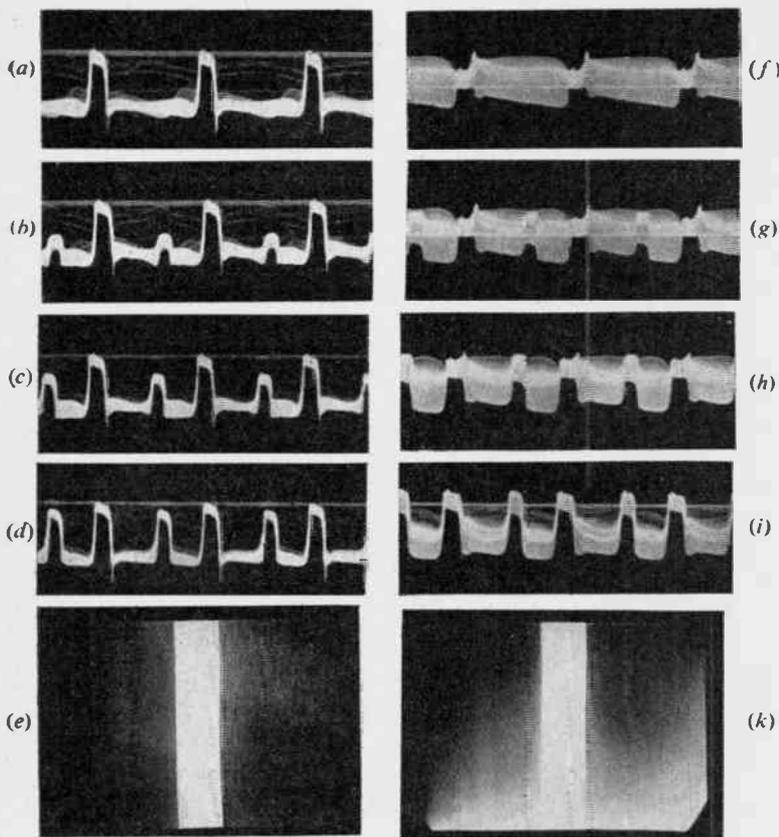
147

Fig. 11.—Oscillograms of the Photicon output signal and television pictures scanning a vertical white bar on a black field:
(a) - (d) line oscillograms obtained under bias operation with increasing scene brightness.
(e) resulting picture at the same light level as (d).
(f) - (k) corresponding to (a)-(k) with bias technique switched off.

photo-surface. The tube can therefore be produced by conventional methods without too much difficulty.

With the moderate degree of potential shift adopted, the shape of the tube transfer characteristic is not appreciably changed and the excellent half-tone rendition is maintained. Measurements taken with and without the application of the bias technique are displayed in Fig. 12. The peak-to-peak signal amplitude is plotted against the average photo-current, while televising a test pattern of vertical black-and-white bars, for two values of beam current. The left-hand column refers to the improved mode of operation. No appreciable change in the signal amplitude or in the shape of the curve is noticeable at high (or somewhat lower operating) values of beam current. With low beam current, where the redistribution is insufficient to develop a strong picture charge pattern, the slope of the curve is considerably increased for low light levels.

At optimum operating conditions, the tube sensitivity is of the same order as the normal Photicon, but since the limitation for low light level operation is normally the appearance of edge flare and shading signals, and not the noise level of the preamplifier input circuit, there is an effective gain in sensitivity.

aberrations in the focusing of the beam and image electrons, effects due to excessive transverse fields in the potential profile developed by the picture, spurious signals due to local differences in the secondary yield and non-uniformities in the irradiation. It is also probable that gamma correction would be necessary in order to obtain a satisfactory overall light transfer characteristic. The optimum compromise, therefore, is the use of a moderate potential shift as the typical faults of normal operation can then be considerably reduced without introducing new difficulties. The example of the P.E.S. Photicon shows that this compromise can be achieved with a simple electrode construction and a homogeneous

The simple arrangement of two biased strips in conjunction with the electron-emitting wall coating compensates the major effects due to the non-uniform redistribution of secondary electrons. By the addition of more electrodes the accuracy of this compensation can be increased, for example, if suitably biased strips are provided along the remaining edges of the storage plate. However, the two-strip construction has proved to be satisfactory in practice as the residual non-uniformity of the black level (Fig. 11) is small and constant in nature; thus preset shading correction can, if necessary, be used to equalize the background.
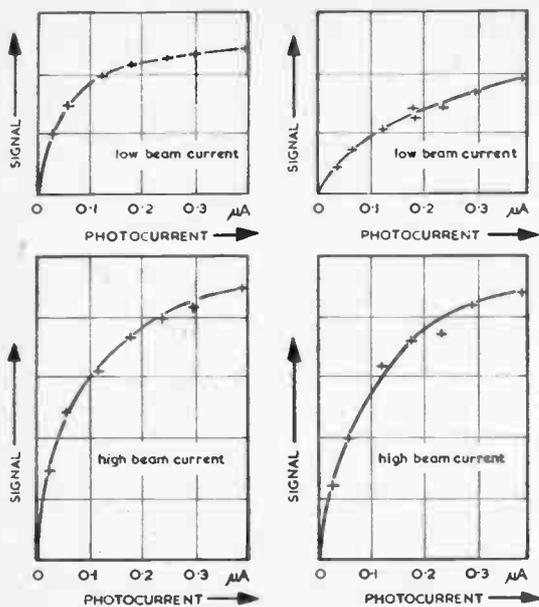
Fig. 12.—Signal output as a function of scene brightness (photo-current) with and without bias technique, televising a pattern of vertical black-and-white strips.

It is possible to obtain the necessary non-uniform low-velocity irradiation by other asymmetric electrode configurations and electron sources.[14] The electron flood, for example, can be produced by extended filament arrangements or by secondary electrons released from high-velocity electron bombardment of the wall coating (not necessarily photo-sensitive in this case), the bombarding electrons originating from an illuminated frame surrounding the picture area on the photo-cathode. All these alternatives possess advantages and disadvantages, but practical experience has led us to adopt the present scheme which has been incorporated in an improved Photicon camera chain and is now being used by the B.B.C.

5. Acknowledgments

6. References

1. Trade mark for an image iconoscope type camera tube, manufactured by Cathodeon, Ltd., Cambridge.

2. McGee, J. D., Lubszynski, H. G. "E.M.I.-Cathode Ray Television Tubes." *J. Instn Elec. Engrs*, **84**, April 1937, pp. 468-475.

3. Iams, H., Morton, G. A., Zworykin, V. K. "The Image Iconoscope." *Proc. Inst. Radio Engrs*, **27**, Sept. 1939, pp. 541-547.

4. Townsend, C. L. "The Clamp Circuit." *Broad. Engrs J.*, 1947, January (Part I) and April (Part II).

5. Schade, O. H.: U.S. Patent No. 2,368,884, issued February 6th, 1945. (British Patent No. 569,436).

6. Helt, Scott. "Practical Television Engineering." pp. 188-190. (Murray Hill Books Inc., New York, N.Y., 1950).

7. Cope, J. E., McGhee, H. A., Theile, R., Pye, Ltd.: British Patent Application No. 29931/50.

8. Percival, W. S., Browne, C. O., Johnson, L. R. J., Blythen, F.: British Patent No. 490,845, accepted August 22nd, 1938.

9. Janes, R. B., and Hickok, W. H. "Recent Improvements in the Design and Characteristics of the Iconoscope." *Proc. Inst. Radio Engrs*, **27**, Sept. 1939, pp. 535-540.

10. Theile, R. and Townsend, F. H. "Improvements in Image Iconoscopes by Pulsed Biasing the Storage Surface." *Proc. Inst. Radio Engrs*, to be published.

11. Vance, A. W., and Branson, H.: U.S. Patent No. 2,147,760, issued February 21st, 1939. (British Patent No. 434,942.)

12. Hergenröther, R. C.: U.S. Patent No. 2,242,952, issued May 20th, 1941.

13. Pierce, J. R.: U.S. Patent No. 2,324,534, issued July 20th, 1943.

14. Patent applications, Pye, Ltd., Cambridge.

149

LINE SCANNING VALVES AND CIRCUITS*

by

B. Eastwood, B.Sc.† and C. C. Vodden, M.Sc.†

A Paper presented at the Second Session of the 1951 *Radio Convention on July 6th
at University College, London.*

SUMMARY

The post-war trend towards higher operating voltages and wider scanning angles in cathode ray tube design has necessitated the development of high efficiency scanning circuits in order that the advantages of these tubes may be realized without unduly high power consumption. This economy has been effected by making use of the resonant return type of time base which recovers a part of the energy stored in the deflection field at the end of each line.

This paper discusses the requirements of scanning valves arising from these circuits. Generally speaking, pentodes have to withstand high anode voltages for a fraction of the cycle with the cathode current off, and thermionic emission from the screen must be kept at a low value under these conditions. This has been achieved by designing the valve so that the screen runs cool (i.e. aligned grids) and also by previous treatment of the screen coupled with suitable processing. Diodes have to withstand a high inverse peak voltage and should have a low forward impedance.

The voltage requirements are not completely new but these are mass produced valves intended for commercial sets, whereas previously such valves were regarded as special low production types. Insulation properties of mica have been investigated under these conditions, and valves using all mica insulation have been rated at 6 kV (design centre) on the anode.

1. Introduction

In comparing the design of present-day television receivers with those in use before 1939, one of the more striking differences is the increase of final anode voltage of the cathode ray tube from around 4,000 or 5,000 V to as high as 13,000 V, whilst at the same time scanning angles have increased from a maximum of 55 deg. to 70 deg. at the present time. This latter change has been more pronounced in American designs than in European.

These changes may be said to have compared roughly to the following pattern. A desire to increase working voltage in order to improve picture brightness soon showed the economic limitations of the scanning methods generally in use before the war, and considerable effort was directed towards the development of high-efficiency scanning circuits. The basic principles of these circuits had been known before 1939,[1,2] but the high loss core materials then in use prevented the achievement of a high enough

power economy to justify the extra cost of components. When improved powdered iron and finally ferrite core materials became available, the full capabilities of these circuits began to be realized in practice.[3,4,5] New valves were developed to exploit to the full the capabilities of the new materials, and with the enormously increased scanning powers now made available, some moves could be made to meet the set designer's persistent cry for a reduction in bulk of the cathode ray tube. This was done by increasing the scanning angle, culminating in recent reports of a proposed 90 deg. tube from the United States.

In this paper it is proposed to review the fundamental principles of operation of scanning methods now in use in commercial receivers, and examine the demands which they make upon the valve designer and to show how valves are designed to meet these demands.

2. The Basic Line-Scanning Circuit

All electromagnetic line-scanning circuits represent an attempt to approximate to the working of the ideal circuit in Fig. 1a, whose operation has been well described on many occasions, notably by O. H. Schade.[4]
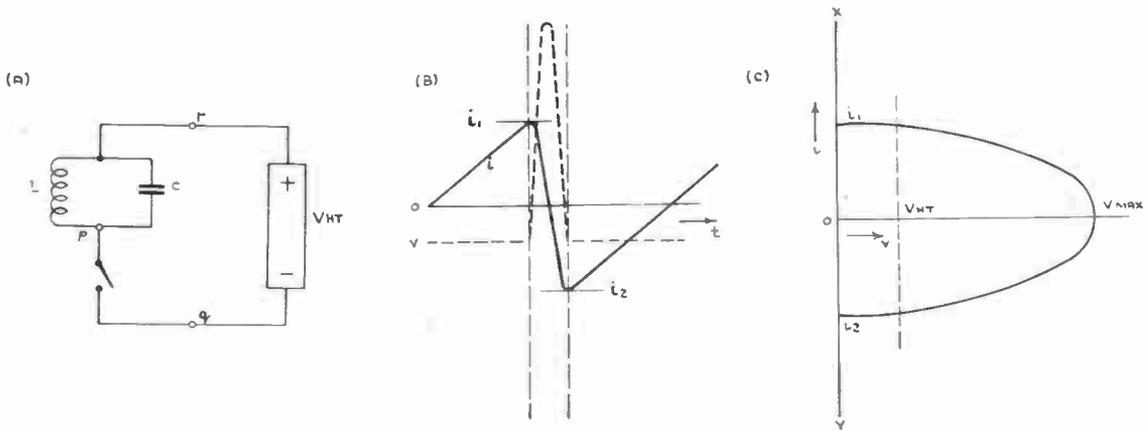
Fig. 1.—*The basic scanning circuit.*

Closing of the switch causes current to be built up linearly in L to a value i_1. The switch is now opened allowing a free oscillation between L and C when the energy of the peak current $\frac{1}{2} L i_1^2$ is converted, first into a high peak of voltage across C of energy $\frac{1}{2} C V^2_{max}$ and then into a negative peak of current i_2 of energy $\frac{1}{2} L i_2^2$. Shortly after this negative peak comes a moment when the voltage on the capacitor is exactly equal to that of the battery, and the rate of change of current is equal to that during the establishment of i_1. At this moment the switch is again closed and the negative current collapses linearly to zero, recharging the battery in doing so.

Figure 1b shows the current through L and the voltage of point p with respect to point r plotted against time. Fig. 1c represents a form of plotting which is of great value in practical circuits since it enables us to examine the coil current and voltage in relation to the current-voltage characteristic of the switch. As horizontal axis we take the voltage of point p with respect to point q and as vertical axis the current through L. Thus XOY represents the voltage-current characteristic of the switch (zero resistance in both directions) and the curve $i_1 V_{max} i_2$ represents the locus of coil voltage and current during the fly-back interval when the switch is open.

3. Practical Line-Scanning Circuits

In this light let us now examine the operation of the circuit of Fig. 2a, which was probably the most widely used before 1939. In this case the circuit is so heavily damped that the negative peak of current practically disappears and consequently there is no need for the switch to be
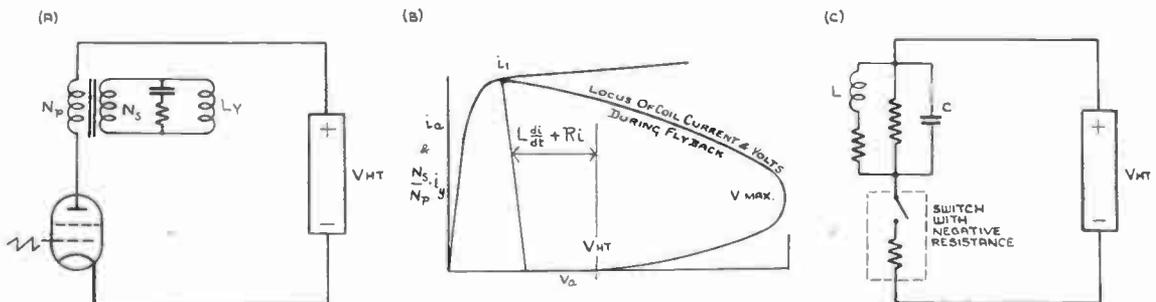

Fig. 2.—*Heavily damped scanning with no energy recovery. Saw-tooth grid drive.*
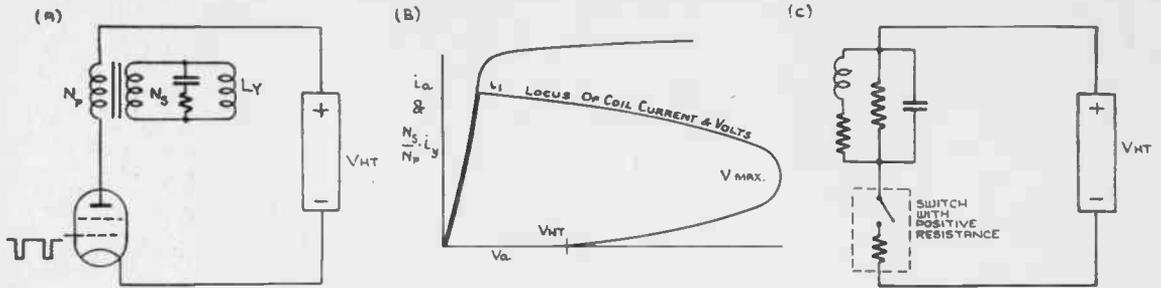
Fig. 3.—Heavily damped scanning with no energy recovery. Square pulse grid drive.

capable of carrying current in the reverse direction. The switch accordingly takes the form of a pentode or beam tetrode.

In order to establish a linear rising sawtooth of current in an inductance with finite resistance, the volts across that inductance must be the sum of a constant reactive component and a linearly rising resistive component. This can be achieved by applying a suitably shaped sawtooth between grid and cathode when the load line during scan

Fig. 4.—Parallel power feedback.

becomes that shown in Fig. 2b. This shows the voltage across the load to be a constant plus the rising resistive component which we require for linearity. This left-hand sloping load line during scan represents the voltage–current characteristic of the switch and shows the valve to be behaving as a switch with negative resistance.

This circuit has also been operated using as grid drive a positive-going square pulse of duration equal to the modulation time of the television signal, often generated by self oscillation. The current–voltage characteristic of the switch now becomes the front of the knee of the pentode which has a positive resistance. If no steps are taken to remedy the defect, the linearity will, in consequence, suffer since the voltage across the load inductance is decreasing with time. An improvement can be effected by including in series with the load inductance a small saturating inductance whose value decreases with increase of current. In the circuits of Figs. 2 and 3, the pentode is called upon to provide the entire current swing with a peak to mean current ratio of about $2 \cdot 3 : 1$.
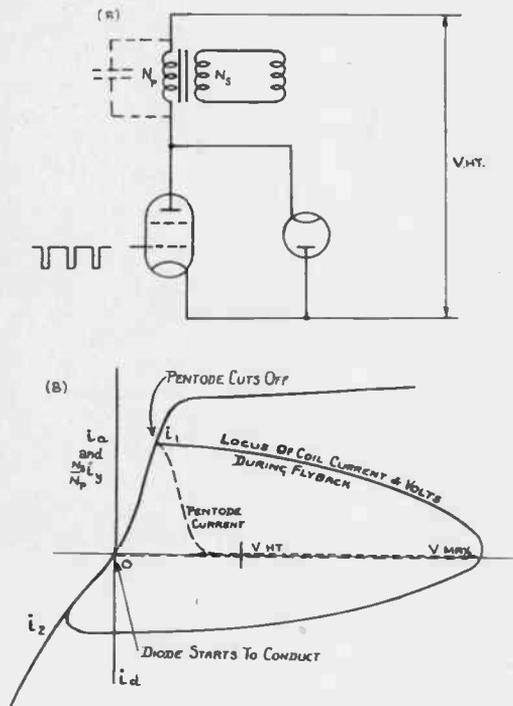
3.1. Parallel Power Feedback

A direct attempt to approximate to the working of the basic circuit of Fig. 1 takes the form shown in Fig. 4a, and if the grid is driven with a positive pulse as in Fig. 3, the combined switch characteristic becomes that of Fig. 4b with the front of the pentode knee and the diode providing the bi-directional conductivity. The negative peak of current is established in the diode through which the almost linear collapse takes place until the pentode again takes over and the diode becomes non-conducting. The pentode no longer has to provide the full peak-to-peak current swing and the power economy is

realized as a reduction in mean current drain from the H.T. supply. The peak-to-mean anode current ratio may now be as high as $3\cdot5:1$ in a practical circuit. This is the case of parallel power feedback.

3.2. *Series Power Feedback*

Imagine now that the diode is transferred to a tertiary winding (this may or may not coincide with the yoke winding), and a biasing battery is connected in series with the diode (Fig. 5a);
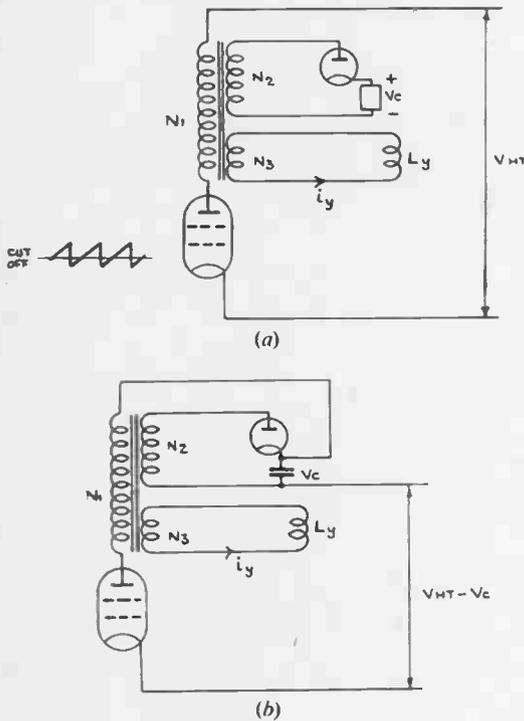

(a)

(b)

Fig. 5.—*Series power feedback basic circuit.*

the saw-tooth grid drive is arranged so that the pentode conducts a chopped saw-tooth of current. Imagine the coil and transformer resistances to be zero but core losses to be finite during the fly-back oscillation so that we have an oscillatory circuit of finite Q. Viewed from the primary the load appears as an inductance L_t and in this the pentode establishes linearly a peak current i_1. The diode is so biased that it is just cut off during this period. This peak current represents a stored energy $\frac{1}{2} L_t i_1^2 = E_o$. During fly-back the pentode is cut off and the circuit

executes the first half cycle of a damped cosine oscillation. This establishes a negative peak of current $i_2 = -i_1 e^{-\pi/2Q}$ representing a stored energy $E_o e^{-\pi/Q}$. The diode with its battery bias now causes the transformer flux (and hence the coil current) to collapse linearly and this energy charges up the battery. The pentode is now brought into conduction again. Hence the mean rate of supply of energy to the primary is $E_o f_H$ where f_H is the line frequency and the mean rate of supply of energy to the battery is $E_o f_H e^{-\pi/Q}$. These energy transfers will take place at the same mean current if the following condition is satisfied:

$$\frac{\text{Primary volts during scan (constant)}}{\text{Battery voltage (constant)}} = e^{\pi/Q}$$

and for this to be true we must have:

$$\frac{N_1}{N_2} = e^{\pi/Q}$$

If these conditions are fulfilled the battery may be replaced by a large capacitor (Fig. 5b) and placed in series with the normal H.T. supply which may now be reduced by an appropriate amount, thus reducing the power requirements of the stage. This is the condition of series power feedback and it will be seen that correct choice of diode winding to primary winding ratio is of first importance.

In practice the presence of finite resistance in the coils and diode prevents this operation being achieved and the characteristic of the combined diode-pentode switch is as shown in Fig. 6a where the equivalent diode characteristic is shown transferred to the primary (diode characteristic 1). As before, the current peak i_2 is established in the diode at the end of fly-back, but to maintain the total left-hand sloping load line $i_1 . i_2$ the diode and pentode currents must increase together. The peak current i_1' which the pentode must supply is now higher than the i_1 of the theoretical no-resistance case for $0i_1' = 0i_1 + 0i_2'$. Plotted on a time scale the currents are as shown in Fig. 6b.

This brings out the fundamental requirements for series power feedback provided that no extra external drain is taken from the boosted H.T. supply:

(a) Mean diode current and mean pentode current must be equal.

(b) The combined pentode current and transferred diode current must together give a linear current.
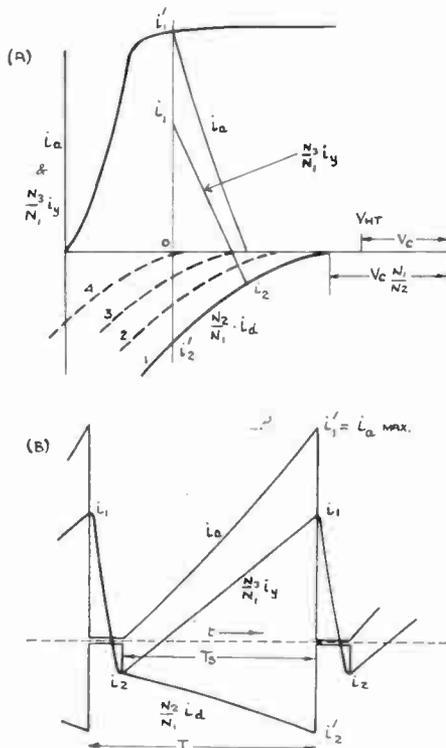
Fig. 6.—Relationship between diode current and pentode current in circuit of Fig. 5(b) when scanning coils have finite resistance and no correcting voltage is applied to the diode cathode.

From these conditions we may derive the following general relationship for diode to pentode winding ratio of which the previous relationship represents a particular ideal case.

Let $i_a = f(t)$ and $i_d = G(t)$

Then expressing the fact that mean currents must be equal:

$$\frac{1}{\tau}\int_0^{\tau_s} f(t)\,dt + \frac{1}{\tau}\int_0^{\tau_s} G(t)\,dt = 0 \ \ldots \ldots (1)$$

The transferred peak-to-peak coil current is:

$$i_1(1 + e^{-\pi/2Q}) = 2\,i_{y\,max}\,.\,\frac{N_3}{N_1} \ \ldots (2)$$

Here we assume that there is no appreciable shorting of the yoke by transformer inductance. So we may express the fact that pentode current and transferred diode current must together give a linear current by

154

From these conditions we may derive the following general relationship for diode to

$$f(t) + \frac{N_2}{N_1}\,.\,G(t) = i_1 - \frac{i_1}{\tau_s}\,.\,(\tau_s - t)(1 + e^{\pi/2 - Q})$$
$$\ldots \ldots \ldots \ldots (3)$$

Integrating (3) between the limits 0 and τ_s

$$\int_0^{\tau_s} f(t)\,dt + \frac{N_2}{N}\int_0^{\tau_s} G(t)\,dt = \frac{1}{2}\,i_{1s}\,\tau(1 - e^{-\pi/2Q})$$
$$\ldots \ldots \ldots \ldots (4)$$

and from (1)

$$\left(1 - \frac{N_2}{N_1}\right)\int_0^{\tau_s} f(t)\,dt = \frac{1}{2}\,i_1\tau_s(1 - e^{-\pi/2Q})\,..(5)$$

but $\dfrac{1}{\tau}\displaystyle\int_0^{\tau_s} f(t)\,dt = I_a$, the mean pentode anode current, so

$$1 - \frac{N_2}{N_1} = \frac{1}{2}\,.\,\frac{i_1}{I_a}\,.\,\frac{\tau_s}{\tau}\,.\,(1 - e^{-\pi/2Q})\ldots(6)$$

This could also be put in terms of the peak-to-peak coil current $2i_{y\,max}$

$$1 - \frac{N_2}{N_1} = \frac{i_{y\,max}}{I_a}\,.\,\frac{N_3}{N_1}\,.\,\frac{\tau_s}{\tau}\,.\,\frac{(1 - e^{-\pi/2Q})}{(1 + e^{-\pi/2Q})}\,.\,(7)$$

From this we see that in practice, besides depending on the Q of the system the diode winding ratio depends on the mode of the operation of the stage which determines the mean anode current for any particular value of transferred peak-to-peak coil current. In any mode of operation where diode current decreases to zero with time during scan, i_1 becomes equal to peak pentode anode current $i_{a\,max}$ and

$$1 - \frac{N_2}{N_1} = \frac{1}{2}\,.\,\frac{i_{a\,max}}{I_a}\,.\,\frac{\tau_s}{\tau}\,(1 - e^{-\pi/2Q})\ \ldots(8)$$

where N_2/N_1 depends on Q and peak-to-mean anode current ratio.

We may now examine the remaining modes of operation of this circuit. The case with saw-tooth drive and steady d.c. bias on the diode has been described (Fig. 6a), but this may be modified to approximate to the ideal zero resistance case by the introduction of a suitable ripple voltage on the diode bias capacitor. This has the effect of moving the diode characteristic successively through the positions 1 to 4 of Fig. 6a at the correct rate as scan progresses.[4] With care the pentode can be made to take over almost exactly when the diode current becomes
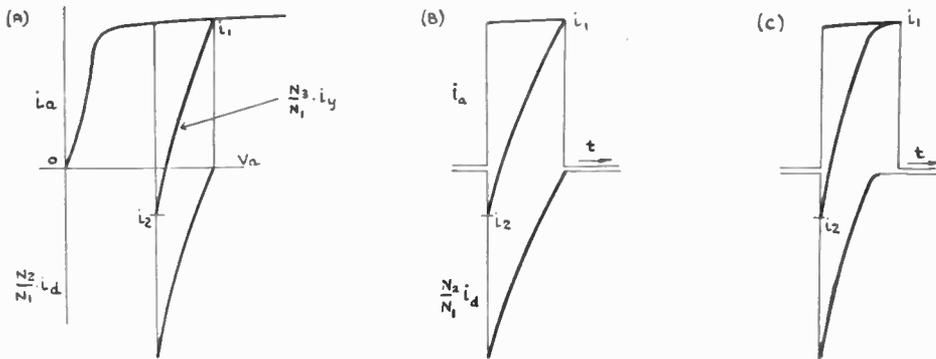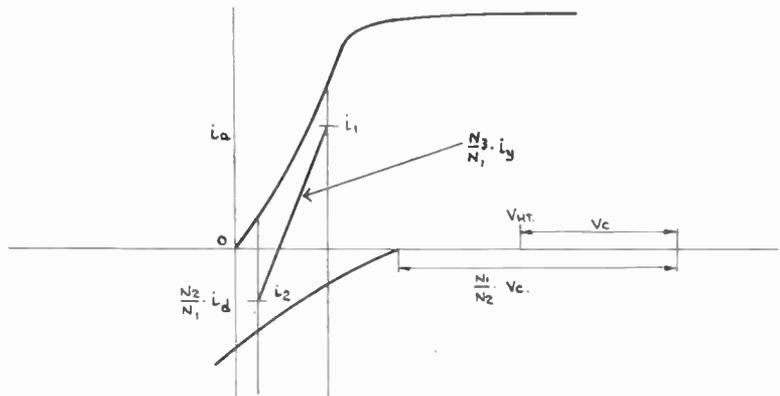
Fig. 7.—*Relationship between diode current and pentode current for series power feedback when grid drive is square pulse.*

zero, but generally some considerable overlap is allowed to take place.

If, on the other hand, the control grid in Fig. 5b is fed with a positive-going square pulse of duration equal to the television modulation period, the operation will in general be of the form shown in Fig. 7 with a right-hand sloping load line. Linearity is determined in this case entirely by the coil and diode resistances. Fig. 7b shows the currents plotted on a time scale. If we regard the pulse of anode current as flat-topped, the general formula for diode winding ratio indicates

$$\frac{N_2}{N_1} = \frac{1}{2}(1 + e^{-\pi/2Q}) \quad \ldots\ldots(9)$$

Fig. 8.—*Series power feedback with square pulse grid drive when load inductance and current swing have been adjusted to move anode voltage during scan below the pentode knee.*

voltage. By adjustment of these factors the working anode voltage can be moved nearer the knee until we reach the condition of Fig. 8a. This will require a further slight adjustment of N_2/N_1 since the shape of the anode current pulse has been altered.

In all modes of operation the elements of the switch, i.e. the diode and pentode, have to stand high peak voltages during the cut-off period amounting to several thousand volts. Low impedance triodes have often been used in place of

for this type of operation to be achieved. If N_2/N_1 is too low we have the condition of Fig. 7c with consequent cramping on the right-hand side. The mean anode voltage Va during scan is determined by the reflected inductance load, peak-to-peak current swing and H.T. supply

diodes on account of the more easily controlled characteristics, but although these have been used in commercial receivers in the United States, their use has not found very wide favour on this side of the Atlantic on account of the high cost of these valves.

155

4. Valve Requirements

Application of the foregoing principles to practical circuits leads us to expect the pentode to have to provide mean currents up to about 100 mA, with peak-to-mean current ratios as high as 3·5 to 1. In addition, these circuits are generally used to generate the high voltage supply for the cathode ray tube by rectification of the positive pulses appearing on an overwind on the primary, so it is most important that the pentode should be capable of being completely cut off during the fly-back or the high voltage pulse will be damped. We may expect the pulse on the pentode anode to be up to about 6,000 or 7,000 V, so we require not only freedom from severe tailing of the I_a-V_g characteristic, but a good "anode-penetration" performance, i.e., there must not be too much change of the cut-off voltage as anode volts are increased. For this same reason, emission from g_2 or any other parts of the assembly (other than cathode) must also be kept low or this will damp the pulse and lower the Q of the circuit in the same way.

If the valve is to be operated in the condition of Fig. 8 the front of the knee should be kept reasonably straight and free from kinks. General requirements of linearity indicate that the knee voltage should be kept as low as possible. For square pulse operation linearity of the I_a-V_g characteristic is not important, but for saw-tooth drive, especially in the older heavily-damped scanning, reasonable linearity is required. In the interests of keeping down screen emission it advisable that the required characteristics should be provided at as low a screen voltage as possible.

4.1. Diodes

The diode has to provide a mean anode current up to about 100 mA with a peak-to-mean ratio as high as 4·5 and should be capable of standing peak inverse voltages up to about 4 or 5 kV. In this case the heater-cathode insulation is important and in a.c. sets the heater-cathode voltage may be as high as 500 V d.c., while in a.c./d.c. sets there will, in addition, be an a.c. component depending on the position in the heater chain.

The diode requirements are rendered more exacting if an auto-transformer is used. Here the diode cathode is connected directly to a point on the primary winding and consequently receives a positive pulse which may be as high as 0·7 or 0·8 of that applied to the pentode anode. If the heater is fed from the same heater line as

the rest of the receiver this means that the heater-cathode insulation has to withstand a pulse of about 4 kV and valves have been made to operate under these conditions, but circuit modifications can be made to render this unnecessary. One approach is to feed the diode heater from a small separate transformer of low capacitance and connect it to a point about halfway up the primary. This still leaves a pulse of about 1·5 kV between heater and cathode, but if care is taken to make the transformer of particularly low capacitance, the heater can be connected directly to cathode without placing too much capacitative loading on the circuit.

The other approach is to feed the diode heater from the normal heater supply, but to place in series with each lead a winding on the line transformer core which feeds the heater with a pulse equal to that applied to the cathode. These windings usually take the form of a single bifilar winding.

5. Line Scanning Pentodes or Tetrodes

Having discussed the set designer's valve requirements for these circuits we can now consider in greater detail how they can be met, bearing in mind that they are required for mass produced sets and hence should be cheap both to make and to use. Other things being equal, a set maker prefers small valves and usually the valve maker is willing to oblige him since, if a suitable design can be evolved, a small valve can be manufactured more cheaply than a large one.

In this paper several references will be made to cost. It is a very important consideration in any extra components or processes which have to be introduced. Basically cost is measured by the total labour involved, plus raw material costs and a factor depending on tools or equipment required. Thus, it is not only a measure of the price of the article as we normally think of it, but, perhaps more important to the engineer, its reciprocal is a measure of the soundness of design from the point of view of overall productivity.

For this reason, other things being equal, we would rather make the scanning valve a beam tetrode than a pentode because beam plates are cheaper to make than another grid. In some respects a line scanning valve is similar to an ordinary audio output tetrode and Fig. 9 shows a cross-section of such a valve. There are, however, certain additional features peculiar to scanning valves.

One of the important differences between normal output valves and line scanning valves is the requirement that thermionic emission from the screen should be kept low. When running, the screen becomes hot, and at maximum ratings some of the helix turns glow-red. If no precautions are taken, these turns will emit electrons. The high voltage pulse induced on the anode by cutting off cathode current and the resulting high field produced at the surface of the helix wires, enhances thermionic emission by the Schottky effect, so that very large currents can be drawn from it. This screen emission can become an appreciable fraction of the original anode current and will reduce the voltage swing.
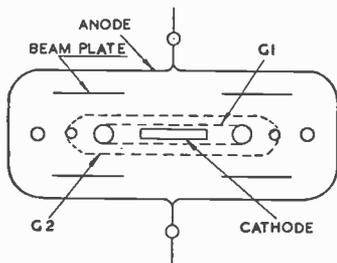

Fig. 9.—Plan of electrodes in a typical beam tetrode.

There are several obvious ways of making screen emission smaller.

(1) Reduce the field at the surface of the screen wires.

(2) Run the helix wire at a lower temperature.

(3) Treat the surface of the screen to increase its work function, and hence produce less thermionic emission.

In practice, it is not possible to do much about (1) in a tetrode as, although an increase in the helix wire size reduces the field, it also increases the available area, so on balance nothing is gained.

Screen watts should be kept low by designing the valve so that the required anode current can be obtained at the lowest possible screen voltage. It is well known that thermionic emission increases very rapidly with temperature so that screens in which the turns are non-uniformly heated will be worse for emission than when they are uniformly heated.

The best way to ensure uniform heating is to align the grids. This technique is widely used in radio valves, and consists of winding the control grid and screen grid at the same pitch, and

adjusting them such that the g_2 turns are in the electrical shadow of the g_1 turns. When the anode voltage is well above the knee, this means that the screen current ratio is low, but more important, the screen current is uniformly distributed (Figs. 10 and 11).

A further advantage of aligning grids is that it makes it possible to use larger helix wire on g_2 than would be possible otherwise for the same g_1-g_2 gap. More heat is radiated by the helix, as its area is larger and also more is conducted to the side rods.

The heat emissivity of the grid helix is greatly increased by spraying it with carbon in a suitable binder. In addition, carbonized fins are sometimes welded to the ends of the g_2 side rods. All these features can be built into a valve to reduce the temperature of the helix.

In theory, it should be a simple matter to use materials with high work functions for the helix wire to prevent emission. Unfortunately there
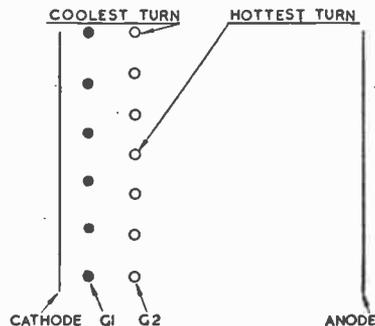

Fig. 10.—Section of a tetrode with non-aligned grids in a plane perpendicular to the helix wires.
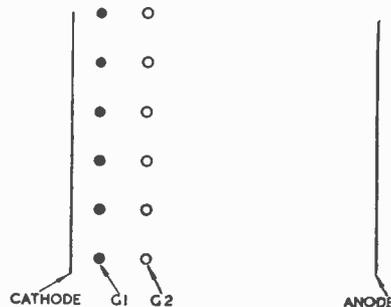

Fig. 11.—Section of a tetrode with aligned grids in a plane perpendicular to the helix wires.

are further complications because, when running at normal temperatures, barium is evaporated from oxide-coated cathodes and deposited on cooler surfaces, including, of course, the grids, which reduces their work functions. Although such a screen would have a low value of emission to start with, it would increase rapidly during running and shorten the useful life of the valve.

It was thus necessary either to find a treatment which would prevent evaporated barium from increasing thermionic emission, or to accept very low temperature ratings. It has been known for a long time that gold- or silver-plating the helix of a control grid would reduce grid emission by a large factor. It was also known, however, that at elevated temperatures which would be met on screen helix wires, such coatings tended to diffuse into the wire and it was found during trials on these surfaces that screen emission started low but rose rapidly during life. The rate of rise depended on screen temperature.

It was then found that a helix of 5 per cent. Mn–Ni coated with a layer of carbon had very low thermionic emission after being bombarded to a bright red heat in a vacuum. Not only was this emission low to begin with but it did not increase under normal running conditions. The exact mechanism of this effect is not known, but it is assumed that during bombardment manganese diffuses to the surface of the helix and combines with the carbon. When barium is deposited, further combination takes place and prevents free barium from increasing thermionic emission. It is a fortunate coincidence that carbonizing the screen has the double virtue of reducing its temperature and inhibiting emission.

From what has been said before we can see how electrical characteristics can be decided for a given receiver. The grid drive available is known, so it is possible to decide what the average cut-off voltage should be, allowing for valve and circuit variations, to ensure that every valve can be driven in all sets. The average current at $V_{g1} = 0$ can also be decided assuming similar variations. It can be seen from Fig. 13 that these two points on the I_{a1}–V_{g1} curve settle the minimum slope. Higher currents are usually required than for output valves, and to keep screen watts low they should be obtainable at low screen voltages.

It is possible to calculate the geometry but the equations are rather complicated, so it is usually

easier, and certainly more instructive for our present purpose to take an existing valve whose geometry is known and decide how it should be modified to produce the characteristics required. This can be done using some very simple formulae, and we can keep a physical picture in our minds all the time.

The most useful formula states simply that, if anode current is space charge limited and all dimensions are divided by a factor n, then the characteristics will remain the same. As the length and breadth of the cathode will each be divided by factor n, then the area will be divided by n^2. This formula is true for any geometry.

Now, for simplicity, we will deal with the case of plane electrode surfaces such as are illustrated in Fig. 9. In this case, neglecting edge effects, which is legitimate if the g_2-cathode gap is smaller than the breadth of the cathode, all space currents, i.e., I_a, I_{g2} and I_k will be normal to the emitting surface and uniformly distributed over it. It is also obvious that, in applying the scaling law mentioned in the last paragraph, only certain valve dimensions will have any effect on electrical characteristics. For plane electrodes, these are the distances between parallel planes containing the cathode coating, grid helices and anode, the grid helix wire diameter, the pitches, and also emitting area.

If the emitting area is varied but all other significant parameters mentioned above are not altered, then I_a, I_{g2} and I_k will be proportional to the coated area, assuming, of course, that this area is still covered by the electrode structure.

Hence, from the first formula, if all dimensions are divided by n, electrical characteristics will remain unchanged and the cathode area will be reduced by a factor n^2. If now the cathode area is increased by a factor n^2, but all other significant dimensions mentioned above are retained, all space currents will be multiplied by n^2. The cathode area will now be the same as it was before the valve was scaled.

These formulae can be restated simply for plane electrode surfaces as

(1) Space currents I_a, I_{g2}, I_2 are proportional to cathode area, inner mu not affected.

(2) If all valve dimensions except cathode area are divided by a factor n, then space currents I_a, I_{g2}, I_k will be multiplied by n^2. Inner mu is not affected.

158

(3) In addition to these parameter changes it is possible to change the inner mu by the approximate formula

$$\mu \propto P_2 \frac{d}{a^2} \quad \text{where}$$

$P_2 = g_1\text{-}g_2$ gap.   ($p_1 = g_1\text{-}k$ gap.)

    $d =$ control grid helix wire diameter.

    $a =$ pitch of control grid.

Variations of $g_1\text{-}k$ gap have only a second order effect on mu, but when $a > \cdot6p_1$ slope begins to fall as a increases, and it falls very rapidly when $a > 2p_1$. Slope also decreases as P_2 gets small.

Suppose, now, we take an existing valve, say an output beam tetrode; to modify its characteristics to fit Fig. 13, the inner mu can be reduced by formulae (3) until the maximum value of I_a at $V_{g1} = 0$ is reached (Fig. 12, Curve 3). Mu cannot be reduced much below 5·0 as slope drops so rapidly that I_a at $V_{g1} = 0$ actually begins to fall. (See Fig. 12, Curve 4.) V_{g2} can then be adjusted to give the correct cut-off (Fig. 13).

I_a at $V_{g1} = 0$ can then be increased to the required value by using formulae (1) and (2). There is a practical limit to the permissible reduction in size of helix wires and gaps, and there is a point where it may be better to increase the cathode area rather than scale down any further. Alternatively, it may sometimes be worth while reducing the control grid pitch to increase slope and run at a higher screen voltage. For example, curve 2 in Fig. 12 may be used. The exact course to be followed depends on individual requirements and cost.

We have mentioned before that it was desirable to use aligned grids for the reduction of screen emission. Small $g_1\text{-}g_2$ gaps and a relatively course pitch make alignment easier, so it is fortunate that the characteristics of these valves are such that these requirements can usually be met.

$I_a\text{-}V_a$ characteristics have to be adjusted by varying g_2-anode gap, which, for the same value of V_{g2}, should be inversely proportional to $I_a{}^2$. This follows from the scaling law discussed earlier. If the gap is too big, the knee voltage will be high, whereas, if it is too small, secondary emission from the anode will not be suppressed and will cause distortion. A rough anode surface
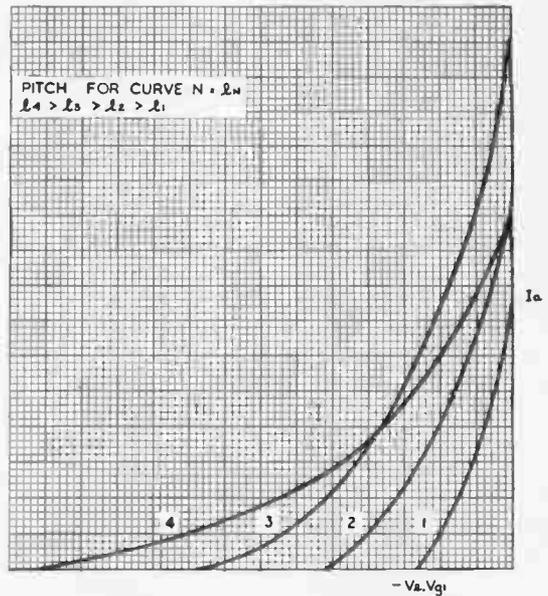

Fig. 12.—Series of curves of I_a versus V_{g1} for an aligned beam tetrode with various pitches on g_1 and g_2 keeping $V_a = V_{g2} = const.$
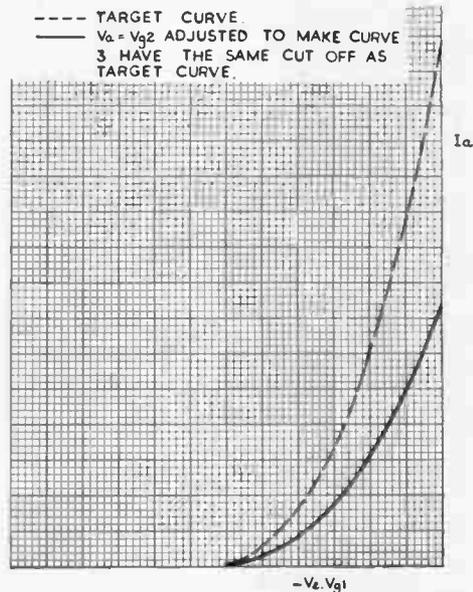

Fig. 13.—I_a versus V_{g1} curve showing the first stage in adjusting the characteristics to fit the target curve.

reduces secondary emission and makes it possible to work with smaller g_2-anode gaps.

We have seen that an additional requirement is that the anode has to withstand high voltages for a fraction of the cycle, and it has been found that mica insulation is satisfactory under these conditions for design centre ratings of 6 kV. That means that occasional valves may go up to 8 kV. High voltage valves normally use ceramic insulators, but they are very expensive to make with sufficient accuracy for this class of valve.

This problem has been solved for some high voltage valves by using mica to space the cathode, grids and beam plate. This is protected by suitably earthed shields from the high field created by the anode which is then supported separately on a ceramic insulator. Ceramics are not fundamentally expensive, unless we require high accuracy, and as the anode need not be located as accurately as the other electrodes it is possible to design a cheap ceramic.

6. Efficiency Diode

Anode voltage insulation requirements are less onerous on the efficiency diode than the scanning pentode, so mica insulation is usually adequate. The design of such a valve is similar to that of a normal power rectifier.

The problem of improving heater-cathode insulation to withstand high voltage pulses is difficult. Heaters usually consist of a tungsten or moly-tungsten alloy wire coated with a layer of alumina several thousandths of an inch thick. This runs at a much higher temperature than the cathode. If precautions are taken to avoid impurities on the coating, and there are no bare or very thin patches, heater insulation is surprisingly good under pulse conditions and could probably be rated at about 2 kV.

To improve it further, a suitable ceramic spacer has to be designed made of alumina to insulate the coated heater from the cathode tube. This spacer will run cooler than the heater coating, and hence its insulating properties will be better. Unfortunately, however, the design of this spacer is a major problem.

An American valve 6AX4GT on which this problem has been overcome has a pulse rating of 4 kV with the heater negative.

7. Conclusions

In this paper no attempt has been made to deal comprehensively with the scanning stage from the point of view of the circuit engineer, since this has been done in other papers [4,5,6,7,8], but rather to consider those features which influence the choice of valve characteristics and ratings. In practice, as we have seen, the provision of these characteristics has to be in the nature of a compromise between circuit requirements and limitations imposed on the valve designer by available materials, cost and ease of manufacture.

8. Acknowledgments

9. References and Bibliography

1. A. D. Blumlein. British Patent 400,976.
2. E. L. C. White and A. D. Blumlein. British Patent 482,370.
3. A. W. Friend. "Television Deflecting Circuits." *R.C.A. Review*, **8**, March 1947, p. 98.
4. O. H. Schade. "Magnetic Deflection Circuits for Cathode Ray Tubes." *R.C.A. Review*, **8**, Sept. 1947, p. 806.
5. O. H. Schade. "Characteristics of High-Efficiency Deflection and High-Voltage Supply Systems for Kinescopes." *R.C.A. Review*, **11**, March 1950, p. 5.
6. A. B. McFarlane and J. R. W. Snith. "A Mathematical Analysis of an Equivalent Scanning Circuit." *J. Brit.I.R.E.*, **11**, Oct. 1951, p. 470.
7. Emlyn Jones. "Scanning and E.H.T. Circuits for Wide Angle Picture Tubes." *J. Brit.I.R.E.*, **12**, Jan. 1952, p. 23.
8. A. B. Starks-Field. "Reactive Time Bases," 1951 Convention Paper. To be published in *J. Brit.I.R.E.*, **12**, 1952.
9. D. A. Wright. "Rare Metals in Electron Tubes." *J. Brit.I.R.E.*, **11**, Sept. 1951, p. 381

RECENT DEVELOPMENTS IN ELECTRONIC INSTRUMEN-TATION FOR CHEMICAL LABORATORIES*

by

Felix Gutmann, Ph.D.,†

SUMMARY

This paper is intended to present some more recent developments in the field covered by the previous review,[1] and is similarly restricted in its scope so that important aspects, e.g. nuclear methods, are again omitted.

1. pH Meters

The reaction of an aqueous medium is either acidic, alkaline or neutral. This property is of paramount importance in a wide range of chemical processes (e.g. electroplating, canned foodstuffs, ore flotation, dairying industry, wool scourers and dyers, tiles and china manufacture, wineries, paper mills, plastics, flour mills, etc.). It depends on the relative concentration of hydrogen-ions, (H^+), and of hydroxyl-ions (OH^-), in the medium. The acid or alkaline behaviour of a solution is measured in so-called pH units, pH being defined as the negative logarithm of the hydrogen-ion concentration in the solution. Pure water is exactly neutral, having equal concentrations of H^+ and OH^-. It has a pH of 7. A fairly concentrated (1N) solution of a strong acid, say, hydrochloric acid, has a pH of 0 and a 1N solution of a strong alkali, say, caustic soda, a pH of 14. It is seen that an acidic solution will have a pH below 7 and an alkaline solution a pH above 7. The lower the pH, the more acid, and the higher the pH, the more alkaline is the solution.

The pH of a solution can be measured by employing the unknown medium as the electrolyte in an electrolytic cell having one inert electrode and one whose e.m.f. depends only on the concentration of the H^+, i.e. on the pH. The potential between these two electrodes is then measured and gives the pH of the solution. The most convenient pH sensitive electrode is the so-called glass electrode, which consists of a small, thin-walled bulb of special glass containing a solution of known pH.

When immersed into the liquid to be tested for its pH, the potential difference set up is

proportional to the difference in pH of the solutions inside and outside the glass electrode. It can be shown from thermodynamics that one pH unit difference generates a potential difference of 59·1 mV at 25°C. However, the measurement of these potentials is not very easy, since the internal resistance of the glass electrode is very ·high, usually in the order of 300 to 900 MΩ. Since a direct potential is generated and an accuracy of 0·05 pH is required, a voltmeter is needed with about 840 mV d.c. full-scale sensitivity, accurate to 0·3 per cent., and having an input resistance of at least 300 times the electrode resistance, i.e. an input resistance of $10^{12} \Omega$ or better.

These instruments have by now been developed to a point where apparatus giving satisfactory performance is commercially available from a large number of manufacturers. Their design centres around the valve employed in the first stage. The Raytheon CK570AX has been used,[2] also the 1Q5 under conditions of constant grid current, and any of the types discussed in Section 2 should be applicable to pH meters.

A new technique has been introduced into the field by Kraus, Holmberg and Borkowski,[3] who used a vibrating reed electrometer for high precision pH measurements, claiming results accurate to better than 0·1 per cent. Unless extreme precautions are taken, this is well above the reproducibility of glass-electrode potentials. A highly accurate mains-operated pH meter, employing vacuum tube stabilization of supply voltages has been developed ·by Belenkii and Rozman.[4]

While all pH meters mentioned so far are of the direct-reading type, a new kind of potentiometric pH meter has been designed by Morton.[5] It uses either positive or negative feedback, and employs a thermistor network for the automatic
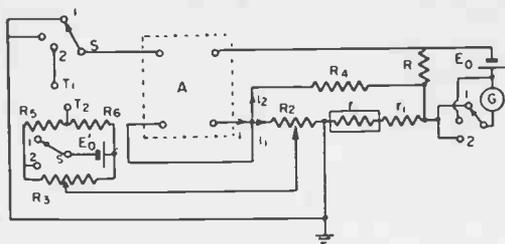
Fig. 1.—*Principle of Morton's potentiometric pH meter.*

compensation of the temperature dependence of the pH of the solution. The principle is shown in Fig. 1. R2 is a calibrated potentiometer, R a standardizing resistor and E_0 a Weston Cell. In operation, the switch S is first thrown to position "1" and the amplifier gain adjusted for zero deflection of G. With S in position "2," G is again balanced to zero by means of R2, which then indicates the pH of the solution. The temperature compensating network comprises R1, R4 and the thermistor r. As the temperature of the solution rises, r decreases so that the current through it increases at the expense of the current through R4, causing the voltage across the main potentiometer R2 to increase. The amplifier uses a space-charge grid tetrode such as the Mullard PM1DG.

2. Current Amplifiers

A survey of circuits suitable for current amplifiers is given by Selby.[6] The use of multigrid tubes as electrometers is discussed by Prescott,[7] who recommends the use of 6BE6 or 7A8, which may be operated under grid currents as low as 10^{-13} to 10^{-14} A. Subminiature tubes employed in electrometers are treated by Victoreen.[8] Commercial valves as electrometer tubes have been investigated by Kreuzer,[9] who finds that the limit of practical usefulness for measurement purposes of a valve lies at about 1/10,000 of its grid-current. The same author employs a KF4 in a single tube circuit, separately compensated for slow changes in filament voltage and mutual conductance.

An efficient method of stabilizing heater voltages is described by Ellenwood and Sorrows,[10] resulting in a stability of better than 0·005 per cent. for changes in line voltage of ±10 per cent.

A new balanced electrometer circuit using a FP54 and operated from a single battery, has been developed by Caldwell.[11] It is well known

that once thermal equilibrium has been attained, the main cause of instability in a balanced circuit is spontaneous changes in emission. This can be largely eliminated by the use of a split electrometer tube, following Lafferty and Kingdon.[12] Caldwell's circuit, shown in Fig. 2, retains the balanced feature of the conventional electrometer circuit, but also enables a single valve to be used in the subsequent d.c. amplifier. The resistances in the electrometer circuit should be so adjusted that the plate voltage at the operating point as measured from the negative side of the grid bias resistor, is independent of small changes in the supply voltage.
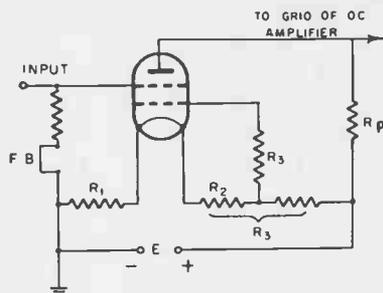
Fig. 2.—*Balanced electrometer circuit (Caldwell).*

A rather novel method for current amplification is described by Rust and Endersfelder.[13] A carbon microphone is energized from the signal and made to respond to a tone of given constant frequency derived from a loudspeaker. The alternating output from the microphone then is proportional to the signal and can be amplified without undue difficulty. The system is essentially a low impedance inverter.

3. Colorimeters and other Photo-electric Instruments

Colorimeters proper are instruments which compare, against a standard, the variations in the absorption of light produced by a colour change in a liquid undergoing a chemical reaction. Here it is intended to summarize under this heading a rather wide variety of instruments which rely on the measurement of light incident on a photo-electric cell. Spectrophotometers employ a monochromatic beam of light of adjustable wavelength and thereby permit a better degree of discrimination. Photo-fluorometers illuminate the solution with —usually ultraviolet—light and measure the

162

fluorescence which it excites by means of a photo-electric cell mounted at right angles to the exciting beam of light. All these instruments employ either photo-voltaic cells (usually selenium) or photo-electric tubes (usually with caesium cathodes). They are much used when rapid semi-quantitative analyses are needed, e.g. testing the chlorine content of water, vitamin analyses, etc.

Many chemical compounds are "optically active": their refractive indices are not the same for right- and for left-circularly polarized light. A beam of plane polarized light may be considered as the vector sum of two circularly polarized beams of equal amplitude but opposite direction of rotation. If such a beam is passed through an optically active medium, the difference in the refractive indices causes a rotation of the plane of polarization through a definite angle. This angle of rotation is linearly proportional to the number of molecules encountered, and therefore to the concentration of the optically active substance. This method is called "polarimetry."

It has many applications not only for quantitative analysis, but also for the determination of chemical structure and of magnetic properties. The first is based on the fact that optical activity is caused by a lack of symmetry in the molecule, while the latter is based on the Faraday Effect, i.e. the rotation of the plane of polarization of light when a beam of light passes through a transparent medium placed in a magnetic field parallel to the beam. Polarimetry is a standard method in sugar analysis and a powerful research tool, particularly in organic chemistry.

Due to their high inherent gain, photo-multiplier tubes have come increasingly to the fore. Larsen[14] has developed a highly sensitive Comparison Fluorimeter which incorporates an automatic device switching the light from a standard to the unknown solution at 60 c/s whilst the sensitive element is switched from one arm of a bridge circuit to another. The meter, in a cathode-follower type valve voltmeter, is first set to zero with the standard solution in both cells. One of these is then replaced by the unknown solution and the bridge is rebalanced by altering the width of one of the illuminating slits.

Two convenient circuits for use in conjunction with photo-multipliers are reported by Ellis and
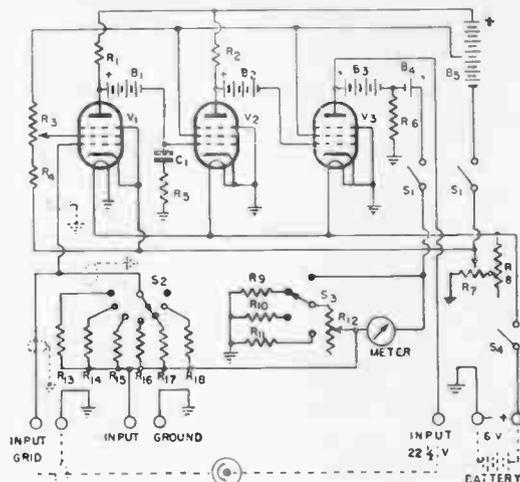

Fig. 3.—Modified Vance amplifier.

R1, 2	2MΩ	R9	1kΩ	R17	1000MΩ
R3	25kΩ	R10	3kΩ	R18	3000MΩ
R4	30kΩ	R11, 12	10kΩ	C1	0·01μF
R5	9kΩ	R13	1MΩ	B1, 2, 3	22½V
R6	100kΩ	R14	10MΩ	B4	1½V
R7	100Ω	R15	100MΩ	B5	90B
R8	30Ω	R16	300MΩ	M	0-100μA

Brandt.[15] Their battery-operated circuit is shown in Fig. 3. It is based upon the Vance electrometer,[16] which, however, is not completely stable for more than a few hours. The modified circuit, as shown in Fig. 3, is claimed to be free from this defect. The mains-operated version is based upon the mu bridge developed by Turner,[17] but is direct reading, and is shown in Fig. 4.

A typical multiplier tube, like the 931-A, readily delivers 100-150 μA. However, operation at such high-current densities is not very satisfactory and it is advisable to limit the output to less than 50 μA.

The difficulties inherent in low-level d.c. amplification have led to many designs involving light-choppers. Two methods have been developed. modulating the light beam. Kalmus and Sanders[18] employ a dial light as source, 100 per cent. modulated at 20 c/s from a two-tube multivibrator, using a 6SN7, followed by a direct-coupled 6V6 with the light globe as plate-load.

Kalmus and Striker[19] convert the d.c. space current within the photo-cell into a.c. by its magnetic deflection or suppression by means of an alternating field applied transversely across

Fig. 4.—*Schematic diagram of line-operated amplifier.*

R1, 2	400Ω	R7	5kΩ	R14	200Ω
R3, 8, 9	220kΩ	R10	270kΩ	R17	10kΩ
R4	50kΩ	R11	250kΩ	R18	1MΩ
R5	300Ω	R12, 15, 16	10kΩ	C1, 2	2μF
R6	50kΩ	R13	300Ω	C3, 4	25μF
				C5, 6	0·05μF
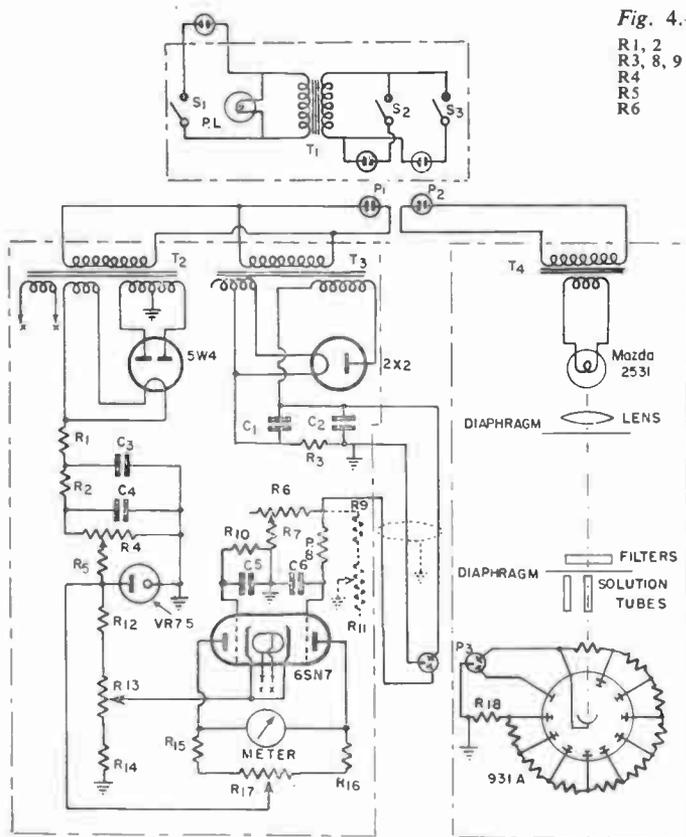
magnetic field of only 200 oersteds amplitude suppresses 90 per cent. of the electron current. The a.c. signal has twice the frequency of the modulating magnetic field and therefore can be readily isolated from fundamental frequency stray e.m.f.'s. This device increases the sensitivity of the photoelectric apparatus up to the limit imposed by thermal motion.

A recording polarimeter has been designed by Levy, Schwed and Fergus.[20] The operator is replaced by a photo-electric servo-system using a multiplier tube in conjunction with a mechanical light-chopper. At a recording speed of $\frac{1}{2}$ deg/min. the instrument is claimed to have a precision of 0·005 deg. There seems to be ample scope for further application of electronic techniques to polarimetry.

Photo-electric methods have been applied successfully to the counting of individual particles in an aerosol (a suspension of minute solid particles in a gas). Gucker and O'Konski[21] have developed two methods to accomplish this. The first system is based upon light scattering. In it, a fine stream of the aerosol, protected by a sheath of a pure gas, passes through a confined region under intense dark field illumination. Every solid particle produces a single flash of scattered light in a forward direction, and this flash then impinges on a photo-multiplier cell.

the path of the photo-electrons, as shown in Fig. 5. The approximate paths of the electrons in the presence and in the absence of the modulating magnetic field are shown in Fig. 6. A
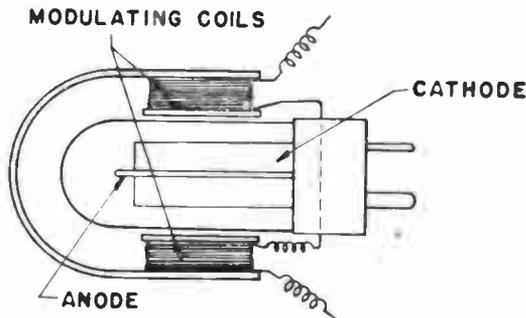

Fig. 5.—*Magnetic modulation of electron current in photo-tubes (Kalmus and Striker).*
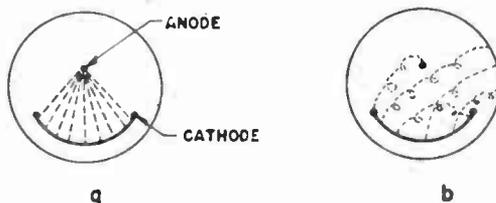

q   b

Fig. 6.—(a) *Approximate path of photoelectrons in the absence of magnetic field.*

(b) *Electron paths deflected by an applied magnetic field. (According to Kalmus and Striker).*

164

Fig. 7.—*Apparatus for size distribution studies in aerosols* (*Gucker and O'Konski*).

Fig. 8. (below)—*Differential pulse-amplitude selector circuit* (*Gucker and O'Konski*).

Each particle of 0·6-micron diameter or larger produces a single pulse, which is amplified and made to actuate a counter. In the second method, the aerosol is forced through a fine jet, and the individual particles are charged by friction. The stream then impinges upon a collector. A single pulse is produced by every particle of diameter exceeding 2·5 microns. The pulse amplitude is proportional to the square of the particle diameter.

The same authors[22] have further improved their first method by the incorporation of a discriminator circuit which limits the count to particles producing pulses within a predetermined range. Because the light scattered depends on the size of the individual particle, this circuit allows the counting of particles within a given range of diameters, i.e. it permits a size-distribution study of the aerosol. Fig. 7 shows a block-diagram of the electronic circuits and Fig. 8 reproduces the differential pulse-amplitude selector circuit. Its resolving time is 4 milliseconds.

4. Polarographs

Polarography is a method of electrochemical analysis, devised by Heyrovsky, which is based on the interpretation of the characteristic current *v.* voltage curves obtained in the electrolysis of solutions. In order to avoid electrode contamination by the products of electrolysis, and for other reasons, a dropping mercury electrode is used in conjunction with a second electrode of an effective area very much greater than the area of a mercury drop. The potential applied to the system is continuously increased and the current flowing determined as a function of the potential. Initially, only a minute current flows. However, when a certain critical voltage is reached, electrolytic discharge commences and the current starts to rise. Eventually, a region of saturation current is reached where the current stays substantially constant till, at still higher potential, another component of the solution enters into the discharge process.

It can be shown that the saturation current is linearly proportional to the concentration of the particles (say, ions) being discharged, while the discharge potential depends on the nature of the particles (e.g. the ion species). The midpoint of the discharge curve, called the half-step potential, serves thus to identify the substance undergoing discharge. The whole curve is termed a polarographic "step" or "wave." The half-step potentials have been tabulated for a large number of ions and other substances which can be reduced or oxidized at a mercury electrode. A quantitative analysis of the substance under electrolysis is thereby possible.

In Alternating Current Polarography a small alternating "exploring" potential of low audio frequency (say, 50 c/s) is superimposed upon the direct voltage which governs the electrochemical process. The cell impedance can be shown to depend on the operating point on the current-voltage curve, which point in turn depends on the chemical state of the reactants in the cell, as determined by the impressed direct potential. The impedance becomes a minimum at the half-step potential. Thus, the magnitude of the alternating current flowing through the cell may be used to measure the concentration of the substance undergoing discharge, and the direct potential at which the alternating current maximum is observed is the half-step potential.

The new method of polarography with alternating current has been further developed by its innovators, Breyer, Gutmann and Hacobian.[23] The sensitivity of the apparatus has been greatly increased by the incorporation of a two-stage pre-amplifier in front of the main amplifier. This pre-amplifier uses two 6AU6 as triodes with the plates grounded, as suggested in an application note by the valve manufacturers.[24]

Instruments similar to those first employed by Breyer and Gutmann[25] have been developed by Randles[26] and by Delahaye.[27] Both employ a cathode-ray oscilloscope as the indicating instrument. Randles, whose work is based upon Matheson and Nichols,[28] succeeds in displaying the whole polarogram on the screen as a series of peaks. D.C. amplifiers are used, in contradistinction to the method originally used,[25] which allows the use of a.c. amplifiers throughout.

An instrument for "Differential Polarography" has been devised by Leveque and Roth.[29] The polarographic diffusion current is claimed to be electrically differentiated by means of a simple addition to the normal, d.c., polarographic circuit. In effect this again is but another version of the method which had been developed by Breyer and Gutmann.[25]

Polarographic analysis operates with currents of the order of microamperes. The same method applied, not to analytical purposes, but to the electrolytic production of a substance, is called "Controlled-Potential Electrolysis." Solid electrodes are used, and a number of circuits have been devised to keep the potential of the electrode *v.* solution rigorously constant. Lamphere and Rogers' circuit[30] is claimed to hold the potential of the electrode at a predetermined value to within 4 mV over a period of 24 hours. The desired potential is set up on a slide wire connected to a reference battery; in opposition to the cathode-solution potential. Changes in the latter cause current to flow through an inverter, which consists of a vibrating chopper, driven from the mains. The phase of the alternating output from the inverter therefore depends only on the direction of the d.c. unbalance current. This a.c. is then amplified and applied to one phase of a two-phase motor, its other phase being connected to the mains. The sense of rotation will then depend on the phase angle and therefore on the direction of the unbalance current through the inverter. The

166

motor then adjusts the electrode voltage. Heavy velocity damping is applied to the motor by means of a selenium rectifier circuit, in order to prevent hunting. A 4,000-μF, 25-V electrolytic capacitor shunts the electrolytic cell to reduce transients.

A similar apparatus has been designed by Chambers.[31] The actual potential and the desired potential, which latter is set on a voltmeter, are fed to a balancing unit consisting of a double triode and a galvanometer relay. The latter, in turn, controls a reversible motor adjusting the main control rheostat.

In controlled-potential electrolysis the completion of the electrode process is followed by a drop in current. This current drop can be made to indicate automatically that the final stage in the electrolysis has been reached. An instrument based on this principle has been designed by Kovalenko.[32] A photo-relay, preset for a certain minimum current, activates a 6F6 to give a signal. The photo-relay operates from a light beam reflected from an aluminium foil attached to the ammeter needle in the deposition circuit.

5. Gas-Analyzers

As far back as 1895, Hardy[33] suggested the analysis of binary gas mixtures by means of differences in the velocity of propagation of sound through them. This idea has recently been taken up by Crouthamel and Diehl.[34] An A.F. generator, operating at 1,000-3,000 c/s, drives a small dynamic loudspeaker which is mounted at one end of a sound-tube. A sensitive microphone mounted at the other end gives maximum or minimum response, depending on the resonance condition of the tube. For a given tube length and a given frequency, the signal amplitude is an unstated trigonometric function of the composition of the gaseous mixture in the tube. Hydrogen in air has been
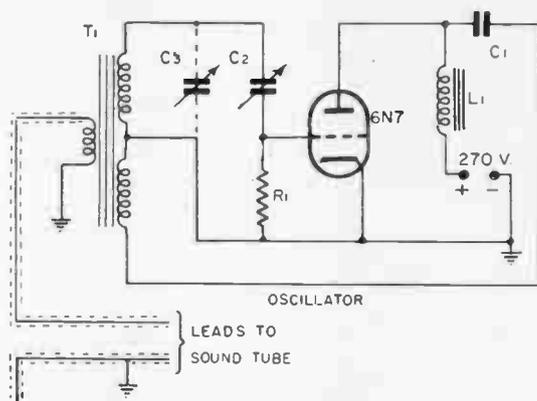

Fig. 9.—*Doubly-stabilized tuned grid oscillator (Crouthamel and Diehl).*

determined on a direct-reading meter, with 10 per cent. H_2 corresponding to full-scale deflection. Methane in air and CO_2 in air can also be estimated. Since the frequency and amplitude of the exciting A.F. are critical, a doubly-stabilized tuned grid oscillator was designed by the authors for this apparatus. This circuit is shown in Fig. 9, and the sound tube itself in Fig. 10. The resulting calibration curves are given in Fig. 11, for three different frequencies.

Oxygen and some of its compounds like nitric oxide, nitrogen dioxide and chlorine dioxide, and many vapours, are strongly paramagnetic.[35] Pauling, Wood and Sturdivant[36] designed an instrument for the determination of the partial pressure of oxygen, based upon its paramagnetic properties. A small test body is placed in a strongly inhomogeneous magnetic field. In a paramagnetic medium the body is deflected. This is used to indicate the concentration of the paramagnetic gas present.

The paramagnetic oxygen analyzer has been further developed by Dyer.[37] This author uses a bridge circuit energized with about 3 V at 20 kc/s from a local oscillator. Two arms of the
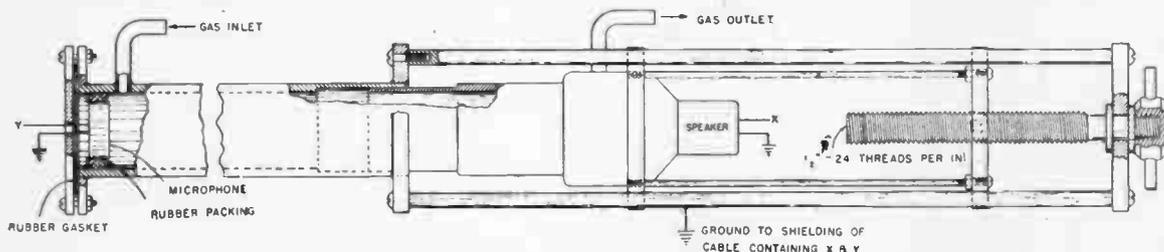

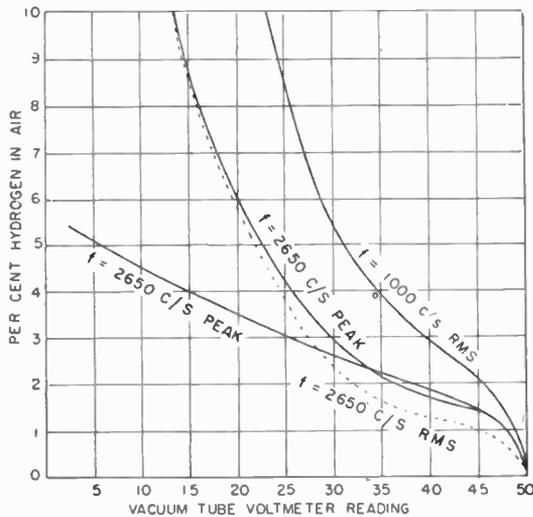Fig. 10.—*Sound tube (Crouthamel and Diehl).*

167

Fig. 11.—*Calibration curves for hydrogen-air mixtures (Crouthamel and Diehl).*

bridge consist of heated platinum wires located in a strong, inhomogeneous field, produced by an alnico magnet. The heated paramagnetic gas suffers a loss in its magnetic susceptibility and is therefore replaced by a cooler gas flowing from regions of higher flux density, cooling the Pt wires. The resulting change in resistance unbalances the bridge and the unbalance voltage is a measure of the oxygen concentration. Change from air to pure oxygen is claimed to produce an output of 60 mV.

Another apparatus for the same purpose is reported by Luft.[38] A modulated magnetic

field, produced by rotating one pole of a permanent magnet, is applied to the gas, and the variations in pressure induced operate a flexible membrane, which constitutes one plate of a capacitor. The capacitance method of pressure determination has been previously described by the same author in an earlier report.[39] The apparatus is claimed to be extremely sensitive, 0·01 per cent. being quoted.

The importance of oxygen analysis has led to the development of yet another method: Toedt[40] utilizes the experimental fact that the potential between metal electrodes immersed into water depends primarily on the concentration of oxygen diffusing towards the nobler electrode. While the exact nature of the effect is not yet understood, good results are claimed to have been obtained with a Pt electrode. The method involves a kinetic quantity and is not based upon a Redox potential determination.

6. Titrimeters

The convenience and rapidity of electronic devices for titration work have led to the design of a large number of instruments. Only a few will be mentioned.

A very simple vacuum tube titrimeter with internal calibration has been developed by Werner.[41] The circuit is shown in Fig. 12. It uses a 0-1 mA meter. The voltage dividing network R7-R8 taps off a calibrating voltage from the stabilized plate supply.

Austin, Turner and Percy[42] place the titration cell into one arm of the feedback loop of a negative feedback amplifier, which automatically equalizes the rate of supply of titrating agent to the rate of addition of titratable compound, resulting in continuous and automatic titration.

According to Delahaye,[43] the charging or discharging current of a capacitor connected to the terminals of a potentiometric titration cell becomes a maximum at the endpoint of the titration, assuming the ohmic resistance of the circuit to be negligible. This is illustrated in Fig. 13. An electronic circuit allows the time constant of the measuring circuit to be made independent of the resistance of the potentiometric cell. This yields a sharper indicator maximum which then represents the true endpoint. Fig. 14 shows the complete electronic
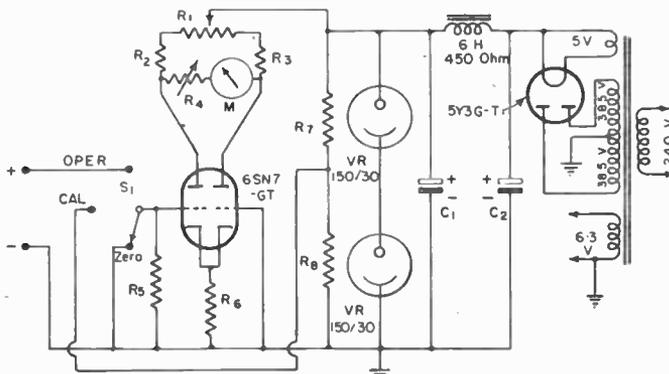

Fig. 12.—*Werner's titrimeter.*

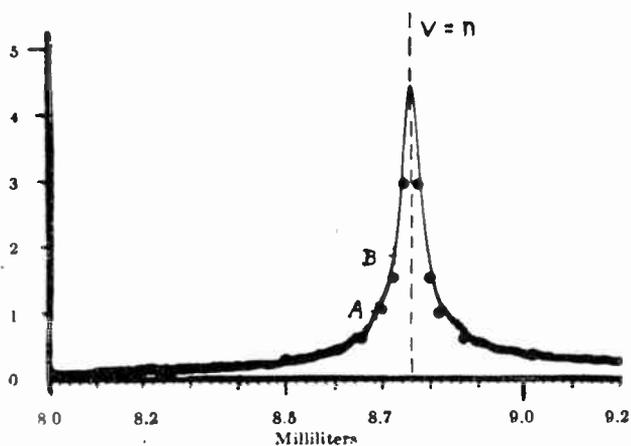|		
R1, 4 1000Ω	R5 10MΩ	R7 0·3MΩ
R2, 3 8000Ω	R6, 8 750Ω	C1, 2 8µF

Fig. 13.—*Variations of indicator current in titration of* $AgNO_3$
by a NaCl solution (Delahaye).

circuit, as developed by Delahaye (*loc. cit.*). A twin triode is employed as amplifier. C4 is the capacitor of the measuring circuit. The switching arrangement allows the use of either the new (indicator-current), the conventional (plotting e.m.f. applied *v.* reagent added) or the so-called Erich Mueller method. The network C3, R5, R6 is a filter to suppress parasitic alternating voltages.

An electronic trigger circuit for precise automatic titrations with a motor-driven, syringe-type burette, is described by Muller and Lingane.[44] The principle is shown in Fig. 15. The twin
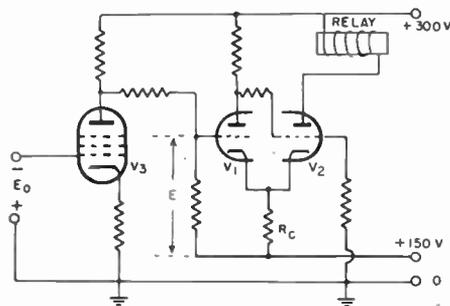
triode V1, V2 is employed in a trigger circuit based upon the one proposed by Schmitt.[45] With no signal, V1 is non-conducting and V2 conducts fully. This represents a steady state. If the grid of V1 is driven somewhat more positive, its plate voltage decreases, driving the grid of V2 more negative. This decreases the voltage drop across R_c making the grid of V1 still more positive. The action is cumulative till V1 conducts and V2 cuts off. The switching action is very positive and takes place within about 1 microsecond. Both final states are quite stable. By decreasing R_c, the difference between the two triggering level can be reduced to as little as 100 mV. On further reducing R_c, however, the circuit tends to fail as a trigger, but becomes an extremely sensitive amplifier. Due to the pre-amplifier
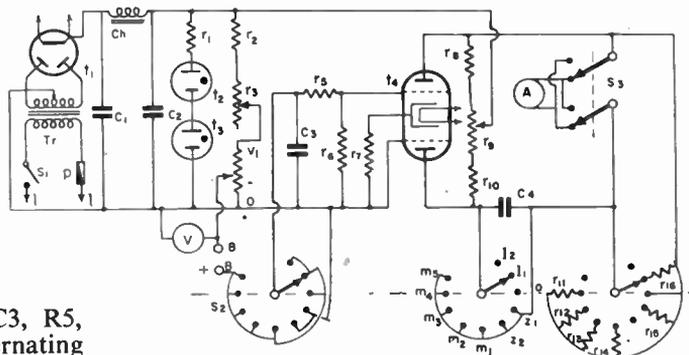

Fig. 14.—*Electronic device for potentiometric titrations*
(Delahaye).

R1 3000Ω	R6 $30M\Omega$	C1, 2 $20\mu F$
R2 $20k\Omega$	R7 100Ω	C3 $0.5\mu F$
R3 1000Ω	R8 $10k\Omega$	C4 $30\mu F$
R4 200Ω	R9 2000Ω	T1 $5Y3$
R5 $0.25M\Omega$	R10 $10k\Omega$	T2,T3 VR105-30
		T4 $6N7$

V3, the authors prefer a difference in triggering levels of about 0.5 V. The complete circuit is shown in Fig. 16. It switches at a predetermined potential and switches back again at a slightly lower voltage, thereby stopping delivery from the burette exactly at the equivalence point.

The use of R.F. oscillators in titrations has been treated by Jensen and Parrack,[46] and by Blaedel and Malmstadt.[47] Any changes in ionic or dipole content in either an ionized or non-ionized medium may be followed by high frequency titrations, as first described by Blake.[48] R.F. titrations require neither electrodes nor

Fig. 15.—*Trigger circuit for automatic titrations (Muller and Lingane).*

169

Fig. 16.—*Automatic titration apparatus (Muller and Lingane).*

R1	9000Ω	R11	2MΩ
R2, 3, 6, 8, 15	100kΩ	R12	100Ω
R4, 16	1MΩ	R13	1000Ω
R5	4000Ω	R14	10kΩ
R7	5MΩ	R17	5MΩ
R9	200Ω	C1, 2	8μF
R10	0·5MΩ	C3	1μF

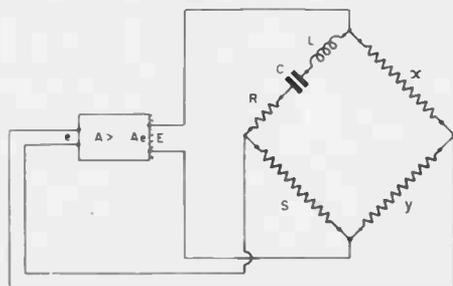|	
B1	22·5V
B2	1·5V
V1	5Z4
V2, 3	VR150
V4	6SJ7
V5	6SN7
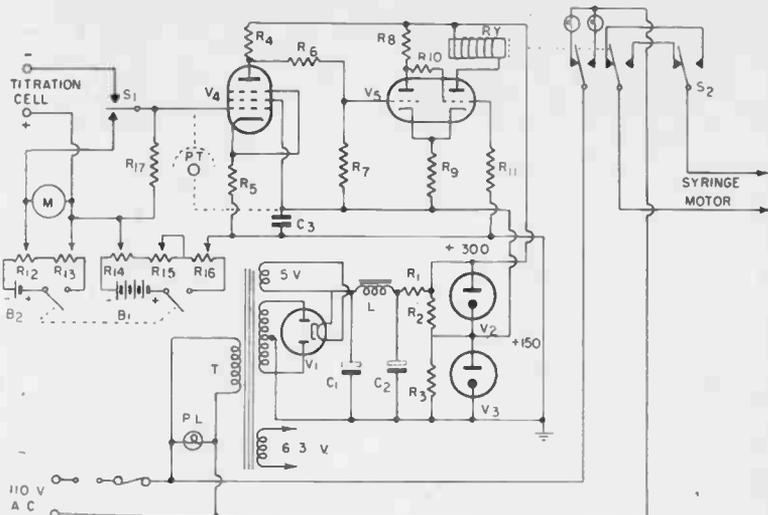
actual physical contact with the solution. They are particularly suited for titrations where the endpoint is difficult to detect by other methods. Blaedel and Malmstadt,[47] describe a titrimeter operating at 30 Mc/s. West, Barkhalter and Broussard,[49] also describe a titrimeter, utilizing a heterodyne principle to detect the detuning and/or loss produced by the progress of titration.

(a)

(b)

Fig. 17.—(a) *Principle of conductivity bridge automatic quadrature balance (Moneypenny).*
(b) *Linear high-gain amplifier with zero phase-shift for Moneypenny's conductivity apparatus.*

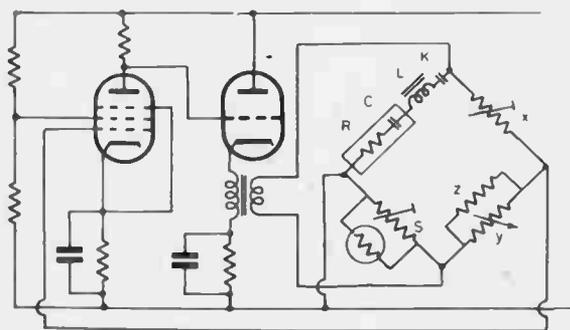## 7. Electrolytic Conductance Apparatus

The R.F. titrimeters mentioned above are all based on the introduction of the reaction vessel into an R.F. field and the relating of the progress of the chemical reaction to changes in some electrical parameter of the oscillatory circuit. The originator of the method, G. G. Blake,[48] claims that this method measures changes in the conductance. In a series of papers,[50] Blake has further developed this promising analytical tool, although, as in the present reviewer's opinion, conductance secures only one single facet of the very complex impedance changes produced by the chemical reaction proceeding within an oscillatory circuit.

An arrangement in many respects similar to Blake's is described by Bever, Crouthamel and Diehl.[51] This also is claimed to respond to conductivity changes.

In conventional conductance determinations by means of some kind of a.c. bridge, a capacitive as well as a conductive balance must be attained. In practice, this constitutes a serious drawback and has tended severely to limit the method. Two devices have been suggested to alleviate this: Vergnolle[52] proposed the application of the Miller effect to compensate for the dephasing. A valve arrangement, equivalent to a variable capacitor, allows a very convenient reactive bridge balance to be obtained. Moneypenny[53] describes an apparatus which provides a direct measure of only the resistive
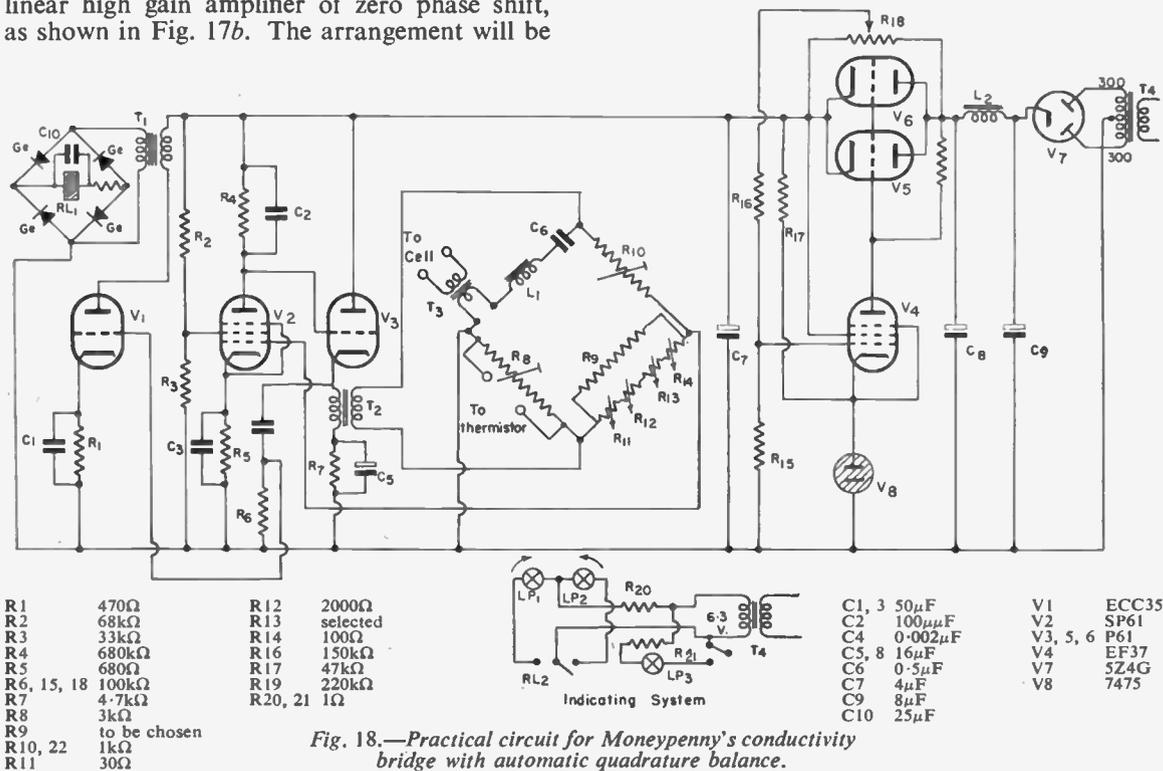
170

component by making use of the boundary conditions between stability and instability in an amplifier in which the actual bridge provides a feedback network. The transition from quiescence to oscillation depends on the resistive balance exclusively. It is thus no longer necessary to obtain a reactive balance at all, the conductive component being the quantity required. In effect the method provides a means to secure an automatic and instantaneous quadrature balance.

The principle of the arrangement is shown in Fig. 17a. The electrolytic cell is to be represented by a series combination of a resistance R and a capacitance C. L is an inductance of negligible resistance. The bridge is balanced, i.e. the output voltage e vanishes, if $yR = xS$ and if, simultaneously, $\omega^2 LC = 1$. Considering y and ω as the independent variables, y will measure R if ω simultaneously satisfies the above criterion. The apparatus designed by Moneypenny makes ω automatically self-adjusting by making the bridge a feedback channel between the output and input of a linear high gain amplifier of zero phase shift, as shown in Fig. 17b. The arrangement will be

stable or unstable (oscillatory) depending on whether the loop gain is less or larger than unity, i.e. its stability will be governed by Nyquist's[54] criterion.

If the amplifier has a high gain and zero phase shift the resistive balance given above represents also the condition obtaining at the boundary between stability and instability. The frequency of oscillation of the system at this transition point is in turn determined by the criterion of zero phase shift after one complete traverse of the loop in Nyquist's diagram. This criterion is satisfied by the second balance condition given above, so that the reactive balance is automatically achieved. Therefore, it suffices to adjust y till the system is brought to the edge of instability, at which point $y = 1/R$, the quadrature balance being automatically attained.

The circuit of the complete instrument shown in Fig. 18 is claimed to be free from unwanted instability, since it employs a direct coupled amplifier drawing its H.T. supply from a low-impedance stabilized source.

R1	470Ω	R12	2000Ω
R2	68kΩ	R13	selected
R3	33kΩ	R14	100Ω
R4	680kΩ	R16	150kΩ
R5	680Ω	R17	47kΩ
R6, 15, 18	100kΩ	R19	220kΩ
R7	4·7kΩ	R20, 21	1Ω
R8	3kΩ		
R9	to be chosen		
R10, 22	1kΩ		
R11	30Ω		

C1, 3	50μF	V1	ECC35
C2	100μμF	V2	SP61
C4	0·002μF	V3, 5, 6	P61
C5, 8	16μF	V4	EF37
C6	0·5μF	V7	5Z4G
C7	4μF	V8	7475
C9	8μF		
C10	25μF		

Indicating System

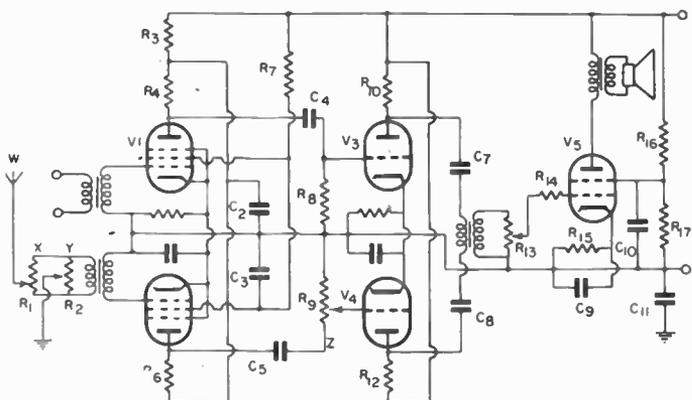*Fig. 18.—Practical circuit for Moneypenny's conductivity bridge with automatic quadrature balance.*

171

Fig. 19.—*Apparatus for the cancellation of stray interferences in conductivity measurements (Ives and Pittman).*

R1	2000Ω	C1, 6, 9	25μF
R2, 5	1000Ω	C2, 3, 10	8μF
R3, 10, 12, 16, 17	20kΩ	C4, 5, 7, 8	0·05μF
R4, 6	200kΩ	C11	2μF
R7, 8, 13	0·5MΩ	V1, 2	6J7
R9	1MΩ	V3, 4	6C5
R11	500Ω	V5	KT33C
R15	200Ω		

Another difficulty encountered in conductance measurements is interference by stray electric fields. Following a proposal by Hartshorn,[55] Ives and Pittman[56] provide two amplifying channels, one fed with the signal plus unavoidable interference, and the other with the interference alone, picked up by means of an aerial mounted in close proximity to the bridge. Before the final stage, the two outputs are combined so that self-cancellation of the unwanted interference takes place. Fig. 19 depicts the circuit of the complete apparatus. X, Y and Z are the compensating arrangements.

Fig. 20.—*Principle of Delahaye's method for electrometric titrations.*

Delahaye[43] reports that the charge or discharge current of a capacitor connected to the terminals of a potentiometric cell becomes a maximum at the equivalence point in an electrometric titration. The same author[57] has applied this principle to conductimetric analyses, using a simple differentiating circuit. The principle is shown in Fig. 20. The conductivity cell

is fed at constant current from a regulated supply. The potential across the cell is rectified and applied to a capacitor and microammeter in series. The endpoint of the titration is then indicated by a reversal in the meter current. Delahaye's method assumes that the capacitor in the measuring circuit (C in Fig. 20) is a pure capacitance, without leakage. Since C, in practice, is an electrolytic capacitor of a few 100 microfarad, its leakage current must be compensated. A suitable circuit is shown in Fig. 21. The output voltage from the amplifier is applied to R1 and R2 in series. Compensation can then be achieved by setting the potentiometer P, and once obtained will hold for all conductances.
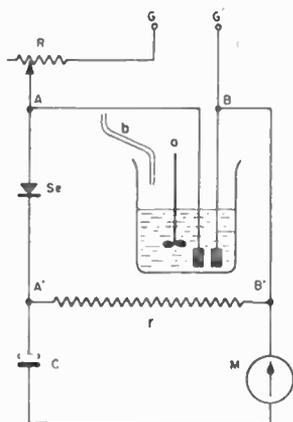
8. Instruments for Determination of Dielectric Properties

The extremely simple dielectric constant meter, described by Alexander,[58] has received a certain amount of attention. The main drawbacks of the original version were its long warming-up time (about 2 hours) and difficulties in maintaining oscillation with substances of high dielectric constant, even if without undue

Fig. 21.—*Circuit for the compensation of capacitor leakage currents (Delahaye).*
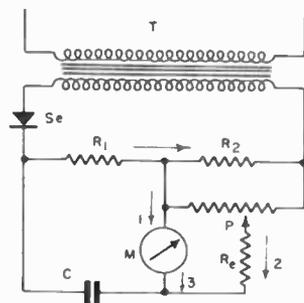
losses. Fischer[59] modified the circuit by placing the sample within the coil. The instrument which is empirically calibrated, is claimed to permit the measurement of permittivities up to 80.

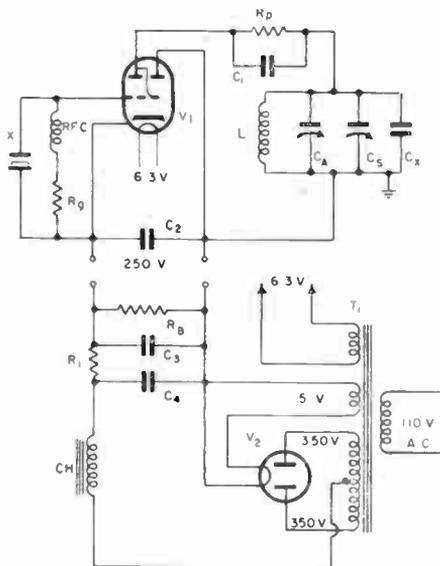Another version has been developed by Bender,[60] and is shown in Fig. 22.

Fig. 22.—*Bender's modifications of Alexander's dielectric constant meter.*

C1 0.001μF	CA $100\mu\mu$F variable	R1 2000Ω
C2 0.01μF	Rg 40kΩ	V1 6E5
C3, 4 8μF	Rp 150kΩ	V2 80
Cs $50\mu\mu$F variable	RB 15kΩ	

An absolute method for the measurement of the dielectric constant of liquids is reported by Greinacher.[61] It measures the rise of a liquid dielectric in a small measuring capacitor upon application of a known voltage. The dielectric constant can be directly calculated if the applied voltage and the density of the liquid are known. The effect depends on the square of the applied potential; 200-2,000 V d.c. or a.c. were found convenient. Only a small quantity of liquid, which may be slightly conducting, is required.

Another apparatus for dielectric constant determinations is reported by Baker.[62] It involves an electric chronometer to measure the time taken for a resistance-capacitance combination to discharge between given potential limits. The method, while very elegant, is restricted to dielectrics of rather good power factor.

A convenient method for the determination of the equivalent capacitance and resistance of rectifiers, reported by Cooper,[63] appears to be capable of application also to other dielectrics of comparatively good conductance. It involves finding the apparent series resistance and reactance by means of a small alternating voltage superimposed upon a polarizing d.c. potential. The measurement is carried out at a number of frequencies and the semi-circular impedance locus is plotted, with its centre on the R axis. The diameter then equals the barrier resistance and the smallest intercept equals the resistance of the selenium layer. An equation is given for the calculation of the true capacitance. The method should be particularly valuable for liquids which exhibit large polarization effects.

Dielectrics containing free charges present certain problems in the interpretation of dielectric measurements. The problem has been treated theoretically by Breyer and Gutmann,[64] who give expressions for the apparent dielectric constant of a space containing free charges, in terms of the field distribution within the dielectric.
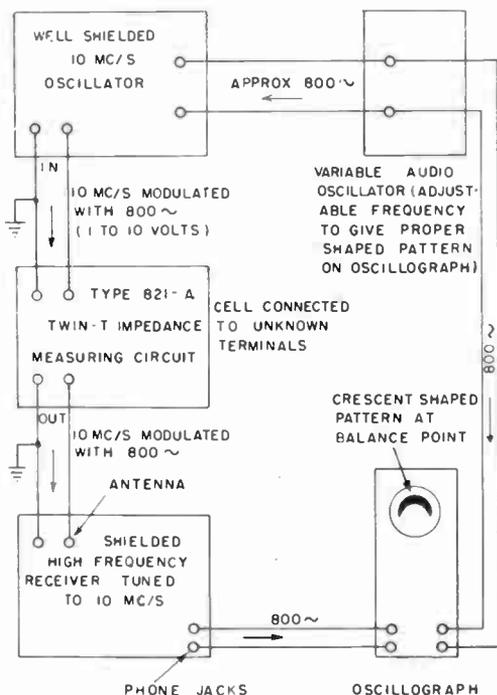

Fig. 23.—*Oscillographic method for dielectric constant determinations (Elliott, Jones and Lockhart).*
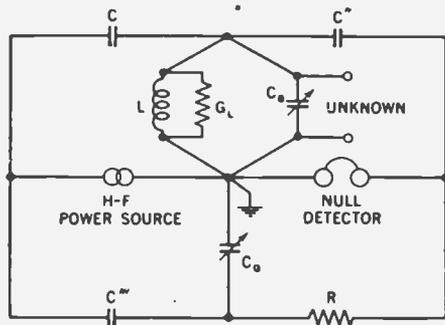
Fig. 24.—*Twin-T impedance measuring circuit* (*General Radio*).

An oscillographic method has been developed by Elliott, Jones and Lockhart.[65] Its basis is shown in Fig. 23. A 10-Mc/s signal from a generator is modulated at an audio frequency, derived from a local oscillator. The receiver is set to normal operation, i.e. with the C.W. beat oscillator switched off. The test capacitor containing the dielectric is connected to the "unknown" terminals of a General Radio type 821-A Twin-T Impedance measuring circuit, depicted in Fig. 24. One set of deflection plates is connected to the receiver output and the other pair to the modulating A.F. source. At the balance point, a horizontal crescent-shaped pattern results. Any deviation from the conductance balance tends to make the crescent tip one way or the other, depending on the sense of the off-balance. Any deviation from capacitance balance makes the crescent appear fatter. Both balances are claimed to be quite independent.

The authors[65] have used this instrument for dielectric identity tests on plasticizers. These materials exhibit characteristic temperature-dielectric loss curves which are very sensitive to contamination. The method involves the determination of the dielectric properties of the sample at 10 Mc/s, as a function of temperature, over an interval of, say, 100°C. It should also be applicable for other polar organic liquids.

An electronic method, based upon a measurement of dielectric properties, for the determination of the solid to gas ratio in dense aerosols has been developed by Dotson and co-workers.[66] It measures the dielectric constant as the mixture flows between the plates of a capacitor. The circuit is shown in Fig. 25.

When both oscillators operate in phase, no current flows in the inductively-coupled circuit. If the capacitance of C1 alters, the two oscillators are no longer in phase and a current proportional to the phase-difference is induced. The R.F. output is rectified by the diode and measured as the voltage drop across R1. A 1 per cent. volume change in a coal-air mixture, producing a capacitance change of only 0·02 pF, is claimed to yield an output of 30 mV across a 1,000-Ω load.

A direct-reading instrument for the measurement of small series resistances in capacitors has been developed by Gutmann.[67] A thermocouple ammeter measures the circulating tank current of an oscillator, first in the absence and then in the presence of the test capacitor. Its decrease then is a measure of the series resistance, if the capacitive reactance of the capacitors can be neglected.
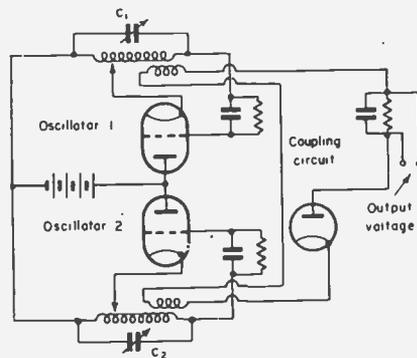

Fig. 25.—*Circuit for the measurement of the solid to gas ratio* (*Dotson and others*).

9. Moisture Meters

An electronic instrument for moisture determinations by means of Karl Fischer titrations (cp. paper 1), has been designed by Kieselbach.[68] The circuit is of interest because it is completely mains operated, is independent of line fluctuations, and is claimed to be relatively independent of the cell impedance. It is shown in Fig. 26. The current through the cell is kept constant and the potential across it measured by means of one section of a 6SL7, directly coupled to a 6E5 electron ray indicator. To minimize grid current, the plate current has been greatly reduced. A reasonable gain is obtained by using a large plate load resistance. Line fluctuations are compensated by the second half of the 6SL7
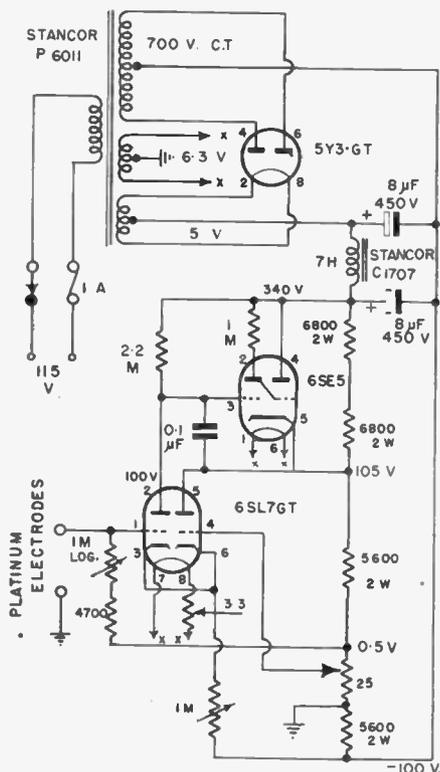
174

Fig. 26.—Mains-operated instrument for Karl Fischer moisture determinations (Kieselbach).

acting as cathode follower, coupled to the amplifier. The low effective plate resistance of the cathode follower minimizes the degeneration produced by the high cathode resistance. Any change in supply voltage affecting the grid potential affects the cathode voltage equally, maintaining a constant bias. Also heater voltage fluctuations are neutralized by the action of the cathode follower part of the 6SL7, if the two halves of the tube are fairly closely matched.

The author reports even better success, as far as matching is concerned, with use of a 6SU7.

An apparatus for the estimation of water in gases has been developed by Weaver and Riley.[59] The electrical conductivity of a thin film of a hygroscopic material like phosphoric acid varies greatly with the concentration of water in its surrounding atmosphere. The method involves the change of pressure of a standard gas of known composition until its conductivity equals that of the detecting film. Water vapour in oxygen, liquid carbon dioxide, freon, moisture in powdered solids, water content of organic liquids, etc., have been estimated. A film of phosphoric acid, sulphuric acid, or a solution containing one or more acids, bases or salts with a binding material like gelatin or a high polymer plastic is spread over an insulator between two solid Pt electrodes. Nitrogen saturated with water vapour is used as standard gas. A local oscillator at audio frequencies powers the circuit, which otherwise is conventional.

10. Electronic Control Circuits

A novel oscillator which can be readily adapted for a multitude of control devices is reported by Mouzon.[70] A movable metallic vane is interposed between the tank coil and the feedback coil in a grounded grid oscillator. The vane can easily be adjusted so that a displacement of 2/1000 in. suffices to stop oscillation. The ensuing change in plate current can be used directly to actuate a relay. The grounded grid makes sure that the coupling between the feedback coils is entirely determined outside the tube. Very good frequency stability even with changing mains voltages has been claimed.

Another versatile control instrument is represented by the Fielden Proximity Meter.[71] Its principle is illustrated in Fig. 27. An oscillator operating at 500 kc/s feeds a phase balancing network producing two earth-free, equal and
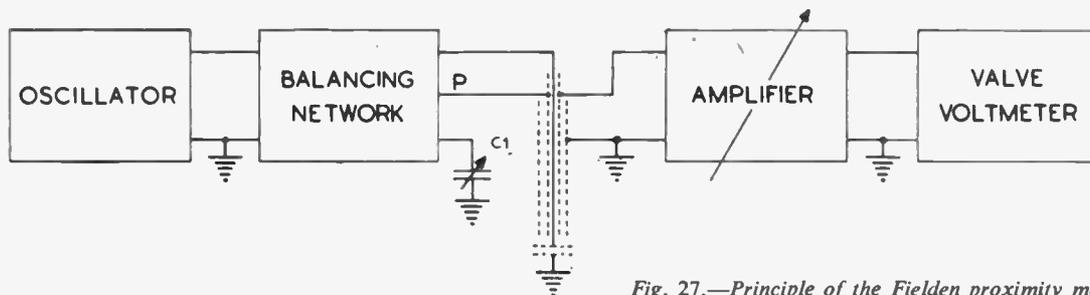

Fig. 27.—Principle of the Fielden proximity meter.

anti-phase voltages in series. One side of this is connected to earth via C1, which constitutes the zero-setting control. The other side is connected to earth via a probe. When C1 is adjusted to equal C2, no voltage appears between the point P and earth, and the deflection of the amplifier-valve voltmeter is zero. Any asymmetry between C1 and C2 produces a deflection. The instrument is fed from raw a.c. and should be applicable to a wide variety of control uses.
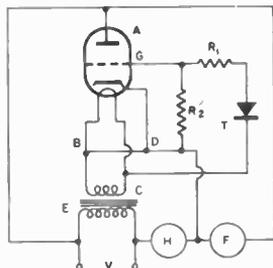

Fig. 28.—*Thermo-regulator for mercury thermostat (Swinehart)*.

A very simple thermo-regulator, intended for work in conjunction with a mercury thermostat, has been developed by Swinehart.[72] It uses an FB57 thyratron in a mains-operated on-off circuit. The current through the thermo-regulator cannot exceed 3-4 μA, thus avoiding corrosion of the Hg contacts. The circuit is shown in Fig. 28. Current is always flowing through the fan F and the heater H. However, since the impedance of the fan is much higher than the impedance of the latter, the heater current will be negligible unless the tube fires, when the fan is shorted out.

A similar circuit, intended for use as a low-power relay, has been designed by Ratchford and Fein,[73] using a 2050 thyratron. It can handle up to 10 W.

An interesting circuit designed as a reflux ratio timer has been developed by Fisher.[74] This instrument is intended for use in fractional distillation, where it controls the periods of reflux and of delivery of distillate from the condenser. The circuit is shown in Fig. 29. The apparatus consists of two interlocked timing units, based on the capacitor discharge

principle, one for "off" or reflux timing and the other for "on" or delivery timing. When S5 is closed, V1 warms up. The tetrode section of V1 acts as a self-rectifying amplifier, drawing current through Ry1 and closing contacts S1 and S2. The diode section of V1 then applies a negative bias across C1 to the control grid of V1, eventually leading to V1 cutting off. Ry1 then drops out and stays open till C1 has discharged through R1 and R2. The cycle is then repeated. The time interval during which Ry1 is energized is set by means of R1. With the constants given, this allows a variation from 4 to 60 sec. The action of V2 is analogous, but its output circuit does not pulse. The delivery period is set by R3, intervals of from 1 to 5 sec being available.

11. Radiometric and Ionization Apparatus

A new Pirani gauge, based upon a suggestion by Knudsen,[75] has been designed by von Ubisch.[76]

The bridge containing the hot wires of the
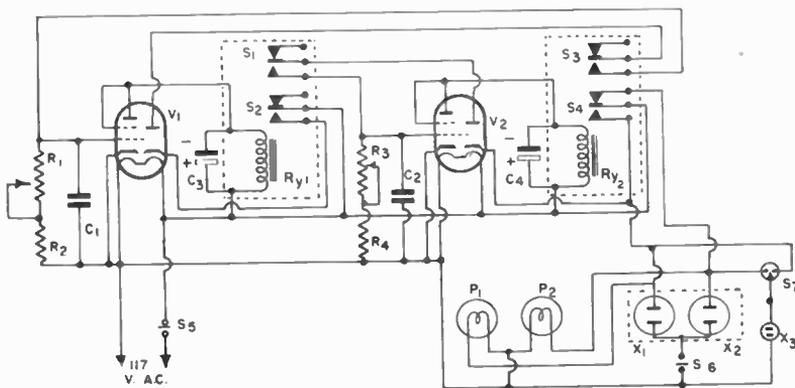
Fig. 29.—*Reflux ratio timer (Fisher)*.

| R1 | 3MΩ pot. | R3 | 1MΩ] | C1 | 4μF | C3, C4 8μF |
| R2 | ·25MΩ | R4 | 50kΩ | C2 | 2μF | |

gauge forms one part of the feedback loop of a regenerative feedback amplifier, tuned to the bridge-supply frequency, viz. 800 c/s. The amplitude of the a.c. can be made to adjust itself so that the temperature of the wires is kept constant at all pressures. The amount of adjustment required is then a measure of the pressure. The instrument is claimed to be applicable to pressures up to 10 mm Hg and even higher.

An ionization gauge of high sensitivity is reported by Mackinson and Treacy.[77] The ion current is appreciably increased by lengthening the mean free path of the ions by means of a

magnetic field. Readings down to 10^{-5} mm Hg can be taken on an ordinary microammeter. The sensitivity is claimed to be 380 μA per micron, at pressures below 0·8 micron.

In the conventional ionization gauge electrons emitted from a hot filament serve as the ionizing agent. The "Alphatron," manufactured by Messrs. British-American Research, Ltd., replaces the electrons by means of alpha particles liberated from a speck of radium. The gauge is claimed to read linearly for pressures ranging from 10^{-5} mm to 10 mm Hg.
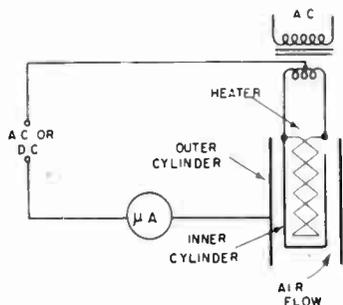

Fig. 30.—*Halogen vapour detector* (*White and Hickey*).

All these ionization gauges operate in at least a partial vacuum. If a platinum filament is heated to incandescence in air at atmospheric pressure, positive ions are emitted. White and Hickey[78] report that within a certain optimal temperature range (around 90°C), the ion current becomes extremely sensitive to the presence of vapours containing halogen compounds, such as freon or carbon tetrachloride. These authors have employed the effect in a detection device for such vapours. Their circuit is shown in Fig. 30.

A promising application of electronic techniques to chemistry is reported by Rius, Balta and Beltran,[79] who applied an R.F. voltage of 2,400 V at 2·7 Mc/s between one electrode in a solution and another immediately above it. The whole apparatus is mounted in vacuo. Currents of 0·1 A were observed and electrolysis occurred, the submerged electrode becoming the cathode. Manganous compounds were oxidized to the manganic state.

Schlesman[80] has devised a system of fractional distillation in the presence of radiant energy, providing a method for separation of fractions comprising two compounds having very nearly identical boiling points. It is based upon differences in the absorption of radiant energy, even of compounds having the same boiling point. A mixture of two such compounds is raised to the common boiling point and passed over a cooled surface. If it is simultaneously exposed to an R.F. field of proper frequency, the compound showing an absorption band in that frequency region will remain vaporized while the other, showing no absorption, is condensed. Good results were obtained with this method in a number of otherwise very intractable cases.

12. Electronic Thermometry

In highly sensitive thermocouple circuits for temperature measurements, particularly if amplification is employed, stray R.F. fields often prove troublesome. Cottrell, Purchas and Winterton[81] have devised a convenient filter arrangement for that purpose, consisting of a low-resistance parallel resonant filter.

The fact that the amplifier valve is essentially a voltage-sensitive device of high input impedance makes its application to low-impedance devices, e.g. thermocouples, somewhat difficult. However, semi-conductors have recently come to the fore which exhibit large negative temperature coefficients and high internal resistances. The variation of the resistance of these thermistors with temperature has been treated by Becker, Green and Pearson,[82] but the simple exponential relationship proposed by these authors yields errors of up to 16·6 per cent., when compared with experimental data. A more recent investigation by Bosson, Gutmann and Simmons[83] proposes a three-constant law which fits the measurements with a standard relative error of fit of better than 1 per cent., and therefore permits accurate interpolation in precise thermometry.

These thermistors are solids. An electrolytic thermistor, using viscous waterglass, has been developed by Gutmann and Simmons.[84] It is three times as sensitive as commercial thermistors, and its cold resistance and sensitivity may be easily controlled. However, while the conduction of solid thermistors is electronic, and therefore allows the use of either d.c. or a.c., electrolytic thermistors are ionic conductors, restricting their use to a.c. circuits.

An electronic thermometer using thermistors is reported by Weiller and Blatz.[85] The circuit is shown in Fig. 31. R_x is the thermistor, con-
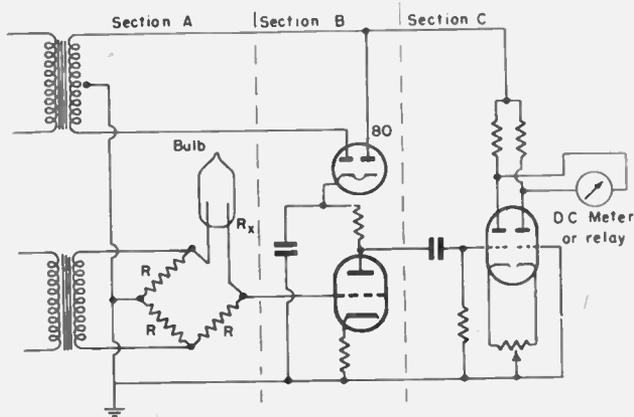
177

Fig. 31.—Electronic thermometer for thermistors (Weiller and Blatz).

stituting one arm of a bridge, which is powered from an a.c. source. Section A represents the temperature-sensitive part, section B is an amplifier, and section C uses a discriminator to produce a pulsating d.c. in either a meter or a relay. The plates of the double triode are fed from the same a.c. source which powers the bridge in section A, thereby providing phase discrimination.

The complicated approximately exponential relationship between resistance and temperature of thermistors has led to the design of a compensating network of fixed resistors to match thermistors to a single resistance v. temperature curve. Such a compensator is reported by Anderson.[86] A mathematical analysis of the non-linear d.c. bolometer circuit has been published by Kerns.[87]

An automatic thermometric recorder has been designed by Herington and Handley,[88] where a thermistor is used as sensing element. The substance is contained in a U-tube and stirred by means of an oscillating gas pressure.

A number of thermostatic control units have been designed, using thermistors and employing electronic amplification. Vodden[89] has developed a control unit of the proportional control type using

gas-filled triodes, capable of controlling up to 250 W heaters. Taylor[90] reports a precision thermistor thermostat capable of holding a heat bath to $0.01°C.$, and a number of similar applications are described by Nguyen Thien-Chi and Suchet.[91]

A high-temperature precision thermostat employing the furnace winding itself as the temperature-sensitive element has been developed by Eubank.[92] It is based upon work described by Roberts.[93] The furnace winding forms part of an a.c. bridge, followed by a high-gain amplifier. The phase angle of the unbalanced bridge controls the firing of a thyratron.

13. The Electronic Balance

An electronic balance indicator based upon radioactivity is reported by Feuer.[94] The principle is illustrated in Fig. 32 which shows the complete instrument. Alpha particles from a radioactive source R_a, attached to the balance arm, strike a 3-plate ionization chamber. If the balance is in equilibrium, the ionization produced between the centre plate and either the upper or lower collector plate of the ionization chamber will be exactly equal. The voltages produced are also equal and cancel if applied to a push-pull amplifier having the centre plate as electric centre. Any departure from balance
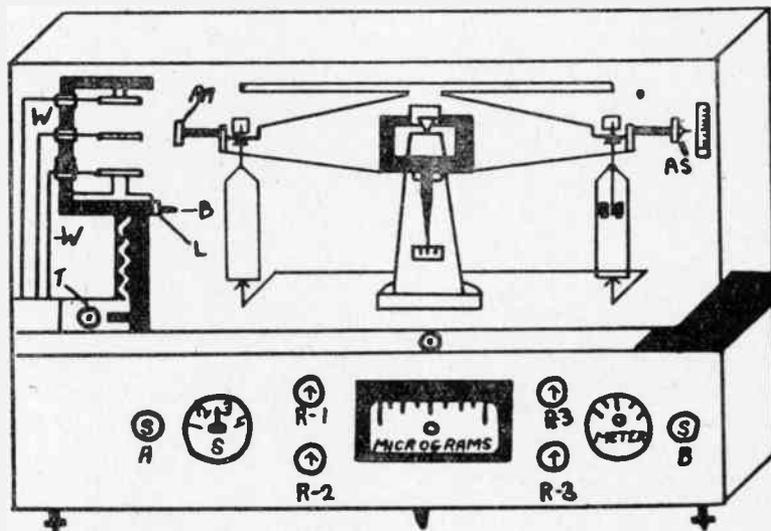

Fig. 32.—Principle of electronic balance indicator (Feuer).

equilibrium will, however, produce a signal. In practice, the single-ended circuit shown in Fig. 33 is used rather than a push-pull arrangement.

A photo-electric balance indicator, which can be attached to any analytical balance, has been developed by Rulfs.[95] A photo-electric cell is placed behind the balance pointer, to which is affixed an opaque vane partially interrupting the illumination. Any deviation from the equilibrium position produces a corresponding change in illumination and in the electric output from the photocell. Using a barrier-layer type cell in conjunction with a 20-0-20 µA meter, the arrangement is said to be capable of being used as a cheap standard balance suitable for semi-micro work.

14. Other Electronic Aids

Electronic techniques have invaded the field of chemistry to such an extent that only a minute selection of interesting applications can here be mentioned. Laszlo[96] employs alternating currents of 50 to 1,000 c/s at 3,500 V in electro-osmosis to achieve separation of liquids with and without permanent dipole moments.

A novel heat-flow meter is described by Hatfield and Wilkins.[97] A small disc of silver-tellurium alloy, coated with copper gauze on both sides, is placed with its plane perpendicular to the direction of heat flow. This causes a small potential difference, proportional to the temperature difference, to be developed between the front and back of the disc. The voltage thus generated is then amplified and measured. An output of 2 mV/ft^2/hour is claimed.

In the "Superstat,"[98] boiler feed water or water which is too hard for any other applications, is subjected to an alternating field. The colloidal state of the hardness salts suspended in the water is claimed to be thus altered in such a way that they are prevented from coagulating and settling out as a hard scale. A fine sludge is formed instead which can easily be removed. The physical basis of the operation of this apparatus appears to be rather obscure.

15. Acknowledgments
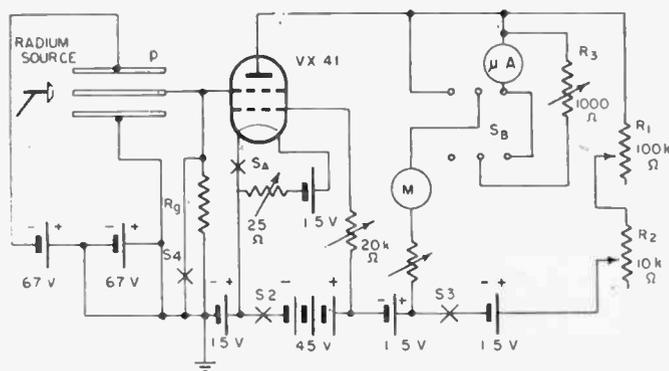
Fig. 33.—Circuit arrangement for Feuer's electronic balance indicator.

16. References

1. F. Gutmann. Proc.I.R.E.Aust., 10, 1949, p. 241; J.Brit.I.R.E., 10, May 1950, p. 194.
2. A. Hemingway and E. B. Brown. Electronics, 23, May 1950, p. 202.
3. K. A. Kraus, R. W. Holmberg and C. J. Borkowski. Anal. Chem., 22, 1950, p. 341.
4. L. I. Belenkii and Ya. B. Rozman. Zavodskaya Lab., 16, 1950, p. 120.
5. C. Morton. Trans. Faraday Soc., 44, 1948, p. 588.
6. M. C. Selby. Electronics, 23, May 1950, p. 110.
7. J. R. Prescott. Rev. sci. Instrum., 20, 1949, p. 553.
8. J. A. Victoreen. Proc.I.R.E., 37, 1949, p. 432.
9. J. Kreuzer. Z.f.Physik, 125, 1948-49, p. 707.
10. R. C. Ellenwood and H. E. Sorrows. Nat. Bur. Stan. J. Res., 43, 1949, p. 251.
11. P. A. Caldwell. Rev. sci. Instrum., 19, 1948, p. 85.
12. J. M. Lafferty and K. H. Kingdon. J. appl. Phys., 17, 1946, p. 894.
13. H. H. Rust and H. Endesfelder. Z. angew. Physik, 2, 1950, p. 39.
14. F. J, Larsen. Iowa State Coll. J.Sci., 24, 1949, p. 66.
15. G. H. Ellis, and C. S. Brandt. Anal. Chem., 21, 1949, p. 1546.
16. A. W. Vance. Rev. sci. Instrum., 7, 1936, p. 489.
17. L. A. Turner. Rev. sci. Instrum., 4,, 1933, p. 665.
18. H. P. Kalmus and M. Sanders. Electronics, 23, July, 1950, p. 84.
19. H. P. Kalmus and G. O. Striker. Rev. sci. Instrum., 19, 1948, p. 79.
20. G. B. Levy, P. Schwed and D. Fergus. Rev. sci. Instrum., 21, 1950, p. 693.
21. F. T. Gucker, Jr., and C. T. O'Konski. Chem. Rev., 44, 1949, p. 373.
22. F. T. Gucker, Jr., and C. T.O'Konski, J. Coll. Sci., 4, 1949, p. 541.
23. B. Breyer, F. Gutmann and S. Hacobian. Aust. J. Sci. Research, 3, p. 558 and p. 567. 1950.

24. Circuit Lab. Report No. 2, Radiotronics No. 142, 45 (April, 1950).
25. See Paper I, ref. 34.
26. J. E. Randles. *Trans. Faraday Soc.*, **44**, 1948, p. 322.
27. P. Delahaye. *J. Phys. Coll. Chem.*, **54**, 1950, p. 402.
28. See Paper I, ref. 33.
29. P. Leveque and F. Roth. *J. Chim. Phys.*, **46**, 1949, p. 480.
30. R. W. Lamphere and L. B. Rogers. *Anal. Chem.*, **22**, 1950, p. 463.
31. F. W. Chambers. *J. sci. Instrum.*, **27**, 1950, p. 292.
32. P. N. Kovalenko. *Zavodskaya*, **14**, 1948, p. 938.
33. E. Hardy. *Compt. Rend.*, **121**, 1895, p. 1116.
34. C. E. Crouthamel and H. Diehl. *Anal. Chem.*, **20**, 1948, p. 515.
35. G. Sivaramakrishnan. *J. Annamalai Univ.*, **3**, 1934, p. 48; Ya. S. Shur. *Physik. Z. Sowjetunion*, **11**, 1937, p. 194.
36. L. Pauling, U.S. Patent 2,416.344, Feb. 25th, 1947; L. Pauling, R. E. Wood and J. H. Sturdivant. *Science*, **103**, 1946, p. 338.
37. C. A. Dyer. *Rev. sci. Instrum.*, **18**, 1947, p. 696.
38. K. F. Luft. *Compt. Rend.*, **230**, 1950, p. 1460.
39. K. F. Luft. *Z. Tech. Physik*, **24**, 1943, p. 97.
40. F. Todt. *Arch. Metallkunde*, **1**, 1947, p. 469.
41. R. L. Werner. *Roy. Aust. Chem. Inst. J. & Proc.*, **17**, May, 1950, p. 208.
42. R. R. Austin, G. K. Turner and L. E. Percy. *Instruments*, **22**, 1949, p. 588.
43. P. Delahaye. *Anal. Chem.*, **20**, 1948, p. 1212.
44. R. H. Muller and J. J. Lingane. *Anal. Chem.*, **20**, 1948, p. 795.
45. O. H. Schmitt. *J. sci. Instrum.*, **15**, 1938, p. 24.
46. F. W. Jensen and A. L. Parrack.¹ *Ind. Eng. Chem. Anal. Ed.*, **18**, 1946, p. 595.
47. W. J. Blaedel and H. V. Malmstadt. *Anal. Chem.*, **22,**, 1950, p. 734.
48. See Paper I, ref. 46; see also ref. 50 below.
49. P. W. West, T. S. Burkhalter and L. Broussard. *Anal. Chem.*, **22**, 1950, p. 469.
50. G. G. Blake. *The Analyst*, **75**, 1950, p. 32; *Aust. J. Sci.*, **11**, 1948, p. 59; *ibid*, **11**, 1949, p. 138; *ibid*, **12**, 1949, p. 32.
51. R. J. Bever, C. A. Crouthamel and H. Diehl. *Iowa State Coll. J. Sci.*, **23**, 1949, p. 289.
52. J. Vergnolle. *Compt. Rend.*, **229**, 1949, p. 831.
53. H. K. Moneypenny. *J. sci. Instrum.*, **26**, 1949, p. 120.
54. H. Nyquist. *Bell Syst. Tech. J.*, **11**, 1932, p. 126.
55. L. Hartshorn. "Radio-frequency Measurements" p. 90, (Chapman & Hall, London, 1940).
56. D. J. D. Ives and R. W. Pittman. *Trans. Faraday Soc.*, **44**, 1948, p. 644.
57. P. Delahaye. *Anal. Chem.*, **20**, 1948, p. 1215.
58. See Paper I, ref. 60.
59. R. B. Fischer. *Anal. Chem.*, **19**, 1947, p. 835.
60. P. Bender. *J. Chem. Education*, **23**, 1946, p. 179.
61. H. Greinacher. *Helv. Phys. Acta*, **21**, 1948, p. 261.
62. G. T. Baker. *Electronic Engng.*, **22**, 1950, p. 280.
63. R. Cooper. *Proc. Phys. Soc.*, B, **63**, 1950, p. 176.
64. B. Breyer and F. Gutmann. *J. Proc. Roy. Soc. N.S.W.*, **83**, 1950, p. 66.
65. M. A. Elliott, A. R. Jones and L. B. Lockhart. *Anal. Chem.*, **19**, 1947, p. 10.
66. J. M. Dotson, J. H. Holden, C. B. Siebert, H. P. Simons and L. D. Schmidt. *Chemical Eng.*, **56**, Oct. 1949, p. 129.
67. F. Gutmann. *J. sci. Instrum.*, **27**, 1950, p. 169.
68. R. Kieselbach. *Anal. Chem.*, **21**, 1949, p. 1578.
69. E. R. Weaver and R. Riley. *Anal. Chem.*, **20**, 1948, p. 216.
70. J. C. Mouzon. *Rev. sci. Instrum.*, **19**, 1948, p. 76.
71. Fielden Electronics Pty. Ltd., Melbourne, Vic., Australia.
72. D. F. Swinehart. *Anal. Chem.*, **21**, 1949, p. 1577.
73. W. P. Ratchford and M. L. Fein. *Rev. sci. Instrum.*, **21**, 1950, p. 188.
74. H. E. Fisher. *Anal. Chem.*, **20**, 1948, p. 982.
75. M. Knudsen. *Ann. d. Phys.*, **34**, 1911, p. 593.
76. H. von Ubisch. *Nature*, **161**, 1948, p. 927.
77. R. E. B. Makinson and P. B. Treacy. *J. sci. Instrum.*, **25**, 1948, p. 298.
78. W. C. White and J. J. Hickey. *Electronics*, **21**, March 1948, p. 100.
79. A. Rius, J. Balta and J. Beltran. *Anales fis. y. quim (Madrid)*, **40**, 1944, p. 14.
80. C. H. Schlesman, U.S. Patent 2,455,812 (1948).
81. C. L. M. Cottrell, J. G. Purchas and K. Winterton. *Nature*, **165**, 1950, p. 857.
82. J. A. Becker, C. B. Green and G. L. Pearson. *Trans. Amer. Inst. Elec. Engrs.*, **65**, 1946, p. 713.
83. G. Bosson, F. Gutmann and L. M. Simmons. *J. Appl. Phys.* **21**, 1950, p. 1267
84. F. Gutmann and L. M. Simmons. *Rev. sci. Instrum.*, **20**, 1949, p. 674.
85. P. G. Weiller and I. H. Blatz. *Electronics*, **17**, July 1944, p. 138.
86. L. J. Anderson. *Bull. Amer. Met. Soc.*, **30**, 1949, p. 192.
87. D. M. Kerbs. *Nat. Bur. Stand. J. Res.*, 1949, **43**, p. 581.
88. E. F. G. Herington and R. Handley. *J. Chem. Soc.*, 1950, p. 199.
89. H. A. Vodden. *J. Soc. Chem. Ind.*, **69**, 1950, p.69.
90. A. H. Taylor, *Electronics*, **23**, July 1950, p. 154.
91. Nguyen Thien-Chi and J. Suchet. *Ann. de Radioelectricité*, **5**, 1950, p. 155.
92. W. R. Eubank. *Rev. sci. Instrum.*, **21**, 1950, p. 845.
93. H. S. Roberts. *Amer. Inst. Physics* "Temperature: Its Measurement and Control in Science and Industry." p. 604. (Reinhold Publishing Corporation, New York, 1941).
94. I. Feuer. *Anal. Chem.*, **20**, 1948, p. 1231,
95. C. L. Rulfs. *Anal. Chem.*, **20**, 1948, p. 262.
96. Z. Laszlo. *J. Chem. Phys.*, **17**, 1949, p. 507.
97. H. S. Hatfield and F. J. Wilkins. *J. sci. Instrum.*, **27**, 1950, p. 1.
98. Superstat Ltd., 155 Minories, London, E.C.3.

PHASE VARIATIONS WITH RANGE OF THE GROUND-WAVE SIGNAL FROM C.W. TRANSMITTERS IN THE 70-130 kc/s BAND*

by

A. B. Schneider, Dipl.-Ing.†

A Paper presented at the Fourth Session of the 1951 *Radio Convention on July 26th at University College, Southampton.*

SUMMARY

Curves of phase variation versus distance for homogeneous and smooth earth of various conductivities are calculated to K. Norton's and H. Bremmer's formulæ. Confirmation of the curves is given by phase measurements within the reactive field of a C.W. radiator and along the base-line extensions of a Decca Navigator Chain. Further, a simple method of assessing the phase variation with distance in the case of inhomogeneous earth is suggested and illustrated by an analysis of readings on the Decca Navigator System.

SYMBOLS

a = radius of the earth in kilometres.

D = distance in kilometres between transmitter and receiver measured along the surface of the earth.

$v = \dfrac{D}{a}$ = angle in radians subtended by transmitter and receiver in the centre of the earth.

c = velocity of light = $2 \cdot 99776 \times 10^8$ m/sec.

f = frequency in cycles per second.

$\lambda = \dfrac{c}{f}$ = wavelength in metres per cycle.

$\omega = 2\pi f$ = angular velocity in radians per second.

ε = dielectric constant of the earth considering air as unity.

σ = conductivity of the earth in e.m.u.

$k_1 = 10^3 \cdot \dfrac{2\pi}{\lambda}$ the wave number.

E_v = vertical component of the electric vector in mV/metre.

E_o = a constant depending on the transmitted power in mV/metre at unit distance.

1. Introduction

In any radio aid to navigation which operates on the principle of phase comparison, a question of primary importance is clearly that of variation of the phase of signals with distance, when they

travel over a spherical earth, under conditions of known frequency of transmission and finite, inhomogeneous ground conductivity.

As a first step to establishing the extent of the phase variations, the existing theoretical solutions for the electromagnetic field based on Maxwell's equations may be used. These solutions all assume ground of homogeneous conductivity and fall into groups for a flat earth and a spherical earth.

2. Historical Note

To illustrate the advances in the philosophy of the phase problems of the electromagnetic field, it is well to recall the original work on the subject, since it is from the basis of the early work that the present paper has been developed. The first work must be attributed to A. Sommerfeld[1] who gave a rigorous solution of the electric field radiated by a dipole over a finitely conducting, flat earth. Later H. Weyl,[2] using a different approach, arrived at a more generalized solution, although in the case of a transmitter and receiver situated at the surface of the earth, the solution may be shown to be identical with Sommerfeld's.

In the case of a spherical earth, it was known, from other physical problems, that the field radiated from a dipole may be expressed in terms of a series of zonal harmonics $P_n (\cos v)$.

The Sommerfeld-Weyl integral and zonal harmonics series had to be converted into a form which was suitable for practical engineering calculations, and this work in itself proved to be a major mathematical task.

Through the medium of the van der Pol[3] transformation, K. Norton[4] finally shaped the integrals of Sommerfeld and Weyl into a formula, for the condition of a flat earth, used in this paper for short distances from the transmitter.

G. N. Watson[5] was the first to convert the series of zonal harmonics into a form usable for practical evaluation, and the major part of later papers is based upon his transformation.

H. Bremmer[6] used a somewhat similar method in order to arrive at his formula for cases where the spherical shape of the earth no longer can be neglected. This later formula is used in this paper for longer distances from the transmitter.

Quite naturally, in the earlier work, interest was directed towards the field intensity, and phase was almost completely neglected until the publication of Norton's work, where generalized curves of phase variation were shown.

The object of the present paper is to extend the work of Norton and Bremmer, with particular reference to phase variations in the frequency band between 70 and 130 kc/s.

3. Sketch of Derivation of Bremmer's Solution

A practical transmitter working in the 70-130 kc/s frequency band will have an antenna system which can be considered as approximating an infinitely short vertical aerial carrying a current $I.e^{-j\omega t}$ of infinite amplitude in such a manner that the product of current and antenna length, or the moment of the aerial, is finite. Were the earth not present, the field surrounding such an aerial would be the undisturbed primary electromagnetic field, characterized by the electric vector E and magnetic vector H. Both E and H are each given in space by a set of three components depending on the chosen system of co-ordinates. Any existing electromagnetic field is determined in the air as well as in the earth by the scalar wave equation obtained from Maxwell's equations. Their solution is in general quite a difficult vectorial problem. To facilitate the mathematical procedure a Hertzian radial vector $r\Pi$ is introduced; it originates at the aerial and is proportional to $e^{jk_1 D}/D$. The scalar value of the Hertzian vector satisfies the scalar wave equation.

$$(\Delta + k^2)\Pi = 0 \quad \ldots\ldots\ldots\ldots(1)$$

where $\Delta = \dfrac{\partial^2}{\partial x^2} + \dfrac{\partial^2}{\partial y^2} + \dfrac{\partial^2}{\partial z^2}$

182

is the Laplacian operator and

$$k^2 = \frac{\varepsilon\omega^2 + j4\pi\sigma\omega}{\sigma^2}$$

with the dielectric constant ε and conductivity of the earth σ expressed in electrostatic units.

The six components of E and H may be obtained from the Hertzian vector by means of differentiation. Thus

$$E = \text{curl curl } (r\Pi)\, e^{-j\omega t} \quad \ldots\ldots\ldots\ldots(2a)$$

$$H = \frac{ck^2}{i\omega} \text{curl } (r\Pi) . e^{-j\omega t} \quad \ldots\ldots\ldots\ldots(2b)$$

The components of the field vectors for the primary field could be worked out from equations 2 in spherical co-ordinates with the axis directed along the aerial, the propagation constant then being real and equal to the wave number k_1.

The presence of the earth will disturb the primary field, so that a different radial Hertzian vector has to be determined whose scalar quantity must satisfy the conditions set by the presence of the earth. These are known as the boundary conditions and are as follows:—

(1) Above the surface of the earth, $r\Pi$ must satisfy the scalar wave equation $(\Delta + k_1^2)\Pi = 0$ as before, with the additional condition that it must be zero at infinity; under the surface of the earth $r\Pi$ must satisfy the scalar wave equation $(\Delta + k_2^2)\Pi = 0$.

(2) The tangential components of the field vectors E and H must be continuous across the boundary between the earth and outer space.

(3) At the antenna itself, $r\Pi$ must become infinite.

These boundary conditions describe completely the required Hertzian vector; unfortunately it is impossible to express it by an integral. One method of approach is to construct outside the earth the primary field Π_{pr} in a series of zonal harmonics and add to it a similarly constructed contribution from the secondary field Π_{sec} reaching the outer space from under the earth's surface. The contribution from the secondary field is always finite.

The expression for the total field Π_{tot} may then be written as

$$\Pi_{tot} = \Pi_{pr} + \Pi_{sec} = \sum_{n=0}^{\infty} (2n + 1) f(n) P_n (\cos v)$$
$$\ldots\ldots\ldots\ldots(3)$$

and it comprises a mixture of zonal harmonics, Bessel and cylindrical functions.

In this series, a predominant part is played by a parameter k_1a. The greater the numerical value of this parameter, the slower is the convergence of the series; also the most important terms of this series are those in which n is of the order of the value of k_1a. In the frequency band 70-130 kc/s for instance, k_1a ranges from 9500 to 17000, which makes the series impracticable to compute in the normal way, although probably some electronic calculator could deal with the problem.

Bremmer transforms this series into another:
$$\Pi_{tot} = S_{-1} + S_0 + S_1 + S_2 + \ldots\ldots\ldots\ldots(4)$$
and gives the following interesting physical interpretation:

The component S_{-1} now represents the new primary field, composed of the sum of the direct ray and that reflected from the earth's surface. During reflection a fraction of the wave is refracted into the earth and part of it may emerge again as the component S_0. In this way several internal reflections and subsequent refractions may take place giving rise to refracted components S_1, S_2 and so on.

In the radio problem only the term S_{-1} is of interest, but the other terms disappear completely only for a perfectly conducting earth.

As the next step, Bremmer considers the component S_{-1} as representative of the whole field, neglecting completely the "rainbow" terms S_0, S_1 and now, following Watson, transforms S_{-1} first into a complex integral whose path of integration embraces the positive part of the real axis and then, changing the sign of n below the real axis and replacing $(n - \frac{1}{2})$ by ν, obtains the integral

$$S_{-1} = j \int_L \frac{\nu + \frac{1}{2}}{\sin(\nu\pi)} g(\nu) P_\nu \{\cos(\pi - \nu)\} \, d\nu \ldots(5)$$

with the integration path lying completely above the real axis. Closing the path of integration upwards at infinity on the n-plane, the value of S_{-1} becomes equal to the sum of residues which are found above the real axis. The last series, which is still in a very complicated form containing cylindrical functions and zonal harmonics, converges more quickly than the original series of zonal harmonics.

The cylindrical functions appearing in the final residue series are approximated by the Hankel or third-order saddle-point approximation, the zonal harmonics are approximated by the saddle-point approximation, and sin v by v. As a result, there emerges Π_{tot}, from which by differentiation one eventually obtains the final formula for the vertical component E_v of the electric vector **E**. Eqn. (9) gives part of the formula for computation of phase correction θ.

It may be shown that, for shorter distances, Bremmer's formula can be transformed directly into Sommerfeld's; therefore it may be considered the more general.

4. Phase Variation Over Homogeneous Soil

Both Norton's and Bremmer's formulæ may be expressed in a form explicitly exposing the three basic components:

(1) Undisturbed primary field,

(2) Complex attenuation factor due to the presence of a spherical finitely conducting earth, and

(3) Function of time dependence,

$$E_v = \underbrace{(E_o/D) \cdot e^{jk_1D}}_{\text{undisturbed field}} \cdot \underbrace{|A| \cdot e^{j\theta}}_{\text{attenuation factor}} \cdot \underbrace{e^{-j\omega t}}_{\substack{\text{function of time} \\ \text{dependence}}}$$

$$\ldots\ldots\ldots\ldots(6)$$

The argument of E_v is the phase Φ:

$$\Phi = (k_1D + \theta) - \omega t \text{ radians} \ldots\ldots\ldots\ldots(7)$$

where θ is the phase correction to be added to the "standard phase" k_1D. The function of time dependence is given here as $\exp(-i\omega t)$, which slightly simplifies the presentation of phase correction curves. Phase measurements were carried out with the aid of the Decca Navigator System, not on the actual transmitted frequencies but on the harmonics (up to the sixth) of the transmitted frequencies. The harmonics were obtained in the Decca receiver itself by suitable distorting circuits. The phase meters used are capable of phase discrimination within an accuracy of $\pm 1/100$ of a cycle or ± 3.6 deg. of phase at the comparison frequency. Taking the case of the sixth harmonica as the most stringent, a phase discrimination of ± 0.6 deg. of the transmitted frequency is obtained.

The curves of phase correction θ given in Figs. 1, 2, 3 and 4 were calculated with a computational accuracy of $\pm \frac{1}{2}$ deg. of phase at the transmitted frequency.

FIGURE 1.

PHASE CORRECTION θ FOR THE
TRANSMITTED FREQUENCY 70·83 kc/sec
AND FOR THE SIXTH HARMONIC

FIGURE 2.

PHASE CORRECTION θ FOR THE
TRANSMITTED FREQUENCY 85 kc/sec
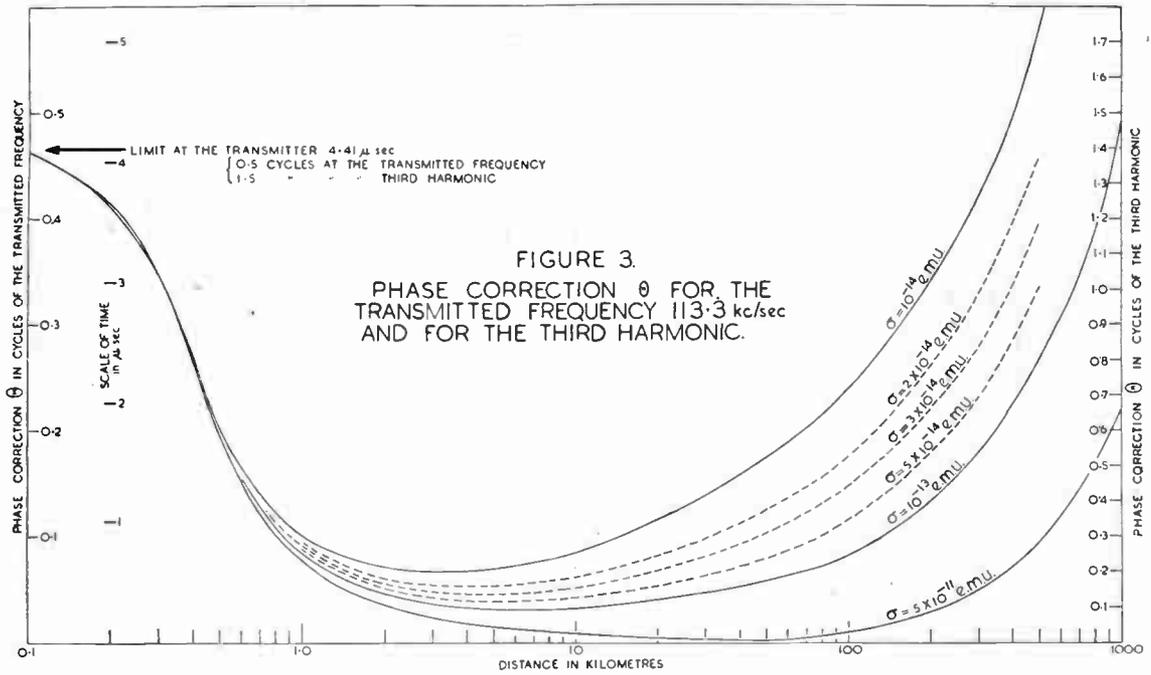AND FOR THE THIRD, FOURTH AND
FIFTH HARMONIC.

184

FIGURE 3.
PHASE CORRECTION θ FOR THE
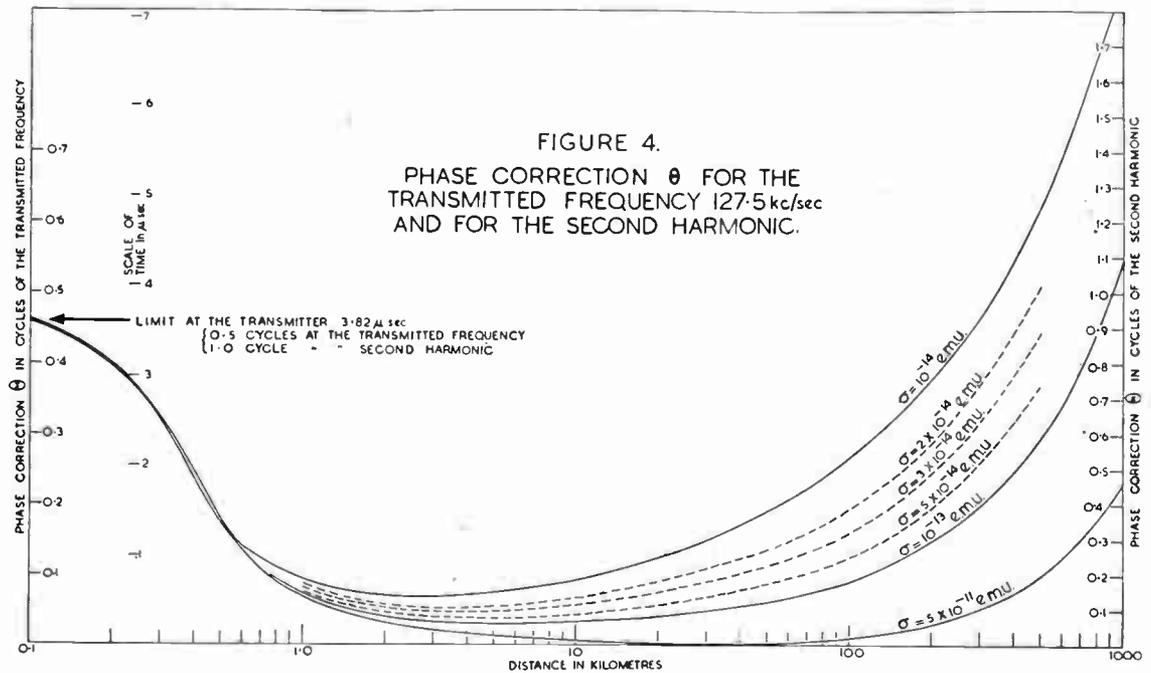TRANSMITTED FREQUENCY 113·3 kc/sec
AND FOR THE THIRD HARMONIC.

FIGURE 4.
PHASE CORRECTION θ FOR THE
TRANSMITTED FREQUENCY 127·5 kc/sec
AND FOR THE SECOND HARMONIC.

185

For short distances from the transmitter, Norton's formula was used in the following form:[7]

$$\tan \varphi = \frac{f(p,b) \sin \varphi + (k_1 D)^{-1}}{f(p,b) \cos \varphi - (k_1 D)^{-2}} \dots \dots (8)$$

where

$$f(p,b) \sin \varphi = -2p \sin b + \frac{(2p)^2}{1 \cdot 3} \sin 2b \dots$$

$$+ \sqrt{\pi p} \cdot e^{-p \cos b} \cdot \cos \left(\frac{360°}{2\pi} p \sin b - \tfrac{1}{2}b \right)$$

$$f(p,b) \cos \varphi = 1 - 2p \cos 2b + \frac{(2p)^2}{1 \cdot 3} \cos 2b$$

$$- \frac{(2p)^3}{1.3.5} \cos 3b + \dots$$

$$+ \sqrt{\pi p} \cdot e^{-p \cos b} \cdot \sin \left(\frac{360°}{2} p \sin b - \tfrac{1}{2}b \right)$$

$$p = \frac{k_1 D}{2} \cdot \frac{\cos^2 b''}{x \cos b'}$$

$$x = \frac{1 \cdot 797.10^{21} \sigma}{f}$$

$$\tan b' = \frac{\varepsilon - 1}{x} \text{ and } \tan b'' = \frac{\varepsilon}{x}$$

$$b = 2b'' - b'$$

This formula takes into account the induction and static fields in the immediate vicinity of the transmitter.

Phase corrections for longer distances were computed to Bremmer's formula and a sufficient number of components of the residue series was taken to preserve an overall accuracy of computations of $\pm \tfrac{1}{2}$ deg. Bremmer's expression given here differs slightly from that given in his book.[6] It is due to the fact that, being concerned with the amplitude only, he accepts an arbitrary phase angle, obtained as a ratio of the primary undisturbed field to the secondary field disturbed by the presence of the earth, omitting the expression $\sqrt{j} \cdot e^{jk_1 D}$. The phase correction, following Bremmer and neglecting induction and static fields, is computed as the argument of the following expression:

$$\sum_{s=0}^{\infty} (2\tau_s - 1/\delta^2)^{-1} \cdot e^{j(x\tau_s + 45°)} \dots \dots (9)$$

where

τ_s = complex numbers whose value depends exclusively on the parameter δ; series for computing τ_s are to be found in the Appendix.

$$\delta = K \exp \left[j(135° - \chi) \right]$$

$$K = \frac{2 \cdot 924 \cdot 10^{-3} \lambda^{\frac{1}{2}} \sqrt{\varepsilon^2 + 3 \cdot 6 \cdot 10^{25} \sigma^2 \cdot \lambda^2}}{\sqrt[4]{(\varepsilon - 1)^2 + 3 \cdot 6 \cdot 10^{25} \cdot \sigma^2 \cdot \lambda^2}}$$

$$\chi = \tan^{-1} \frac{\varepsilon}{6.10^{12} \cdot \sigma . \lambda} - \tfrac{1}{2} \tan^{-1} \frac{\varepsilon - 1}{6.10^{12} \cdot \sigma . \lambda}$$

The curves of θ computed by the means of the two formulæ are reasonably coincident with each other at the intermediate distances.

Figures 1, 2, 3 and 4 show the curves of θ computed for 70·83, 85, 113·3 and 127·5 kc/s respectively for various conductivities of the earth. The scales at the left-hand side of the Figures are expressed in cycles of the transmitted frequency and the scales on the right-hand side are in cycles of the n-th harmonic actually used for the phase comparison measurements in the Decca Navigator System. An additional scale of time is provided on each drawing and the advantage of this conception is discussed in the next paragraph.

5. Phase Velocity Over a Homogeneous Earth

The phase Φ in equation 7 may be written as the product of the angular velocity and time:

$$\Phi = (k_1 D + \theta) - \omega t = (\omega/c.D + \theta) - \omega t$$
$$= \omega \underbrace{\left[(D/c + \theta') - t \right]}_{\text{time}} \dots \dots \dots (10)$$

Here $\theta' = \theta/\omega$ is the time correction in seconds to be applied to the time D/c which would be necessary for the phase-front moving with the speed of light to reach a point on the earth's surface distant D km from the transmitter. This implies that, since a longer time is now necessary for the equiphase front to cover the distance D, the phase velocity over a finitely conducting earth is less than that of light.

The condition for remaining on the face of the same equiphase surface is that $d\Phi = 0$, that is:

$$d\Phi = \frac{\partial \Phi}{\partial D} \cdot dD + \frac{\partial \Phi}{\partial t} \cdot dt$$

$$= \omega \left[\left(\frac{1}{c} + \frac{\partial \theta'}{\partial D} \right) \cdot dD - dt \right] = 0 \dots (11)$$

The instantaneous phase velocity (I.P.V.) is obtained by definition from

$$V_i = \frac{dD}{dt} = \frac{c}{1 + c \dfrac{\partial \theta'}{\partial D}} \text{ km/sec} \dots \dots (12)$$

186

If the curves of time correction θ' in seconds versus D in km are drawn to a linear scale, $\partial\theta'/\partial D$ is simply obtainable graphically as the slope of the curve at any point.

Rewriting equation 12, one obtains

$$\partial\theta' = \frac{c - V_i}{c \cdot V_i} \cdot \partial D \dots\dots\dots\dots\dots(13)$$

from which the scale of velocities was constructed in Fig. 5.

The I.P.V. is found in Fig. 5 by drawing a parallel through the origin 0 to the tangent at the required point P, up to the intersection with the scale of velocities.

At sufficiently large values of D, where only the first component of the Bremmer residue series is significant, the time correction θ' is virtually proportional to D; that is to say, the curve of θ' degenerates then into a straight line. Now $\partial\theta'/\partial D$ becomes constant and the I.P.V. settles down to a constant value which is smaller than c.

Norton's curves of θ' for a flat earth become parallel to the axis of D at large distances and the inference would be that the I.P.V. reaches the value of c at points sufficiently far away from the transmitter. These two inferences are the basic difference between the two solutions as far as the phase is concerned.
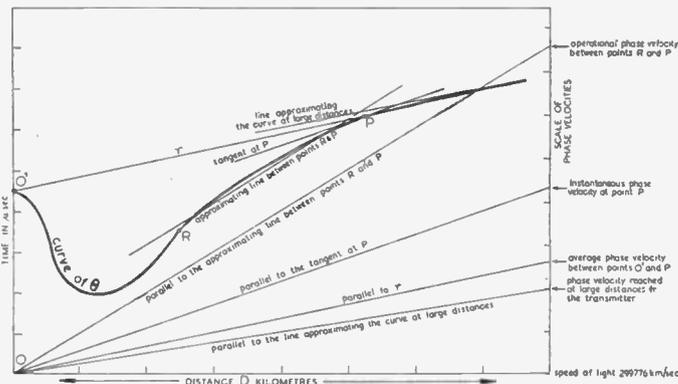

Fig. 5.—Phase velocity diagram.

The advantage of using θ' expressed in seconds rather than in cycles becomes apparent in Fig. 6 where curves of θ' for different frequencies and conductivities can be compared directly with each other. It is evident that the worse the conductivity the lower is the I.P.V. reached by the signal at large distances (cf. Fig. 7).

In addition to I.P.V. two more phase velocities can be defined: the average and the operational phase velocity.

The average phase velocity V_a for the path from the transmitter to the receiving point P may be obtained from the scale of velocities in Fig. 5 by connecting point 0' through a line r and drawing parallel to r through the origin 0.

The operational phase velocity within a certain region, for instance from point R to point P in Fig. 5, may be obtained by by approximating the section of the curve θ' from R to P by a straight line and then drawing a parallel to this line through the origin 0. The computation of charts is greatly simplified by assuming a constant phase velocity, and charts computed for the operational phase velocity would give the smallest errors within the region for which the operational phase velocity was determined.

6. Practical Phase Measurements Over Homogeneous Earth

A number of experiments have been carried out in South-West England[8] and in Sweden[9] in order to test the validity of the curves of θ computed on the assumption of a homogeneous earth, using the Decca phase comparison technique. Two C.W. signals transmitted on different frequencies are converted in the receiver to a common comparison frequency and the phase difference of the two signals on the common value is displayed on a phase meter called a Decometer. Lines of equiphase-difference form the position lines from which the navigational aid is derived.

The experiments were divided into two parts :—

(a) investigations of the induction and static fields

(b) investigation of the distant zone.

6.1 Induction and Static Fields

(i) Two C.W. signals on the frequencies $72 \cdot 916$ and $87 \cdot 5$ kc/s, giving the comparison frequency $447 \cdot 5$ kc/s, were transmitted from the same aerial. The Decca position lines in this case were circles centred on the transmitter and were predicted by subtracting the values given by the curve for conductivity 5×10^{-14}

187

Fig. 6.—Time correction θ′ in μ sec versus range D in km for frequencies 70·83, 85, 113·3 and 127·5 kc/s and conductivities 5 × 10⁻¹¹, 10⁻¹³ and 10⁻¹⁴ e.m.u.
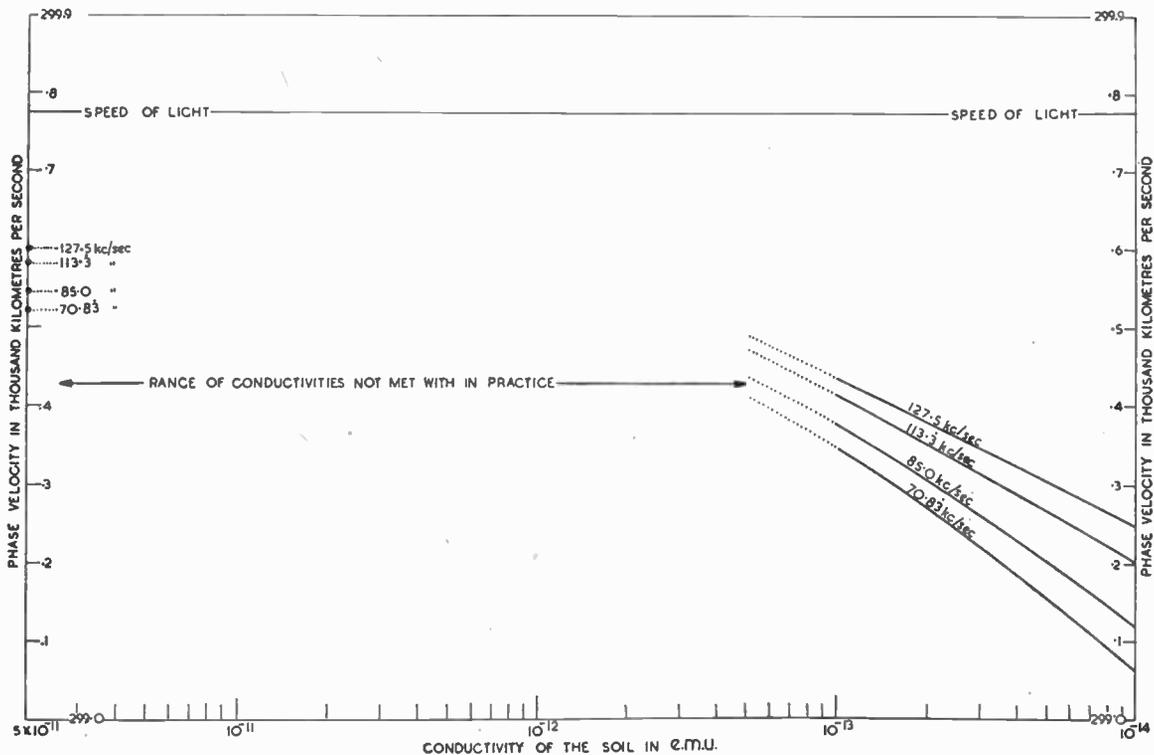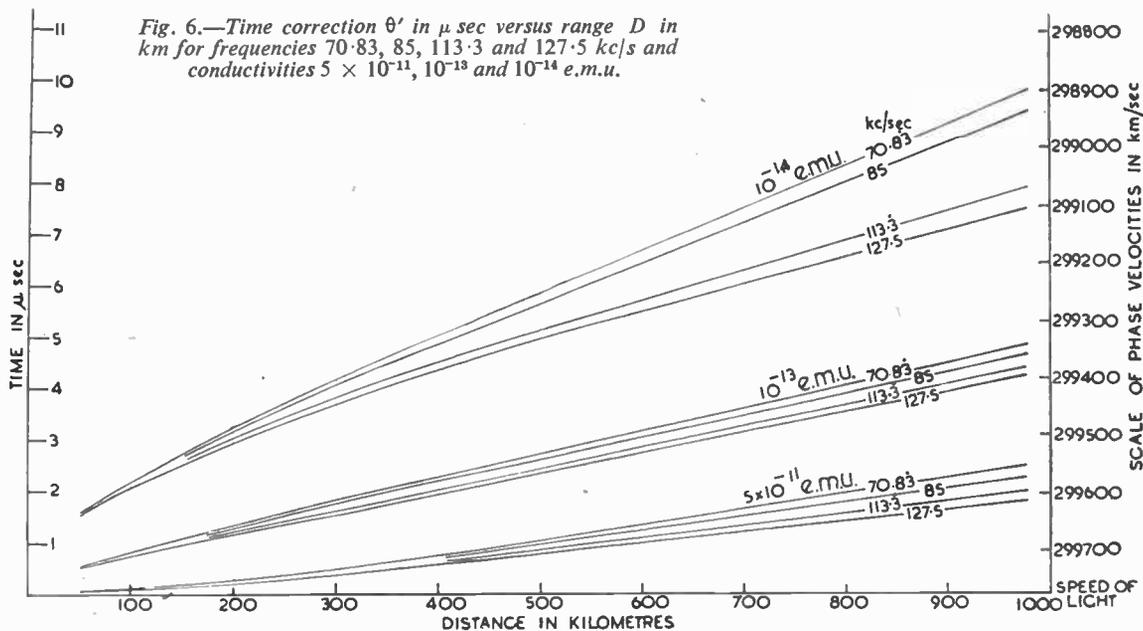

Fig. 7.—Phase velocity at long range versus homogeneous soil conductivities.

188

e.m.u. in Fig. 1 from that for the same conductivity in Fig. 2 in units of the sixth and fifth harmonics respectively. Observations were taken at ranges up to 100 km and the results are plotted as shown in Fig. 8, together with the theoretical curve.

To obtain the best fit near the transmitter, the theoretical curve has been shifted up by 0·05 cycles of the comparison frequency relative to its position based on the average observed readings beyond 10 km.

Subject to this adjustment (since readings beyond 10 km do not come under the homogeneous earth heading), it will be seen that the fit near the transmitter is extremely good, the standard deviation of the errors being only 0·015 of a cycle of the comparison frequency up to the distance of 10 km.

(ii) Two C.W. signals on frequencies 87·5 and 116·6 kc/s (comparison frequency 350 kc/s) were transmitted from two different aerials, distant from each other by about 98 km. Equiphase lines round each transmitter are circles and the phase Φ corresponding to each radius may be found from equation 7 as $\Phi = (k_1 D + \theta)$. By connecting the equiphase-difference points the Decca position lines round the 87·5 kc/s transmitter were drawn for a conductivity equal to 5×10^{-14} e.m.u. and observations made at points shown in Fig. 9. The general agreement between theoretical and observed values, down to ranges of 200 yd or so from the transmitter is good, the standard deviation of the errors being less than 0·05 cycle of the comparison frequency.

6.2. *Investigation of the Distant Zone*

It is very difficult to stage an experiment to test the theory over a homogeneous earth in the distant zone. The nearest approach to the ideal conditions would be to let two signals, whose relative phase is being compared, run over the same path. Such conditions arise along the base-line extensions of a Decca Navigator Chain.

A surveying chain in Sweden[9] offered almost perfect facilities for the experiment. The conductivity of the earth along the base-line extensions was of the order of 10^{-14} e.m.u.
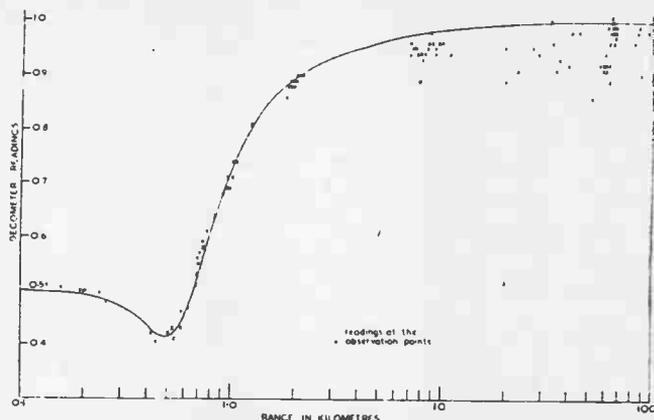

Fig. 8.—*Decca S.W. experimental chain. Comparison of predicted and observed readings in terms of cycles of the comparison frequency 447·5 kc/s. Both frequencies 72.916 and 87·5 kc/s radiated from the same aerial.*

making the order of phase corrections very much greater than the errors of the instruments. Figs. 10 and 11 show the expected phase corrections versus distances for the comparison frequencies 265 and 354 kc/s and various earth conductivities. The curves were set to arbitrary zeros at points shown on the drawings. The experiment shows a fair agreement with the theory.

7. Smooth, Inhomogeneous Earth

In the case of a C.W. wave travelling a distance D over a spherical, smooth and homogeneous earth characterized by the electric constants σ_1, ϵ_1, let the phase correction to be applied to the standard phase $k_1 D$ be θ_1; similarly if the distance D is over earth characterized by the electrical constants σ_2, ϵ_2 the phase correction will be θ_2. Suppose now that the distance D is broken up for the sake of simplicity into only two paths D_1 and D_2 km characterized by the electrical constants σ_1, ϵ_1 and σ_2, ϵ_2 respectively. The phase correction θ_t to be applied in the case of the composite path must have a value, one feels intuitively, lying somewhere between the values of θ_1 and θ_2. To the author's knowledge there does not exist a rigorous mathematical solution to this problem. In default of theory a practical alternative is to extend G. Millington's[10] idea to cover the problem of phase. For the amplitudes of groundwave he suggested a semi-empirical value of the geometric mean of the amplitude obtained by interchanging paths of

189

Fig. 9.—Theoretical equiphase-difference pattern drawn for the comparison frequency of 350 kc/s for conductivity of 5×10^{-14} e.m.u.
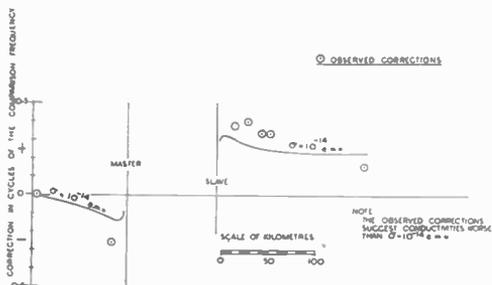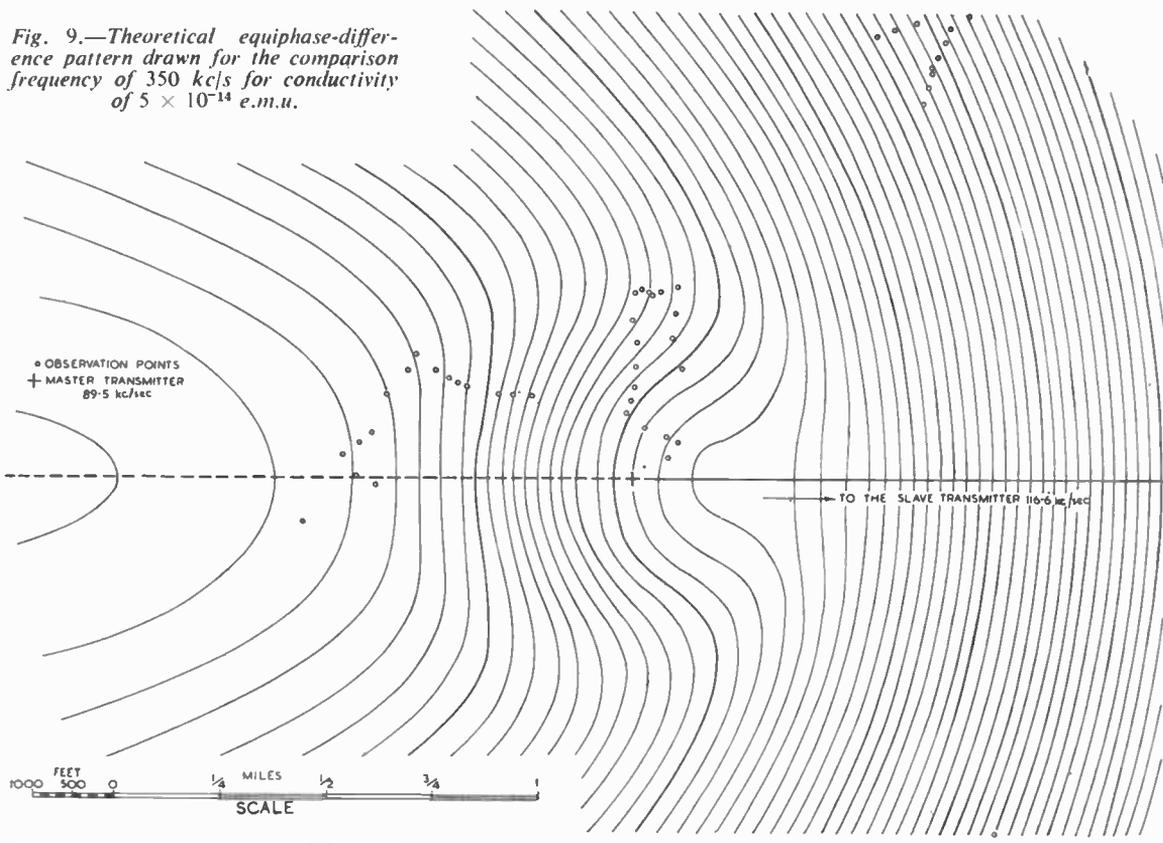

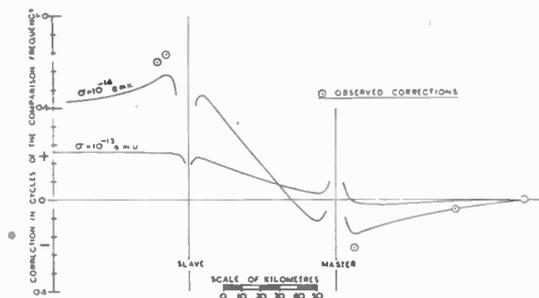Fig. 10.—Decca survey chain in Sweden: comparison frequency 265 kc/s.

Fig. 11.—Decca survey chain in Sweden: comparison frequency 354 kc/s.

different conductivities and sliding up or down curves of field strength calculated for a smooth and homogeneous earth.

If the two fields are $E_1 . e^{j(k_1D + \theta_I)}$ and $E_2.e^{j(k_1D + \theta_{II})}$ then the geometric mean of the two is equal to $\sqrt{E_1E_2} . e^{j\left(k_1D + \frac{\theta_I + \theta_{II}}{2}\right)}$ or the phase

correction is equal to the arithmetic mean of the two corrections.

The following example illustrates the practical procedure:

D_1 and D_2 in Fig. 12 represent stretches of land and sea respectively. The appropriate curves of phase corrections are to be

190

taken from Fig. 6 where the effect of the reactive field is neglected. A curve of θ'_1 corresponding to land conditions is chosen and followed along the distance D_1, then a curve of θ'_2 corresponding to sea conditions is selected and slid up till it meets the end of curve θ'_1 at the distance D_1; the curve of θ'_2 is then followed along the distance D_2, obtaining total phase correction θ'_I. A similar procedure is repeated with the distances D_1 and D_2 reversed; first comes the distance D_2 over the sea and then D_1 over land. In general a different phase correction θ'_{II} is obtained in the second case.

Finally $\theta'_t = (\theta'_1 + \theta'_{II})/2$ is accepted as the required phase correction along the mixed paths D_1 and D_2.

In Fig. 13 are shown curves of the combined correction θ'_t for different lengths of sea-land or land-sea paths, for frequency equal to 85 kc/s, $\sigma_1 = 5 \times 10^{-11}$ and $\sigma_2 = 10^{-14}$ e.m.u.

The shortcomings of this method are obvious and are exactly the same as in Millington's problem. It is true

the intermediate region is negative. There is a corresponding slowing down of the phase velocity when crossing a sea-land boundary.

8. Practical Phase Measurements Over Inhomogeneous Earth

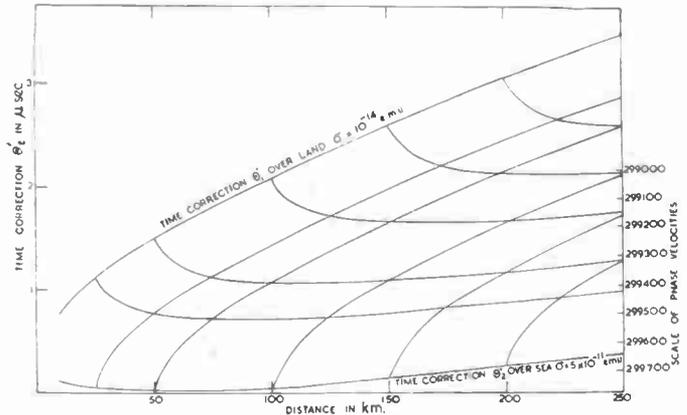The usefulness of this intuitive procedure is best illustrated by the experimental evidence.

Fig. 13.—*Time correction θ'_t for mixed sea-land and land-sea paths for frequency 85 kc/s.*
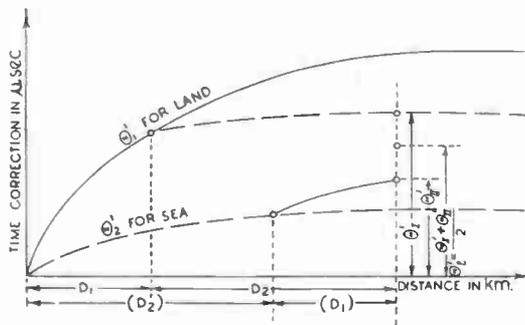

Fig. 12.

that the conditions of reciprocity are satisfied and that the combined curves in Fig. 13 prove that some time after the boundary is passed the phase correction becomes conscious of the electric constants of the new path, but the criticism is that it happens too suddenly, immediately after the boundary has been crossed. Another interesting point may be noted, that corresponding to Millington's field recovery, when crossing the land-sea boundary, there is an accompanying phase velocity acceleration and the instantaneous phase velocity reaches values higher than c, because the slope of the θ'_t curves in

Let A and B in Fig. 14 represent Master and Slave transmitters of a Decca Chain and P an observation point, distant S_A and S_B km from A and B respectively. The time taken by an equiphase front to travel from A to P will be equal to $(S_A/c + \theta'_1)$ seconds where θ'_1 is the time correction obtained by the previously described method; similarly the equiphase front arrives at P from B in $(S_B/c + \theta'_{II})$ seconds. The theoretical time difference Δ_t of the arrival of the two signals is therefore:

$$\Delta_t = \left(\frac{S_A}{c} + \theta'_1\right) - \left(\frac{S_B}{c} + \theta'_{II}\right)$$
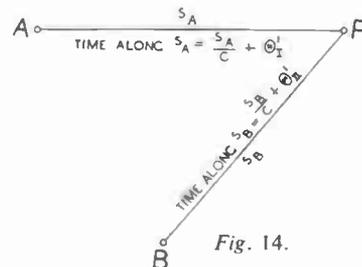$$= \frac{S_A - S_B}{c} + (\theta'_1 - \theta'_{II})$$

Fig. 14.

191

Δ_t is made up of two components:

(1) $\dfrac{S_A - S_B}{c}$ .. the ideal time difference of the arrival of the two signals built upon the velocity of light c,

(2) $(\theta'_I - \theta'_{II})$ .. the theoretical time correction to be applied to that ideal value in order to cater for the imperfections of the earth's conductivity.

An actually observed time difference of the two signals at point P, measured with the aid of a Decometer, contains three components:

(1) $\dfrac{S_A - S_B}{c}$ .. the already mentioned ideal time difference,

(2) .. .. the true time correction due to the electrical constants of the earth,

(3) .. .. probably a constant time delay M (called the monitoring figure) which is introduced at the Slave station to make the actual reading at the monitor point agree with some arbitrary, predetermined value.

For analysis purposes the decometer readings which are originally in cycles, are converted into time differences in seconds by dividing by the comparison frequency in c/s. Further, as the discrepancies from the ideal time differences are small the usefulness of any calculated correction can easily be appreciated by eliminating the first term from both the computed and observed results. The residual components of the observed values are then plotted as abscissae against the theoretical corrections as ordinates.

In the case of a perfect agreement of the observations with the theory, all the plotted points will lie along a straight line, subtending 45 deg. with the axes and displaced sidewards by a constant equal to the monitoring figure M.

Figure 15 shows the theoretically predicted and observed time corrections plotted for several points taken at random from the English Decca Chain on comparison frequencies 255 and 425 kc/s. The monitoring figures were extracted before plotting. Bearing in mind the uncertainty with regard to the conductivity contours, the agreement of observations with theory is very good, the standard deviation being of the order
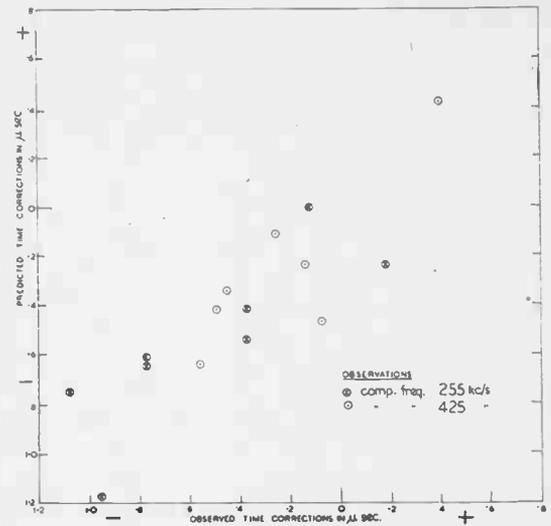
Fig. 15.—*Theoretically predicted time corrections v. observed corrections.*

of 0·2 μsec, which corresponds to distance difference of 60 metres.

9. Estimation of Phase Velocity for Chart Computations

It has been mentioned before that the adoption of a uniform phase velocity greatly simplifies the calculation of charts for use with radio navigational aids working on the phase comparison principle.

From the foregoing analysis it is clear that the operational phase velocity is generally lower than c and as computations for a Decca system must be put in hand well before the time when the system is to come into operation, it was therefore necessary to evolve a method of estimating the best phase velocity to use. One such method is as follows:—

When the positions of the transmitters have been decided, representative observation points within the coverage of the system are selected and marked on a map on which ground conductivities are shown. For each of the chosen points the path distances to Master and Slave are measured and the estimated time correction for each path determined. The difference between the time corrections for the Master and Slave paths for each point are then plotted as ordinates against the corresponding distance differences. A best straight line is fitted through the obtained points, and the slope of

this line' determines the required chart phase velocity.

The accuracy of the estimate can be checked at a later date when observations are available at a large number of points, by the same method, but substituting the observed time corrections for those predicted theoretically.

Figure 16 illustrates the method applied to the green pattern (comparison frequency equal to 253.9 kc/s) of the North British Decca Chain The straight line shows the best fitting line derived theoretically, before the chain was put into operation. The phase velocity indicated by this line was 299,200 km/s. The plotted points were obtained from observations during trials, after the chain had been put into operation. Owing to the wide variations in soil conductivities met with in this case, the results, as expected, show a considerable scatter, but it is clear that a marked overall improvement is obtained by using the selected phase velocity.

10. Conclusions

It is known that the phase angle and hence the phase correction of a C.W. signal cannot be measured directly because of the time factor, $\exp(-j\omega t)$. One way to eliminate the time factor is to use the method employed by the Decca Navigator System, where a standing wave pattern from two synchronized transmitters is formed and the phase correction can be assessed indirectly. On the basis of numerous observations it is probably true to say that the theoretical curves for homogeneous earth are good to the order of accuracy of the measurements. It must be emphasized that the experiments are handicapped by many factors oversimplified by the theory or impossible to account for practically, such as refraction in the troposphere, unsmooth earth, uncertainty of the conductivity contours and difficulty of exact assessment of the geographical position of the transmitter and observation point, leading to wrong
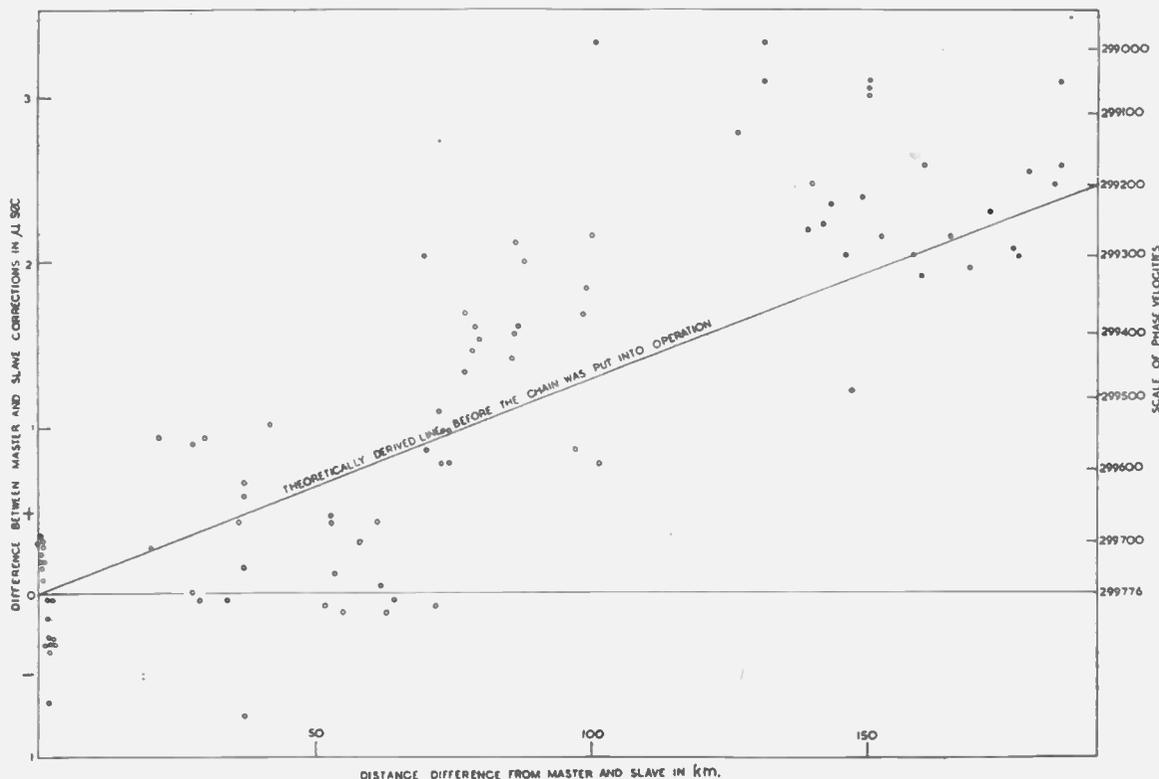

Fig. 16.—*North British Decca Chain: results of observations on the comparison frequency* 253·9 *kc/s.*

distances between them. The method suggested in this paper for dealing with the problems of inhomogeneous earth proved very successful in practical analysis. It is simple, quick in use and gives the right order of predicted phase velocities for chart computations; it also allows the areas most likely to exhibit larger errors to be foreseen. No doubt the rigorous mathematical solution to the problem of inhomogeneous earth will be found in time and some semi-graphical methods will be evolved to short-cut the extremely laborious computations invariably connected with the electromagnetic field problems. However, it is doubtful whether all the factors required for a real appreciation of the exact solution will ever be known sufficiently well for the exact solution to be much more effective and useful in practice than that outlined in this paper.

11. Acknowledgments

The author is indebted to the Decca Navigator Co., Ltd., for permission to publish this paper, to Mr. W. T. Sanderson for his encouragement during the preparation of the paper and to Messrs. R. Martin and H. Oliver who made the computations. The paper reviews a lot of thoughts and ideas developed during the last five years and it is impossible to mention all those whose work was used, and to whom the author offers his sincere thanks.

12. References

1. Sommerfeld, A.: *Ann. Physik*, **28**, 1909, p. 665; "The Propagation of Waves in Wireless Telegraphy," *ibid.*, **81**, 1926, p. 1135-1153.

2. Weyl, H.: *Ann. Physik*, **60**, 1919, p. 481.

3. Pol, B. van der, and Niessen, K. F.: *Ann. Physik*, 1930, p. 273, equations (21) and (23a).

4. Norton, K. A.: "The propagation of radio waves over the surface of the earth and in the upper atmosphere, Part I." *Proc. Inst. Radio Engrs*, **24**, 1936, pp. 1367-1387. Part II, *ibid.*, **25**, 1937, pp. 1203-1236.

   "The calculation of ground-wave field intensity over a finitely-conducting earth." *ibid.*, **29**, 1941, pp. 623-639.

5. Watson, G. N.: *Proc. Roy. Soc.*, **95**, 1918, p. 83.

6. Bremmer, H.: "Terrestrial Radio Waves" (Cleaver-Hume Press, London, 1949).

7. A.S.R.E. Monograph No. 817.

8. Decca Navigator Publ. Plans 108 (1950).

9. Decca Navigator Publ. Plans 92 (1949).

10. Millington, G.: "Ground-wave propagation over an inhomogeneous smooth earth, Part I." *Proc. Instn Elec. Engrs*, **96**, Part III, 1949, pp. 53-64.

    Ditto, Part II: "Experimental evidence and practical implications." *ibid.*, **97**, Part III, 1950, pp. 209-217.

13. Appendix

Evaluation of $\tau_s = \mathrm{Re}\tau_s + j\,\mathrm{Im}\,\tau_s$ for K large as in the case of frequency band 70-130 kc/s.

(a) *Imaginary terms*

$$\mathrm{Im}\tau_0 = 0\cdot7003 - 0\cdot6183.K^{-1} . \sin(15^0 - \psi)$$
$$+ 0\cdot2634 . K^{-2} . \cos(2\psi)$$
$$- 0\cdot0533 . K^{-3} . \sin(15^\circ + 3\psi)$$
$$- 0\cdot00226 . K^{-4} . \sin(60^\circ - 4\psi) + ..$$

$$\mathrm{Im}\tau_1 = 2\cdot232 - 0\cdot1940 . K^{-1} . \sin(15^\circ - \psi)$$
$$+ 0\cdot0073 . K^{-2} . \cos(2\psi)$$
$$+ 0\cdot0120 . K^{-3} . \sin(15^\circ + 3\psi)$$
$$+ 0\cdot00160 . K^{-4} . \sin(60^\circ - 4\psi) + ..$$

For $s > 1$

$$\mathrm{Im}\tau_s \simeq 1\cdot932\left(s + \tfrac{1}{4}\right)^{2/3}$$
$$- 0\cdot2241 . K^{-1} . \left(s + \tfrac{1}{4}\right)^{-2/3} . \sin(15^\circ - \psi) + ..$$

(b) *Real terms*

$$\mathrm{Re}\,\tau_0 = 0\cdot4043 + 0\cdot618 . K^{-1} . \cos(15^\circ - \psi)$$
$$- 0\cdot236 . K^{-2} . \sin(2\psi)$$
$$- 0\cdot0533 . K^{-3} . \cos(15^\circ + 3\psi)$$
$$+ 0\cdot00226 . K^{-4} \cos(60^\circ - 4\psi) + ..$$

$$\mathrm{Re}\,\tau_1 = 1\cdot288 + 0\cdot194 . K^{-1} . \cos(15^0 - \psi)$$
$$- 0\cdot0073 . K^{-2} . \sin(2\psi)$$
$$+ 0\cdot120 . K^{-3} . \cos(15^\circ + 3\psi)$$
$$- 0\cdot00160 . K^{-4} . \cos(60^\circ - 4\psi) + ..$$

For $s > 1$

$$\mathrm{Re}\,\tau_s \simeq 1\cdot116 . \left(s + \tfrac{1}{4}\right)^{2/3}$$
$$+ 0\cdot2241 . K^{-1} . \left(s + \tfrac{1}{4}\right)^{2/3} . \cos(15^\circ - \psi) + ..,$$

RANDOM PHASE VARIATIONS OF C.W. SIGNALS IN THE 70-130 kc/s BAND*

by

W. T. Sanderson, M.A. †

A Paper presented at the Fourth Session of the 1951 Radio Convention on July 26th at University College, Southampton

SUMMARY

The accuracy of C.W. navigational aids in this frequency band depends fundamentally on the phase stability of the received signals, which in turn is determined by skywave effects. The r.m.s. phase errors depend on the relative amplitude of skywave and groundwave, and a method is given for assessing the phase errors in Northern Europe at any given time and range from the transmitter.

For the sake of simplicity a number of approximations are made and the resulting limitations are discussed.

The predicted and observed errors on the Decca Navigator Chains in England and Denmark are compared, and it is concluded that the method gives sufficiently accurate results for most practical purposes. Some comments are added on the variations of errors with height.

1. Introduction

Interest in the propagation of low frequencies has recently revived, owing to the possibilities they offer for the provision of navigational aids giving wide coverage at sea level.

All radio navigational aids depend on measuring the difference between the time of arrival of two signals. At low frequencies the time-difference measurement takes the form of phase comparison. Any disturbance of the phase of the received signals due to reflection effects will introduce inaccuracies into the system.

From an engineering viewpoint, small phase variations are of interest in this respect only, and the present paper is concerned essentially with how skywaves, which are the principal cause of phase instability, affect the performance of navigational aids in this band.

The answer to the question "What errors can be expected here?" can vary from a few yards to as many miles according to how, when and where a particular aid is used. The practical difficulty lies in conveying to the user what a given accuracy figure means or how to get the best use from a particular system, rather than in saying what the errors are likely to be under precisely specified conditions. For this reason quite wide tolerances are permissible in estimating errors and many approximations are justified which would be unacceptable in a more precise art.

2. Nature of Skywave Errors

Owing to signals reflected from the ionosphere, the phase of the resultant signal picked up by the receiver, which is a combination of groundwave and skywave, generally differs from that of the groundwave alone. The magnitude of the resultant errors varies with time and season, being greatest at night and practically negligible up to 300 miles during summer day.

The difference in path length between groundwave and skywave, for a layer height of 90 km, varies from 180 km immediately over the transmitter down to 30 km at about 300 miles; at this latter range a change in the height of the ionosphere of 5 km results in a change of path difference of some 3 km, or about one wavelength. With the variations in apparent ionospheric height which are normally encountered, there is some tendency for the reflected signal to produce a systematic error in the resultant phase at long ranges, but for practical purposes it was assumed that the phase of the resultant has a random distribution about that of the groundwave as mean.

If the variance of this random error can be determined under any required conditions, the performance of C.W. navigational aids can be predicted.

In practice, it is generally impossible to receive the groundwave alone and compare its phase with that of the resultant signal in order to get a direct measurement of the variance required, and indirect methods must be resorted to.

195

One method is to determine the relative amplitude of groundwave and skywave, and deduce the phase variance from this. Another is to observe the errors of some system, such as Decca, and endeavour to break down these errors into the components contributed by the various transmission paths.

The remarks in this paper are chiefly concerned with the latter method as adequate data on skywave conditions on these frequencies is only just becoming available.[1] However, to enable the Decca observations to be applied to solving error problems under different conditions to those obtaining when the observations were made, it is necessary to consider how the errors are related to the ratio of skywave to groundwave field strength.

3. The Relationship Between Phase Errors and the Comparative Strength of Groundwave and Skywave Signals

The following considerations show how the phase variations may be found if the relative amplitude of skywave and groundwave are known.

In Fig. 1, G represents the groundwave vector and x the skywave vector at some instant, making an angle φ with the groundwave, so that the resultant signal R is displaced from its mean direction (G) by an angle θ.

We are making the assumption that all values of φ are equally probable and that x is small compared to G.

Then $\theta = \dfrac{x}{G} \sin \varphi$ radians

or $\dfrac{x}{2\pi G} \sin \varphi$ cycles

The r.m.s. values of $\sin \varphi = 1/\sqrt{2}$, so that the r.m.s. value of θ in cycles due to skywave of amplitude x is

$$\sigma = \frac{1}{2\pi\sqrt{2}} \cdot \frac{x}{G}$$

Fig. 1.

and if the amplitude of the skywave varies and has an r.m.s. value S, the overall r.m.s. value of θ will be

$$\sigma = \frac{1}{2\pi\sqrt{2}} \cdot = k \cdot \frac{S}{G} \quad \dots\dots\dots\dots (1)$$

where $k = 0\cdot 113$ or about $1/9$.

196

We may therefore say that the standard error in phase in cycles of a transmission at a point where the groundwave field strength is G and the r.m.s. value of the skywave S is numerically equal to $\dfrac{S}{9G}$.

The author does not know of any analytical method of determining k for various distributions when possible values of x are not small compared to G, but a graphical method shows that for either a Gaussian or Rayleigh distribution of skywave intensity the value of k is virtually constant up to the values of S equal to one-third of G.

The above expression can be used to assess the phase error of a transmission at any range in the following way:—

Figure 2 shows the estimated field strength in μV/metre against range for a radiated power of 1 kW at 85 kc/s, over soils of varying conductivity. The broken curves lower on the same figure show the corresponding skywave intensities for various reflection coefficients assuming cosine polar diagrams for both transmitting and receiving aerials.

At a range of 450 km over sea water (conductivity 5×10^{-11} e.m.u.), G is seen to be 500 μV/metre, and S, for a reflection coefficient of $0\cdot 15$ (representative of night conditions) is 160 μV/metre.

Under these conditions, $S/G = 0\cdot 32$ and the standard error of phase of this transmission (σ) will be $S/9G = 0\cdot 035$ cycle.

4. Determination of Random Errors in C.W. Navigational Aids

It is proposed to illustrate how this information can be used to calculate the errors of a C.W. navigational aid by reference to the Decca system, which lays down hyperbolic patterns between transmitters whose frequencies are different multiples of a frequency which will be called the basic frequency, f.

Suppose from one station (A) we radiate $6f$, and from the other (B) we radiate $8f$, then at the receiver we can take the fourth harmonic of the A transmission and the third harmonic of the B transmission, both now at $24f$, and compare their phases. $24f$ is called the comparison frequency. The scheme is pictured in Fig. 3.

The $6f$ station (A) is called the Master, as it radiates the controlling transmission. The two
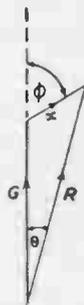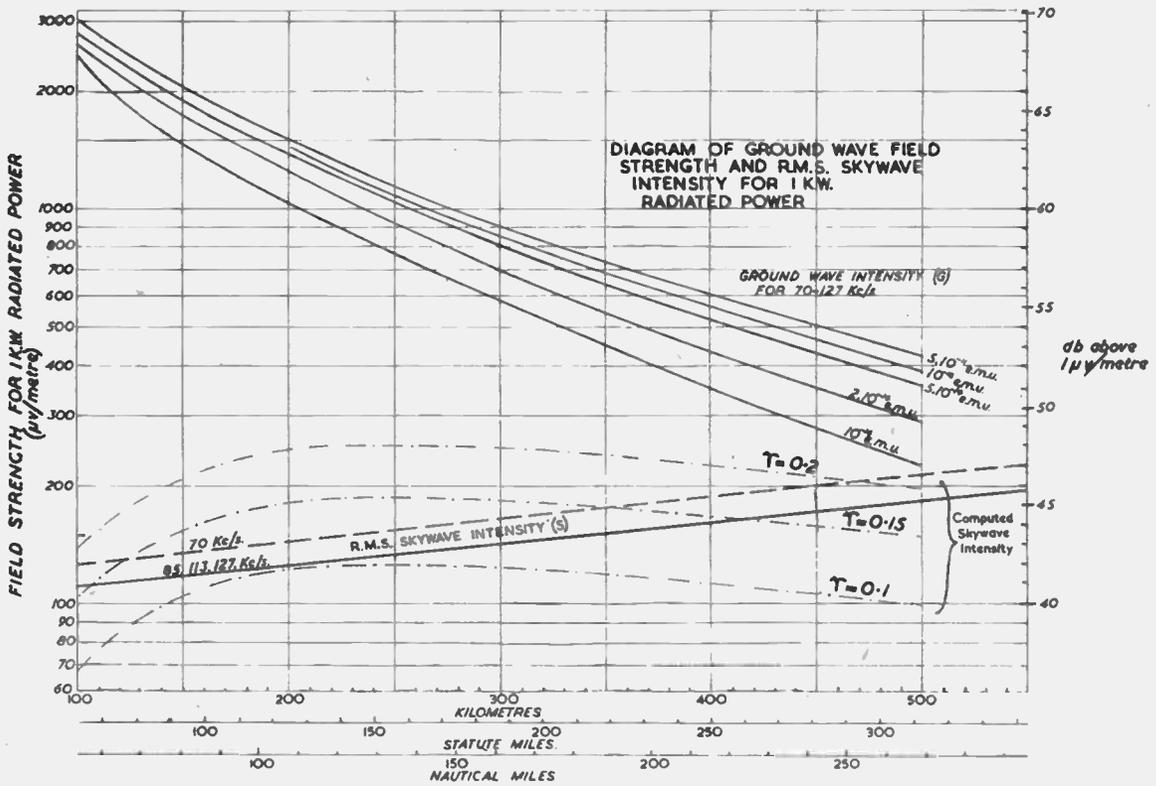
Fig. 2. *Diagram of ground wave field strength and R.M.S. skywave intensity for 1kW radiated power.*

stations together lay down the Red pattern, so called because the position lines from this pair are shown in red on charts prepared for use with the system. The $8f$ station (B) is known as the "Red" Slave, and the phase of its transmission is controlled by the signal received from the Master. To get a fix, two non-parallel lines are wanted, and if good fixing is to be obtainable all round the Master station, this necessitates two other slaves. The theoretically ideal arrangement is to have the three slaves symmetrically placed on a circle round the Master so that the angle formed by the lines joining the Master and any

pair of slaves is 120 deg. The arrangement is not critical and, in practice, widely different layouts may be desirable.

One of these slaves, the "Green," radiates $9f$ and a comparison frequency of $18f$ is used. The other, the "Purple," radiates $5f$ and the comparison frequency is $30f$.

Taking, for example, the Red pattern, shown in Fig. 3, suppose the standard error in the phase of the A transmission over the path a is σ_a and over s, σ_s, and that of the B transmission over the path b is σ_b.

The variance of the error in cycles at the comparison frequency over the path a is then $v_a = M^2\sigma_a^2$ where M is the factor by which the Master frequency is multiplied. The B station is locked in phase to the incoming signal A and has a variance $M^2\sigma_s^2$ initially, and by the time the signal has reached the receiver there is the added variance over the b path, amounting to $S^2\sigma_b^2$ where S is the factor by which the slave frequency

Fig. 3

197
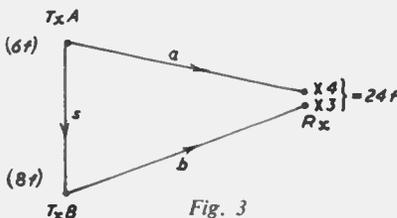
is multiplied. If, as is generally the case, there is no correlation between the errors over the various paths, the total variance observed at the receiver is

$$v_p = \sigma_p{}^2 = M^2(\sigma_a{}^2 + \sigma_s{}^2) + S^2\sigma_b{}^2 \ldots \ldots (2)$$

where σ_p is the standard error of the observed reading in cycles.

If the baseline length s is short compared to a and b, this expression may be simplified to $M^2\sigma_a{}^2 + S^2\sigma_b{}^2$. Over sea water the fall off in groundwave field strength is not greatly affected by frequency over the band considered and we may, along the perpendicular bisector of the line AB, simplify still further by putting

$$\sigma_a = \sigma_b = \sigma \text{ so that } \sigma_p = \sqrt{(M^2 + S^2)}.\sigma$$

For the example given $M = 4$, $S = 3$, so that $\sqrt{M^2 + S^2} = 5$ and $\sigma_p = 5\sigma$.

For the conditions previously considered at 450 km from a transmission with a reflection coefficient of $0\cdot15$, σ was estimated at $0\cdot035$ cycles, so that "Red" phase comparison meter at such a point would be expected to have a standard deviation by night of about $0\cdot17$ cycle. What this means in terms of yards, cables or miles in the error of the derived position line depends on the geometry of the system, but can be quite easily worked out when the transmission frequencies and positions of the station, relative to the observed point, are known.

A similar analysis can be made for any type of C.W. aid and its errors evaluated, provided it is possible to derminate the standard errors of phase over the various transmission paths involved.

It will be seen, however, that to break down observed errors in different parts of an existing system requires several assumptions as the number of unknowns is always greater than the number of observations.

From this point of view it is fortunate that the variations in performance with time and place are large and if the observed value under any conditions is not less than half or more than double the predicted value the prediction may be considered adequate. Rather sweeping approximations can be made in order to derive a simple way of estimating these errors. For example, the groundwave propagation curve may be taken as independent of frequency. This is reasonably true over soils of good conductivity and a drop in reflection coefficient at the higher frequencies largely compensates for their more

rapid attenuation. On this assumption an error-range curve could be drawn which would apply to all frequencies over sea water or good soil.

To obtain a first approximation to this curve, random Decca errors at a large number of points spread over the coverage were obtained from observations made in various trials, σ_p was plotted against range from the midpoint of the base-line, and a smooth curve drawn through these points at the longer ranges, and extended to pass through the origin. For the Red pattern (i.e. $6f$ and $8f$ transmissions) this curve was taken as representing 5σ, and the final curve obtained by replotting with the ordinates marked with values one-fifth of those indicated by the original curve. When reduced by the appropriate factors, the curves for the Red and Green patterns lay practically on top of each other, but the Purple lay somewhat above the other two, indicating a greater skywave effect at the lower frequency ($5f$).

Once this σ-range curve had been estimated the expected errors at the various observation points were derived, taking into account the baseline and the actual ranges from the two stations concerned. As a result the curve was slightly modified and the final results indicate that the effective skywave field strengths for 1 kW radiated are as shown by the full lines on Fig. 2.

It will be noticed that the vertical scale of Fig. 2 is logarithmic so that the intercept between the groundwave and skywave curves at any point corresponds to the logarithm of S/G. For convenience in practical use, Fig. 4 was prepared from Fig. 2 to enable the variance and standard error of a transmission at night to be read off quickly for any given soil conductivity.

As the range is increased the skywave level approaches, and eventually passes, that of the groundwave. When S is more than $1/2$ G the assumptions made in deriving the diagram break down, and if the skywave happens to exceed the groundwave and at the same time shift in relative phase, the resultant signal may rotate by a whole cycle. The phase comparison meter then rotates M or S revolutions according to which of the transmissions has lost or gained the cycle in this way. If the skywave then fades, the comparison meter indicates varying errors about a new mean M or S revolutions away from the original, and will continue to do so unless reset. When this can happen the possible errors in the meter reading suddenly jump. As any expression
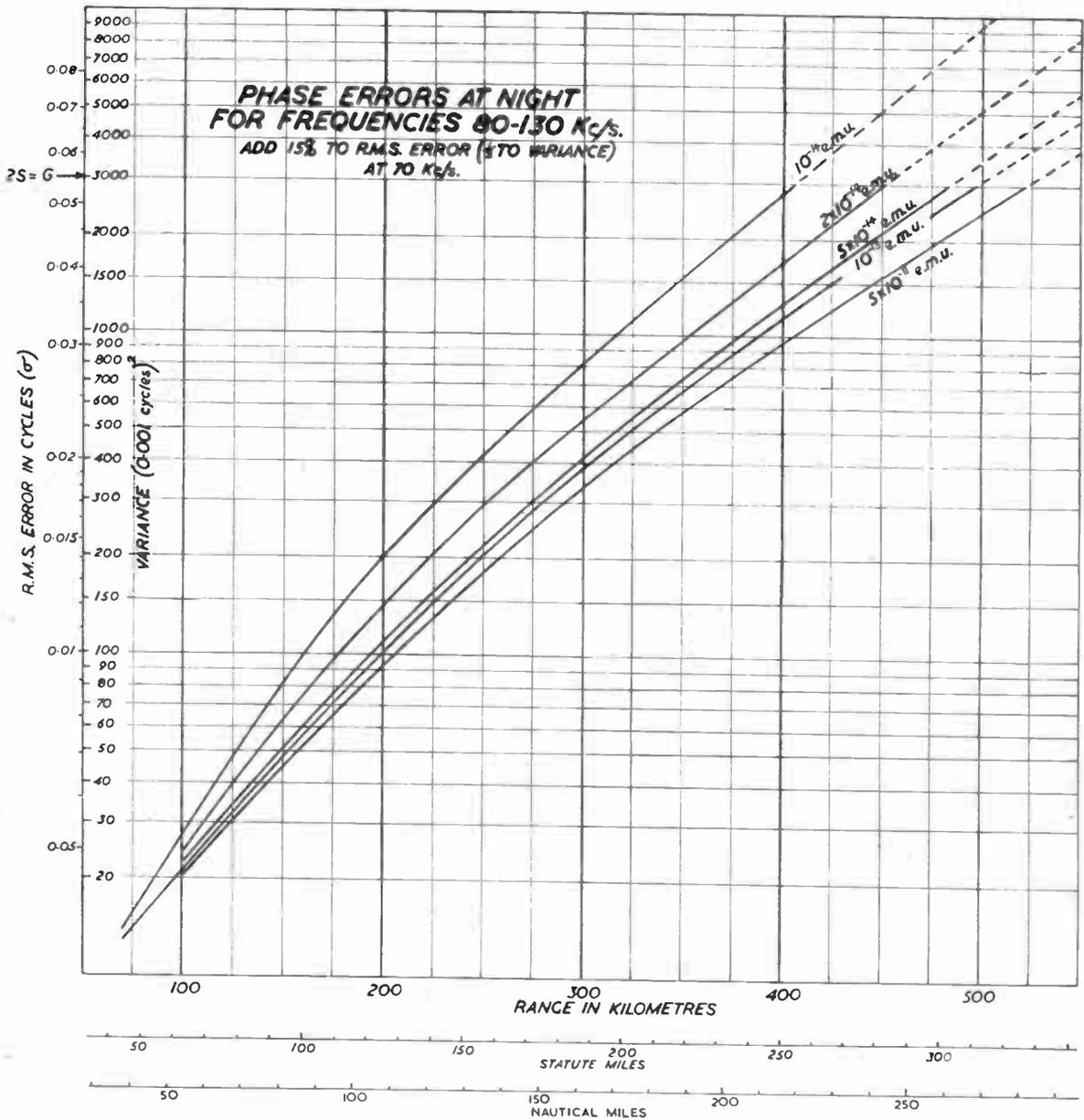
198

Fig. 4.   Phase errors at night for frequencies 80-130 kc/s.

for the standard error of phase then becomes almost meaningless, the use of Fig. 4 must be restricted to ranges where $2S < G$ and this point is indicated on the diagram. Owing to the more rapid attenuation of the higher frequencies, values derived for their errors over very poor soil at limiting ranges should also be treated with reserve.

Before giving a comparison of the predicted and observed readings the changes in the errors to be expected at different times and seasons will be considered.
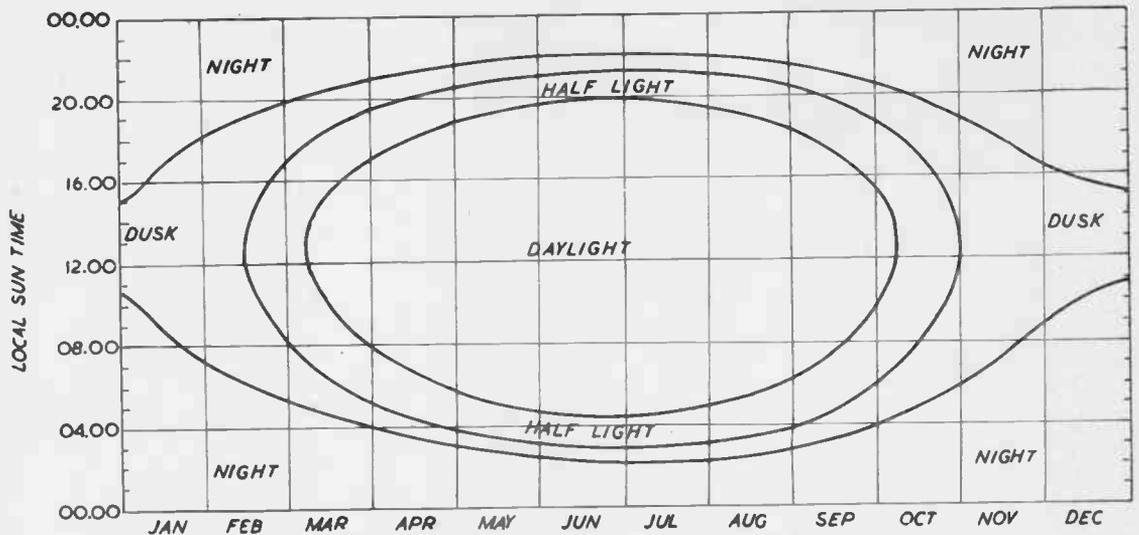
199

Fig. 5. Contours of R.M.S. phase errors (Lat. 55°N).

5. Variation of Errors with Time and Season

The foregoing analysis enables the night errors to be found, but it was known that there was a big difference between daylight errors in summer and winter, and the problem arose as to how daylight observations should be grouped so that each group would be respresentative of a particular skywave condition. At the time this work was under consideration, the author received from Ing. S. Dorph-Petersen a most interesting analysis of some observations which had been taken at five-minute intervals throughout a year at Copenhagen on the Purple pattern of the Danish Decca Chain. The analysis included a diagram with time of day as ordinate and date as abscissa showing error contours, and enabled observations to be grouped into periods during which errors could be expected to be of the same order of magnitude.

Figure 5 is a copy of Dorph-Petersen's diagram, but showing only four periods, denoted *Night, Dusk, Half-light* and *Daylight*. In each period the errors may be expected to be half those in the preceding period, i.e. those during the times marked Dusk will be half the night errors, and so on. There is a strong indication that there is a further sub-division of the Daylight period in which the errors are halved once again, but skywave errors at the ranges at which adequate data are available are so small during Daylight that analysis becomes difficult.

The shape of the contours is clearly dependent on latitude and the diagram is, strictly speaking, applicable to about 55°N, but it may be applied between about 50° and 58°N.

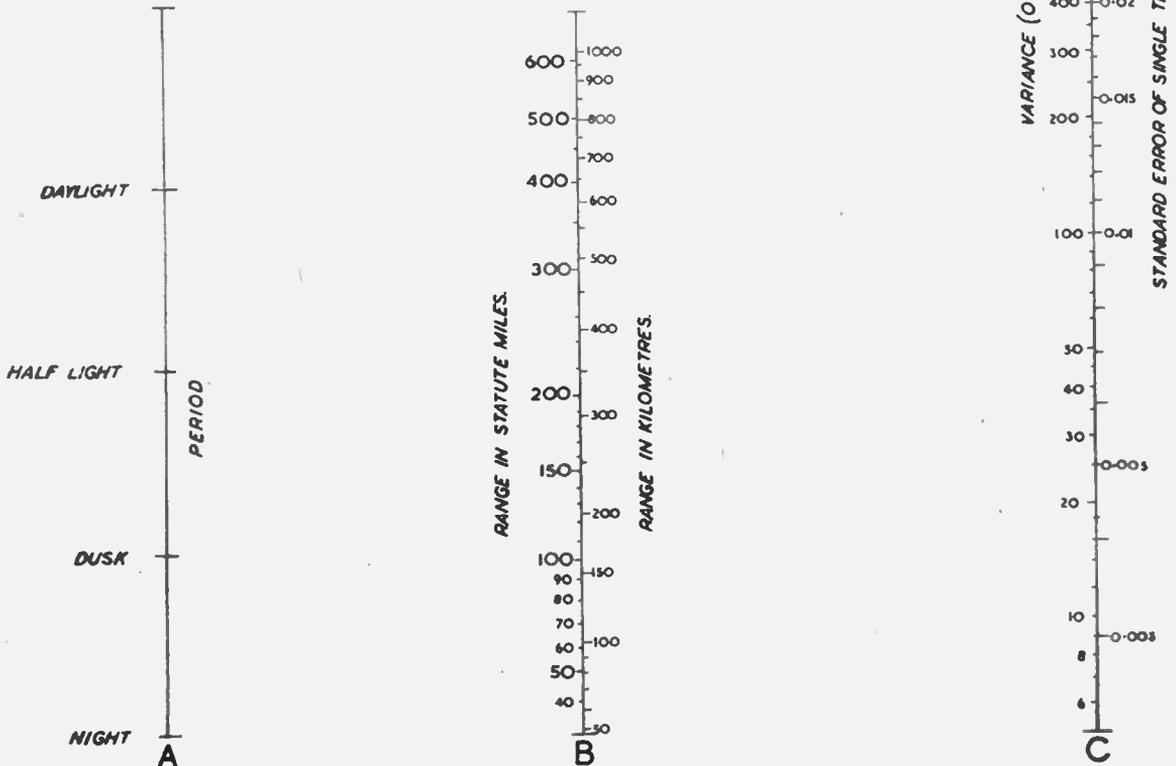## 6. Extension of Predictions to Long Range During Daylight

The reduced errors during periods other than night result from reduced skywave signals and during the Dusk period the skywave field strength lines, shown in Fig. 2, would be dropped to half the values shown. Consequently the range at which the diagram breaks down owing to the skywave becoming comparable with the ground-wave is considerably greater. On the other hand, at such ranges it is no longer a reasonable approximation to take the groundwave attenuation as the same for all soils and frequencies. However, for Northern Europe when a transmission path is over 300 miles long it will, in most cases, be largely over sea or good soil. A nomogram was therefore devised which enables errors at any period over longer ranges to be assessed, but which is restricted to paths of good average conductivity.

This nomogram is shown as Fig. 6. To use it, the ionospheric conditions are found from Fig. 5 for the time at which it is required to know the likely errors. A straight line is then drawn from the appropriate point on Scale A, through the range on Scale B, and where this line cuts Scale C the value of σ for the transmission is read off.

200

7. Comparison of Predicted and Observed Results

The nomogram shown on Fig. 6 was used to predict the Decca errors for all cases where reasonably reliable observations were available and a comparison of the predicted and observed results is given on Fig. 7. If the predictions were perfect all points would lie along the full line running diagonally across the diagram. The broken lines each side enclose the region where the observed errors lie within a factor of $\sqrt{2}$ of the predictions. In view of the likely variations in the observed results, which will be discussed later, the agreement is remarkably good and results partly from using the same observations to construct and check the nomogram. Nevertheless, it is considered that the observations were made under sufficiently diverse conditions to justify the use of the diagram for practical purposes.

8. Variation of Errors from Night to Night

It was mentioned above that part of the disagreement between the predicted and observed errors might be ascribed to inaccuracy of the observed results. This is because the skywave conditions vary considerably from night to night and unless observations are extended over a long period the true standard error will not be obtained. To get some idea of how the errors varied from night to night, and how many nights' observations would be required to give a
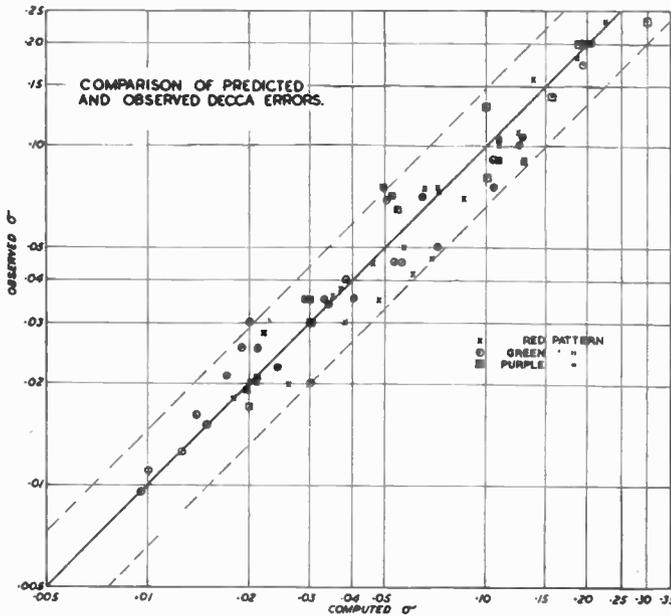

Fig. 6.   Nomogram for estimating R.M.S. phase errors.

Fig. 7. *Comparison of predicted and observed Decca errors.*

The diagram is useful in planning trials when it is desirable to keep the probable error of the results within predetermined limits, or for estimating whether the difference between observed and predicted results is significant. It has, however, not been checked by a similar analysis of results at other ranges and must be treated as giving only an indication of the order of variations to be expected.

9. Short-period Changes in Reading

Skywave errors would be of no consequence if they resulted in rapid flutter of the phase comparison meter, as, by the introduction of suitable time constants in the circuits, the fluctuations could be smoothed out and the meter made to indicate the true average reading.

Unfortunately, the variations take the form of a slow wander and the meter may show a positive error for an hour or more. It is therefore desirable

result which might be expected to be within certain limits of the true (long period) figure, the r.m.s. errors at a point some 100 miles from the transmitting stations were determined for each separate night for a period of 100 winter nights. A histogram of these results was drawn and it was noticed that the distribution was reasonably symmetrical about the mean value if the horizontal scale was logarithmic, indicating that nights with errors twice the average value were about as common as those with errors half the average value. The distribution curve was roughly Gaussian and can be represented by the straight line marked (1) on Fig. 8.

The ordinate of the graph gives the percentage of occasions on which the value of r.m.s. error deduced from observations over a short period (in this case one night) will be below the value shown on the horizontal scale. The latter scale is marked in units of the true value (taken as that derived by considering the 100-night period as a whole). For example, on only 2 per cent. of occasions will the results derived from a single night's observations be less than half the true value.

The analysis was repeated, dividing the period up in groups of two consecutive nights, and gave the line marked 2 on Fig. 8, and so on.
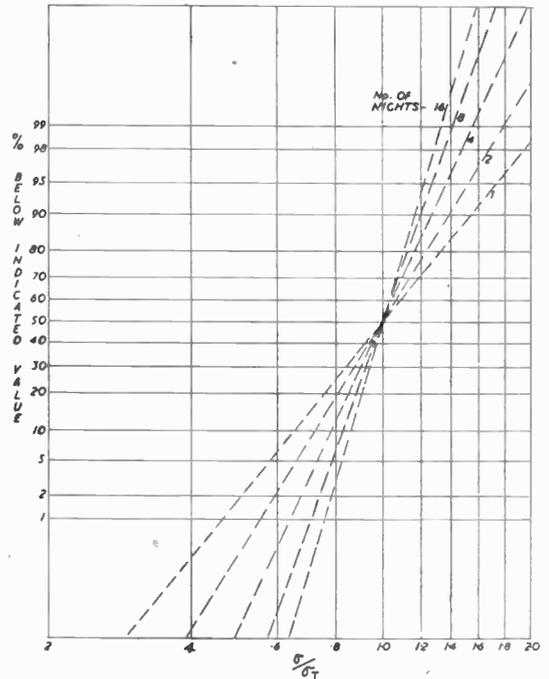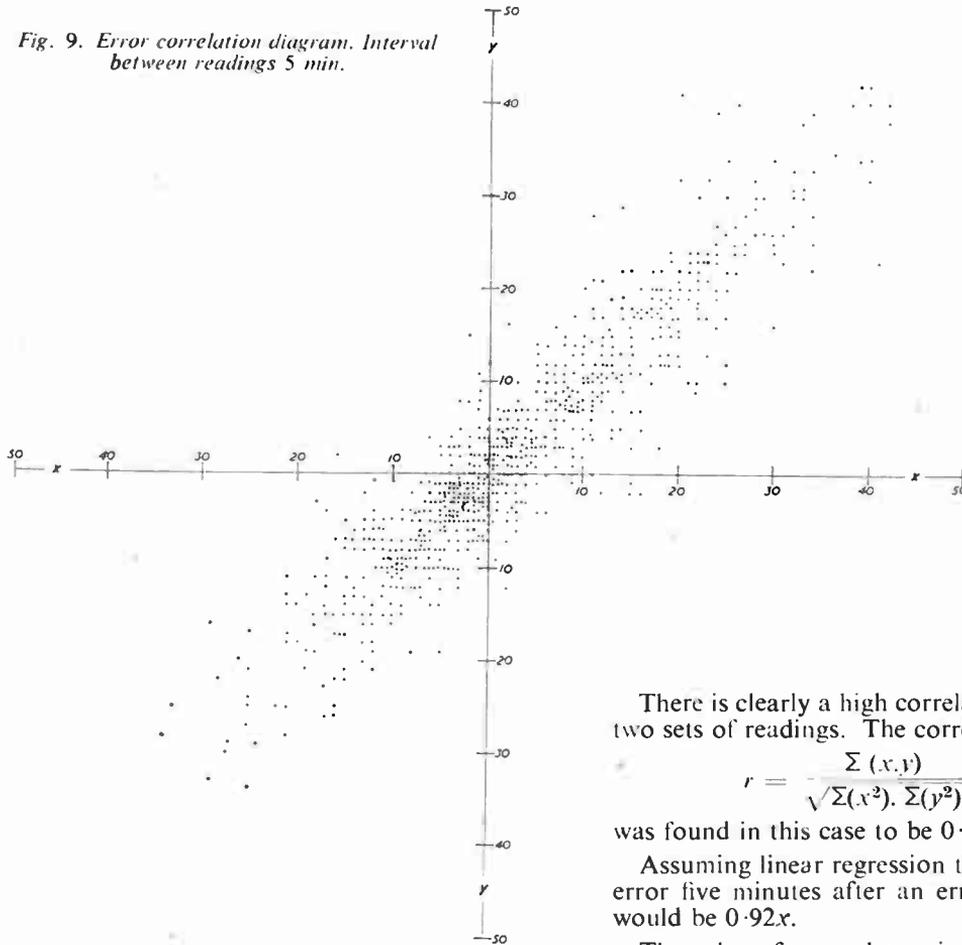

Fig. 8. *Graph showing the number of whole nights' observations required to obtain an error value within any specified limits.*

Fig. 9. *Error correlation diagram. Interval between readings 5 min.*

There is clearly a high correlation between the two sets of readings. The correlation coefficient

$$r = \frac{\Sigma(x.y)}{\sqrt{\Sigma(x^2).\ \overline{\Sigma(y^2)}}}$$

was found in this case to be 0·92.

Assuming linear regression the most probable error five minutes after an error x is observed would be 0·92x.

The value of r was determined over a number of different time intervals up to one hour, and it was found that the expression $r = e^{-t/a}$ fitted the observed results well using a value of α of 30 minutes. Readings must therefore be spaced by about half an hour before they can be regarded an independent, and it takes quite a long time to get any appreciable advantage from averaging a number of readings. A check showed that averaging readings taken every five minutes over half an hour resulted in a 30 per cent. reduction in the probable error compared to a single observation.

However, if the observation point is moving, which is the case when such a system is used as a navigational aid, the skywave interference pattern changes fairly rapidly with range. If some device is used which continuously plots the

to know what advantage can be gained by averaging a number of readings.

For truly independent readings one can expect the error of the average of ten readings to be one-third that of a single reading. In the case of C.W. aids of the Decca type, this is not true unless the readings are widely spaced in time. because if an observation at one instant has an error x, the most probable error five minutes later is not zero (as would be the case for random readings), but something in the neighbourhood of x.

This is illustrated in Fig. 9, which shows a number of Decca errors plotted, in each case, against the errors observed five minutes later. The scales are marked in units of one hundredth of a cycle.
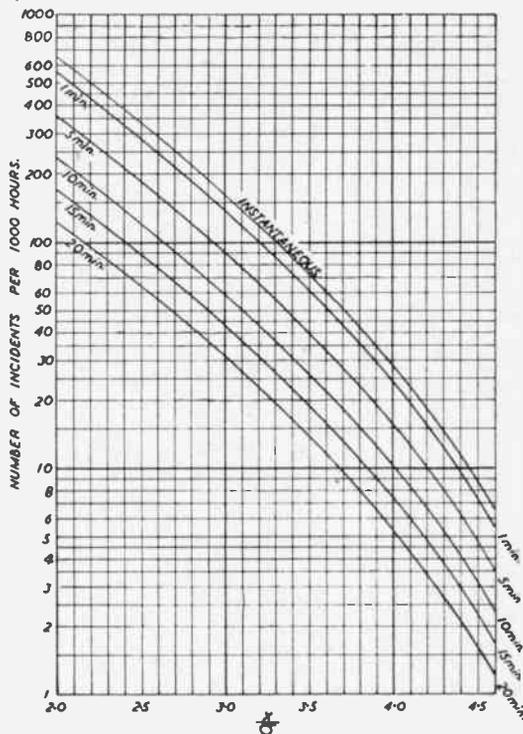
203

Fig. 10.   *Number of separate occasions per 1,000 hours'*
observation when error is likely to exceed a given value of
x/σ.

indicated track of a vessel or aircraft travelling on a straight course, the result is a wavy line and the true track can be quite well estimated. The time required to get a position within specified limits depends on the speed and general location of the observing point. Practical data are somewhat scanty and consideration will be confined here to errors at a fixed point.

10. Distribution and Duration of Errors

The foregoing paragraphs have been concerned with determining the r.m.s. errors. The user is interested not only in the average sort of error he may expect, but also the extreme errors, and how long they are likely to persist. Fig. 10 summarizes the results of an analysis of the Danish Chain Purple pattern readings at Copenhagen to obtain answers to these questions.

The top curve gives the number of occasions per 1,000 hours continuous observing on which error values shown by the abscissa may be expected to occur, and the lower curves how long they will persist.

For example, errors can be expected to reach or exceed 3σ on 170 occasions during 1,000 hours of night observation. On 90 occasions the error will continue in excess of 3σ for five minutes and on about 30 occasions such errors will persist for 20 minutes. How far this graph can be used for conditions widely different from those under which the observations were taken is not known, but it is included to indicate the order of the factors involved.

11. Errors in Observations Made at a Height Above the Earth's Surface

If the ionosphere is regarded as a smooth reflecting shell, then at a receiver some distance above the earth's surface, skywave signals arrive by two paths. One portion of the skywave is coming down after reflection from the ionosphere and the other coming up after reflection from both the ionosphere and the ground. It can be shown that for a flat earth the latter path is longer by an amount δ such that

$$\delta \approx \frac{2h}{\left[1 + \left(\dfrac{d}{2H}\right)^2\right]^{\frac{1}{2}}}$$

where H = height of ionosphere
h = height of receiver
d = ground distance between the transmitter and a point immediately below the receiver.

The computations for a spherical earth are tedious, but checks show that the simple expression given above remains a close approximation.

At a given range the path difference in cycles becomes

$$\theta = k \, \frac{h}{\lambda}$$

and if H is taken as 50 nautical miles (about 92 km), and d is expressed in hundreds of nautical miles, the numerical value of k is

$$k = \frac{2}{(1 + d^2)^{\frac{1}{2}}}$$

and drops from 2 at zero distance to 0·63 at 300 miles.

Until grazing incidence is approached the vertical component of the electric vector undergoes no appreciable change of phase or amplitude on reflection from the earth, and consequently the phase difference between the two skywave

204

signals will be directly proportional to height and will cancel each other at a height h_c where

$$h_c = \frac{\lambda}{2k}$$

They will come into phase again when $h = \lambda/k$, and oppose once more at $3\lambda/2k$, and so on, the relationship between amplitude and height following a cosine law.

The effect of normal changes of apparent height of the ionosphere at night is not critical. The most rapid change in h_c with H occurs at long ranges when h_c is inversely proportional to h, so that variations in h_c of only about 5 per cent. may be expected.

In practice complete cancellation would not be expected as the ionosphere is not a smooth reflecting surface and there is a small degree of dispersion on reflection from the earth. Complete summation at twice the cancellation heights must be rejected for the same reason and consequently the performance in the air should always be better than on the ground, irrespective of height or range.

The cancellation heights for the frequencies used in Decca are shown on Fig. 11, and it will be seen that they are well spread over normal aircraft heights at ranges where skywave effects are of importance.

If a vertical aerial is used a considerable improvement in performance may be expected in aircraft. The benefits may be partly nullified if the aerial picks up an appreciable horizontal component, as the amplitude of this component changes with height according to a sine law, having a minimum at ground level and maximum at h_c.

Williams[2] found that the performance with a vertical aerial was, in fact, better than other types and errors experienced in the air seem to be generally lower than on the ground, but quantitative data are not yet available.

It does appear, however, that the effective coverage of C.W. aids at these frequencies might well be considerably extended by taking advantage of this effect.[3]

12. Acknowledgments

The author is indebted to The Decca Navigator Co., Ltd., for permission to publish this paper, and particularly to Mr. Oliver and Mr. Martin, of that company, who carried out most of the
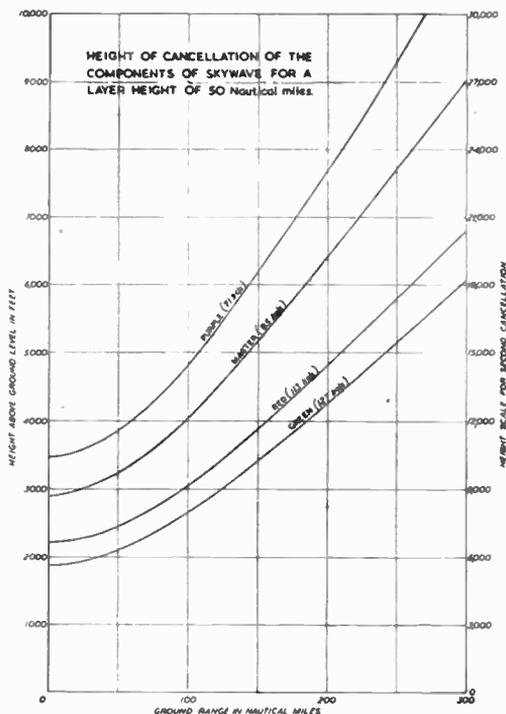

Fig. 11.   Height of cancellation of the components of skywave for a layer height of 50 nautical miles.

analysis work, and Ing. S. Dorph-Petersen for Fig. 5, and much of the data used in the analysis. The paper gives some account of the conclusions reached from a study of Decca performance over the last five years and it is impossible to mention all those who have contributed to this work, to all of whom the author is indebted.

13. References

1. R. N. Bracewell, K. G. Budden, J. A. Ratcliffe, P. W. Straker, and K. Weekes: "The ionospheric propagation of low- and very-low-frequency radio waves over distances less than 1,000 km." *Proc.Instn Elec.Engrs*, **98**, Part III, May 1951, pp. 221-236.
   See also list of references given in this paper.

2. C. Williams: "Low frequency radio wave propagation by the ionosphere, with particular reference to long-distance navigation." *Proc.Instn Elec.Engrs*, **98**, Part III, March 1951, pp. 81-99.

3. J. A. Fejer. South African C.S.I.R.: Telecom. Res. Lab. Reports ETM-6 and ETR-10.

APPLICANTS FOR MEMBERSHIP (JANUARY)

The following new proposals were considered by the Membership Committee at a meeting held on January 29th, 1952: 37 proposals for direct election to Graduateship or higher grade, and 3 proposals for transfer to Graduateship or higher grade ; also 12 applications for Student registration.

The following are the names of those who have been properly proposed and appear qualified. In accordance with a resolution of Council and in the absence of any objections being lodged, these elections will be confirmed 14 days from the date of the circulation of this list. Any objections received will be submitted to the next meeting of the Council, with whom the final decision rests.

Direct Election to Full Member

BALIGA, Bantwal Vittal, B.A. *Mangalore. India.*
NEMET, Anthony, Dr.-Ing.(Zurich). *Richmond, Surrey.*
THRIPP, Gordon. Group Captain. *Jalahalli, India.*

Transfer from Associate Member to Full Member

TURNER, Raymond John Arthur. *Ontario.*

Direct Election to Associate Member

BARFORD, Frederick William. *Richmond, Surrey.*
CLARK, Raymond Laurence. *London, N.12.*
CORDONNIER, Joseph Girard, B.Sc. *Neuilly-sur-Seine, France.*
JUNGALWALLA, Jehanbux Nanabhoy, B.Sc., B.A.(Hons.). *Bombay.*
KAGALI. Sidamallappa Tulajappa, B.Sc. *Belguam, India.*
LAKHANPAL, Dev Datta, B.A.. B.Sc.(Tech.) *Bombay.*
PRAKASH. Narayana Murti, M.Sc. *Bangalore.*
RAJAGOPAL, Damal, B.Sc. *Madras.*
SINGH, Amarjit, M.Sc., Ph.D. *Pepsu, India.*
SRINIVASAN. Thirumalai, Squadron Leader, B.Sc.(Hons.) *Madras.*
STEVENS, Samuel John Henry, B.Sc.(Eng.) *Ilford, Essex.*
TAYLOR, Maurice. *Nicosia, Cyprus.*
WILSON, John. *Bombay.*

Direct Election to Associate

ASHTON, Harold Leslie. *Barking, Essex.*
BROWNE. Joseph Adolphys Adebayo. *Lagos, Nigeria.*
COLBY, Reginald George. *Ilford, Essex.*
DEB, Bipul Chandra. *Karimganj, India,*
DEVANATHAN, M.R., M.A. *Cuddalore, India.*
HABIBULLAH, Mohamed, Captain. M.A. *London, S.W.1.*
LATHAM, Colin. *Walton-on-Thames.*

MACDONALD. Bruce. *Nairobi.*
MENON, Gopal Krishna. *Malabar, India.*
RAMNANY. Parmanand, Flight Lieutenant. *Madras.*
SECKER, Henry Leslie, Squadron Leader. *Hillingdon, Middlesex.*
SENGUPTA, Rabindra, B.Sc. *Calcutta.*
SINGH, Gurmukh, Flight Lieutenant. *Amritsar.*
STAMPOULOS, Charalambos. *Athens.*
WORTH, Donald, Flight Lieutenant. *Birmingham.*

Direct Election to Graduate

BULSARA, Minoo Sorabji, B.Sc. *Bombay.*
HAILE, James Neville, B.Sc. *Coventry.*
ITTER, Charles. *Greenford, Middlesex.*
LAW, Peter Anthony. *Northampton.*
MCLACHLAN, Malcolm John, B.Sc.(Eng.) *Johannesburg.*
SEYMOUR, Roy Eric, B.Sc.(Eng.) *Watford, Herts.*

Transfer from Student to Graduate

AGARWAL, Chunni Babu, B.Sc. *Allahabad, India.*
CASS, Wilfred Richard. *London, S.W.15.*

Studentship Registrations

ACHARYA, Harsukharai. *London, W.2.*
BARRON, Frederick Cusack. *Sydney, Australia.*
HARKNETT, Maurice Richard. *Southsea, Hants.*
HEAL, John William. *Bristol.*
KLAPPOTH, Gerhard Wilhelm. *Earlston, Berwickshire.*
MACDOUGALL, John Duncan. *Romsey. Hants.*
MACLEAN. Duncan MacTavish. *Weymouth.*
MASTER, Minoo Ratansha. *London, W.2.*
MIGAWSKI, Bernard Bronislaw. *London, N.8.*
PEARSON. Gordon Pitt. *Limpsfield, Surrey.*
SHAH, Sunderlal Ghhotalal. *Bombay.*
TOWNSEND, William Harry. *London, S.E.9.*

APPLICANTS FOR MEMBERSHIP (FEBRUARY)

The following new proposals were considered by the Membership Committee at a meeting held on February 27th, 1952 : 29 proposals for direct election to Graduateship or higher grade and 28 proposals for transfer to Graduateship or higher grade ; also 28 applications for Studentship registration.

The following are the names of those who have been properly proposed and appear qualified. In accordance with a resolution of Council and in the absence of any objections being lodged, these elections will be confirmed 14 days from the date of the circulation of this list. Any objections received will be submitted to the next meeting of the Council with whom the final decision rests.

Direct Election to Full Member

BANNERJEE, Sudhansu Shekhar, D.Sc. *Banaras, India.*
SENGUPTA, Monoranjan, B.Sc.(Eng.) (Hons.). *Banaras, India.*

Transfer from Associate Member to Full Member

DATTA, Saroj, M.Sc.. Ph.D. *Calcutta.*

Direct Election to Associate Member

BESWICK, George Robert. *Birmingham.*
GAIROLA, Shekharanand, M.Sc. *Naini Tal, India.*
JOSEPH, Theverthundy Titus, Squadron Leader. B.A., M.Sc. *Maramon, India.*
RAO, Hundi Joga, B.Sc.(Hons.). *Madras.*
WAGLE, Moreshwar Mangesh, B.Sc. *Bombay.*

Transfer from Associate to Associate Member

BROWN, Donald Peter Ernest. *St. Albans, Hertfordshire.*
CHATTERJEE, Inan Saran, M.Sc. *Chelmsford.*
DANZIGER, Rudolf. *Tel-Aviv.*
JEFFERY, Anthony David. *Watford, Hertfordshire.*

Transfer from Graduate to Associate Member

FULLER, Frederick Reginald. *Accra, Gold Coast.*
O'BRIEN, Timothy Patrick. *Kilmainham, Dublin.*
STORER, John Derek. *Sevenoaks, Kent.*
YOUNG, John Robert, M.A., Lieutenant (L), R.N. *Southsea, Hants.*

Transfer from Student to Associate Member

JUDE, Peter Vivian Wilson, B.Sc. *Reading.*

Direct Election to Associate

BOICE, Cyril John. *Gillingham, Kent.*
BOWERMAN, Esmonde Frederick George. Lieutenant (L.), R.N. *Melbourne.*
BRIGHTMORE, Percy Edwin Albert, Flight Lieutenant. *Scunthorpe, Lincolnshire.*
DREW, Kenneth Hamilton, Commander, R.N. *Ross-on-Wye, Herefordshire.*
HENDRY, Dennis James. *Ickenham, Middlesex.*
HORRIGAN, Edwin William, Warrant Officer. *Bristol.*
MARSHALL, Sidney Field. *Erith, Kent.*
PARCHMENT, Ernest David. *London, S.W.9.*
TOMLIN. Laurence. *New Romney, Kent.*

APPLICANTS FOR MEMBERSHIP—*(contd.)*

Transfer from Student to Associate

NOONAN, William Edward. *Walton, Liverpool.*
PHILLIPS, Maurice Marcus. *Ashford, Middlesex.*

Direct Election to Graduate

DENBY, Peter. *London. W.4.*
EDGAR, Ronald Ian. *Romford.*
EDWARDS, Vivian Cecil Wynne, B.Sc., Lieutenant (L), R.N. *Merthyr Tydfil, Glamorganshire.*
FISHER, Bernard, B.Sc. *Sidcup, Kent.*
HUTTON, Leslie. *Sheffield.*
KHAN, Sultan Ahmad, B.Sc.(Eng.). *Karachi.*
MANIAK, Joseph Robert, B.Sc. *Ontario.*
MAURICAKIS, Jerome. B.Sc.(Eng.) (Hons.). *Beckenham, Kent.*
NAYAR, T. N. K., B.Sc.(Eng.). *Trivandrum, India.*
RICHES, William Henry. *Selsdon, Surrey.*

Transfer from Student to Graduate

BAXTER, John Campbell. *Hamilton, Lanarkshire.*
CRYER, Frank Stanworth. *Liverpool.*
GAULDER, Clifford Francis Kerry. *Warlingham, Surrey.*
RAJWADE, Gajanan Vinayak. Lieutenant, B.Sc. *Akola, India.*
SKINNER, Peter. *Surbiton, Surrey.*

Studentship Registrations

AHMED, Nazir. *Gujrat, Pakistan.*
BARTLETT, Thomas Henry, Second Lieutenant. *Sheringham, Norfolk.*
BELL, Ronald James. *Khartoum.*
BLUM, Ruben, Captain. *Tel-Aviv.*
CHACKAL, Joseph Farouk. *London, W.2.*
CORDEIRO, Joseph Rufino, B.Sc. *Indore, India.*
DIN, Shua-Ud. *Kallar Kahar, Pakistan.*
DUNLOP, Edward Goodwin. *Prestwick.*
GILVARY, David Francis. *Bray, Eire.*
HALLS, Richard Walter. *Chelmsford.*
HORNE, Jerome. *East London, South Africa.*
HUSSAIN, Mohd. *Rawal Pindi, Pakistan.*
KANTHASAMY, Chelliah. *Manipay, Ceylon.*
KRISHNAMURTHY, K. Taurus. *Hamble, Hants.*
KUKJAZADA, Fouad. *Limassol, Cyprus.*
MACARTNEY, Robert Alan. *Christchurch, New Zealand.*
MAGUIRE, James Patrick. *Dublin.*
MAHY, John Cecil. *St. Sampson's, Guernsey.*
MOHAMMAD, Mian. *Kufri, Pakistan.*
MURTY, Burra Srirama Chand.a. *Madras.*
NADKARNI, Vasant Anant. *Bombay.*
NELSON, George. *Dumfries.*
NIWAZ, Haq. *Ramdyal, Pakistan.*
PRADHAN, Suresh Mahadeo. *Bombay.*
RAMADAS, Bulusu, M.Sc. *Palakonda, India.*
RAMALINGAM, V. K. *Madras.*
RIDOUT, John Richard. *Bournemouth.*
SMITH, Edward James. *Ilford, Essex.*

SCHOLARSHIPS FOR PRODUCTION TECHNOLOGY AND MANAGEMENT

The Ministry of Education announces that, with the aim of contributing to industrial productivity in this country, 75 scholarships are to be awarded this year for the study of production technology and management in selected universities or technological institutes and in industrial undertakings in the United States.

The Mutual Security Agency (formerly the Economic Co-operation Administration) is to supply the dollar equivalent to meet tuition fees, travelling expenses in the United States and suitable maintenance allowances. The approximate cost will be $250,000. Return passages to the United States will be paid for from public funds.

In previous years most of the candidates qualifying for these awards have been employees of the country's larger firms and organizations. It is hoped that this year employees of the smaller firms, which form such a considerable part of the national economic system, will share in the scheme to a greater degree.

The awards will be made in two groups. In the first group, 40 awards, available for the study of management and normally tenable for a period of nine months, will be open to persons between the ages of 23 and 35 of adequate educational standard, who are potential managers or occupying positions of responsibility in industry, or who propose to teach management subjects. A minimum of three years' industrial experience will be a condition of entry.

In the second group, 35 awards, available for the study of production technology combined with management and normally tenable for a period of one year, will be open to students who hold good honours degrees in either Pure Science or Technology, who have had at least two years' industrial experience and who are now working in industry or research associations or are teaching in universities or technical colleges.

Successful candidates will be expected to leave for the U.S.A. early in September 1952. The closing dates for applications are April 16th and 30th for the technological and management awards respectively.

Full details may be obtained from the Ministry of Education (F.E. Division 1), Curzon Street, London, W.1.

FORTHCOMING MEETINGS

WEST MIDLANDS

Mar. 25th Wolverhampton and Staffordshire Technical College, Wulfruna Street, 7 p.m.

"Short Wave Radio Propagation and the Ionosphere."

W. J. G. BEYNON, Ph.D., D.Sc.

SCOTTISH

Mar. 25th Institute of Engineers and Shipbuilders, Glasgow, 7 p.m. (Please note altered arrangements.)

"The Future of Broadcasting."

P. ADORIAN (*Member*).

LONDON

Mar. 27th School of Hygiene and Tropical Medicine, Gower Street, W.C.1, 6.30 p.m.

"The Application of Magnetic Amplifiers to Industrial Measurement and Control."

H. M. GALE, B.Sc.

NORTH WESTERN

Mar. 27th College of Technology, Manchester, 7.15 p.m.

"Improvements in Loudspeaker Design."

R. T. LAKIN (*Associate Member*).

LONDON

April 3rd School of Hygiene and Tropical Medicine, Gower Street, W.C.1. 6.30 p.m.

A Discussion on

"V.H.F. and U.H.F. Broadcasting."

(Opened by the President)

It is hoped that it will be possible to demonstrate some new equipment during the meeting.

NORTH EASTERN

April 9th Neville Hall, Newcastle, 6 p.m.

"V.H.F. Broadcasting: the Case for Amplitude Modulation."

J. R. BRINKLEY (*Associate Member*).

SCOTTISH

April 10th Works of Metropolitan-Vickers Ltd., Motherwell, 7 p.m.

"X-ray Equipment and its Control Gear."

C. S. NORTON

(Lecture to be followed by a tour of the works.)

LONDON

April 16th School of Hygiene and Tropical Medicine, Gower Street, W.C.1, 6.30 p.m.

"Current Radio Interference Problems."

E. M. LEE, B.Sc. (*Member*).

NORTH WESTERN

April 30th College of Technology, Manchester, 7.15 p.m.

"V.H.F. Broadcasting: the Case for Amplitude Modulation."

J. R. BRINKLEY (*Associate Member*).

LONDON

May 7th School of Hygiene and Tropical Medicine, Gower Street, W.C.1, 6.30 p.m.

"An Aerial Analogue Computer."

W. SARAGA, Ph.D.

NORTH EASTERN

May 14th Neville Hall, Newcastle, 6 p.m.

ANNUAL GENERAL MEETING

To be followed by a programme of technical films.

SOUTH AND WEST MIDLANDS

May A joint meeting will be held in Birmingham during May on a date to be announced later. Details will be circulated by the respective local honorary secretaries.

LONDON SECTION MEETING   –

Wednesday, 16th April.

" CURRENT RADIO INTERFERENCE PROBLEMS "

E. M. LEE, B.Sc. (*Member*)

After a brief historical survey of work in overcoming radio interference, the author will pass to a consideration of current problems. The statistics on interference recently published by the General Post Office emphasize the magnitude of the problem, and the most prominent items revealed in these statistics will be discussed. The problems posed in the field of television interference will receive particular attention.

Recent work in the suppression of interference by screening and by improvements in the receiver will be dealt with, including that of the Electrical Research Association. Some of the forms of interference which are extremely difficult or at the moment impossible to suppress will be mentioned; various examples of interference will be analysed and the cures discussed and, in some instances, demonstrated.

A brief discussion of modern measurement techniques and a summary of the present legal position with reference to the Wireless Telegraphy Act will conclude the paper.